Stochastic Road Infrastructure Management with Empirical Implementation in Uganda

2023

OBUNGUTA FELIX

Acknowledgements

Words cannot fully express how grateful I am to Prof. Kiyoshi Kobayashi (initially my main supervisor) for letting me work and learn in his laboratory. Unfortunately, Prof. Kobayashi retired during my term as a student and this was very challenging because the laboratory would miss his invaluable guidance. Despite this difficulty, Assoc. Prof. Kakuya Matsushima and Assist. Prof. Shunsuke Segi steered the laboratory exceptionally well given the workload and number of students they had to manage. I am deeply indebted to both Professors (Senseis). Specifically, I am appreciative to Assoc. Prof. Kakuya Matsushima (my main supervisor) for his guidance, help with data acquisition and encouragement to do research. I am also profoundly glad that I held fruitful discussions with Assist. Prof. Shunsuke Segi.

During the transition, the laboratory received Prof. Junichi Susaki (my sub supervisor) and Assist. Prof. Kotani Hitomu. The Senseis made the transition smooth and seamless. I am extremely appreciative of the Senseis for their invaluable comments, guidance and availing necessary resources such as text books, and software that were necessary for study. I deeply appreciate Assoc. Prof. Yasuo Sawamura (my sub supervisor) and Prof. Nobuhiro Uno for their guidance and encouragement.

I am thankful to the laboratory secretaries; firstly, Sayaka Hosomi San, who helped me settle in well at the laboratory and secondly, Nakao Satoko San, who helped me until my graduation. I am also very happy to have associated with and learnt from other laboratory members. Certainly, the laboratory parties and gatherings were very memorable and I will cherish them for a lifetime.

I would like to also extend thanks to my teachers at Makerere University who hosted the team from Kyoto University in Uganda and held fruitful discussions. I am indebted to Dr. Hilary Bakamwesiga (my supervisor at undergraduate level) and Dr. Gilbert Kasangaki for leading the Makerere University team and for the great reception and ideas they offered.

Lastly, Eight Japan Engineering Consultants Inc. (EJEC), Japan International Cooperation Agency (JICA), Sekimoto Laboratory at the University of Tokyo, Ministry of Works and Transport

(MoWT) Uganda, Uganda National Roads Authority (UNRA) and Kampala Capital City Authority (KCCA) are appreciated for providing data for this dissertation. I am deeply grateful to the expert engineers from PASCO Corporation for grading the road pavement images. The Japan Society for the Promotion of Science (JSPS) is acknowledged for supporting the work presented in Chapter 5 with a grant – KAKENHI [Grant Number: 21K04288].

Publication Acknowledgement

The bulk of the work presented in this thesis has been published as peer reviewed articles and conference proceedings as listed below:

Article 1

Obunguta, F. and Matsushima, K. (2020). Optimal pavement management strategy development with a stochastic model and its practical application to Ugandan national roads, *International Journal of Pavement Engineering*, Vol.23, No.7, pp. 2405–2419, DOI: 10.1080/10298436.2020.1857759.

The work presented in this article appears in Chapter 3 and has been enhanced with more illustrations and literature. Following the journal and publisher's guidelines, it is stated that: *"This is an original manuscript of an article published by Taylor & Francis in the International Journal of Pavement Engineering on 29 December 2020, available at: http://www.tandfonline.com/10.1080/10298436.2020.1857759."*

Article 2

Obunguta, F., Matsushima, K. and Bakamwesiga, H. (2022). Social Cost Optimization Model and Empirical Evaluation of Intervention Effects on Ugandan Road Pavements, *American Society of Civil Engineers (ASCE) Journal of Infrastructure Systems*, Vol.28, No.4, 05022005, DOI: 10.1061/(ASCE)IS.1943-555X.0000707.

This appears in Chapter 4 with necessary improvements and augmentation.

Article 3

Obunguta, F., Matsushima, K. and Susaki, J. (2022). Probabilistic Management of Pavement Defects with Image Processing Techniques. Submitted to the *Journal of Civil Engineering and Management.*

The contents of this article appear in Chapter 5.

Conference Proceeding 1

Obunguta, F. and Matsushima, K. (2020). Comprehensive Pavement Management with Network Effect: Practical Application to Ugandan Pavement Network, *Proceedings of the 62nd Civil Engineering Planning Division of the Japanese Society of Civil Engineers (JSCE)*; Nagoya, Japan.

Dedication

To my father: Eng. Adongu Richard, mother: Mrs. Adongu Anna Grace Akello, siblings: Jane, Jacob, Eric and Laura, and friends; I am enormously thankful for the moral support during my studies.

Executive Summary

In recent years, many developing countries have had a significant increase in their road infrastructure stock. The increased pavement stock has posed a new challenge of how to manage these roads cost effectively and avoid the total dilapidation of the network without deriving any economic gains. This has generated interest in road infrastructure asset management, a relatively new field in developing countries such as Uganda; which has seen the introduction of Pavement Management Systems (PMSs) and Bridge Management Systems (BMSs) to scientifically manage roads and bridges, respectively.

In the management of infrastructure, it is necessary to estimate the deterioration rate so as to proactively plan for intervention. The estimation requires significant amounts of time series data including condition, inventory and maintenance history. The stochastic Markov hazard model is among the most popular models in the probabilistic estimation of infrastructure deterioration rates for network (macro) level planning. Infrastructure planning mainly involves optimizing costs including travel, intervention, environmental, safety, etc. involved in the usage of infrastructure; and utility to determine the optimum management strategy. This dissertation's main theme is to improve road infrastructure management technologies in developing countries using proactive rather than reactive methods. The thesis contains the following chapters:

Chapter 1: Provides a general introduction on infrastructure asset management and includes the background and motivation. It discussed the total Asset Management Cycle with special interest given to the Plan-Do-Check-Act (PDCA) cycle. It explained the cycle from inception to end and identified the areas of interest in asset management.

Chapter 2: Presents a review of relevant literature that the subsequent chapters look at in detail. The reviewed literature includes infrastructure asset management with a special interest to road pavements; transportation mainly the aspect of travel time and the factors that affect it; and image processing and deep learning with their applications majorly in transportation and infrastructure asset management research.

Chapter 3: Explains pavement management using stochastic Markov models to proactively plan for road infrastructure intervention optimally. This research work involved modeling the deterioration process of road pavements using Markov models and Markov Chain Monte Carlo (MCMC) methods, and planning for optimum road intervention while incorporating the aspect of increase in deterioration rate due to past maintenance works. Specifically, the study examined the applicability to developing countries of a Pavement Management System (PMS) with less data (two-point) requirement to complement current practice. The study compared the current PMS based on specified time intervals regardless of deterioration rate (i.e., time-dependent policy) and a proposed PMS based on deterioration rate (i.e., condition-dependent policy) for the surveyed Ugandan national road network considering a basic plan and a fixed budget, and also investigated the effect of preventive works using a greedy algorithm. The results showed that a shift to the condition-dependent policy increased percentages of network in good and fair condition by 8.6% and 2.5%, respectively, and reduced percentages in poor and bad condition by 8.5% and 2.6%, respectively. Preventive maintenance further increased percentage in good condition by 27.4% and reduced percentages in poor and bad condition by 11.6% and 4.2%, respectively, with a 53.5% reduction in life cycle costs (LCC). This research formed a strong basis to encourage a shift to the condition-dependent policy and preventive maintenance while discouraging the worst first basis, and could be used to support the improvement of PMSs in developing countries.

Chapter 4: Describes the effect of condition on travel time on roads, an extension of Chapter 3 that dwells on road infrastructure condition. Specifically, it looked at management of multiple pavement sections considering varied interventions on pavement durability and capacity and their effects on travel time. Road data was used to build an asset management model applied to determine the intervention choice for multiple road sections concurrently by optimizing social costs (travel and road improvement) incurred by society. The model innovatively combined condition improvement (e.g., patching) and capacity increase (e.g., increasing number of lanes) in a joint decision framework to facilitate socially optimum intervention choice after meeting minimum safety levels. Empirically, the model showed the contribution to decrease in travel time on account of condition improvement and capacity increase for Ugandan roads. Optimal intervention strategies were proposed within a set budget limit and it was suggested that there may be no need to arbitrarily increase intervention budgets. This study may positively impact timely

multiple pavement intervention decisions and can be applied to other infrastructure such as bridges and tunnels. It can be adapted to optimally decide effective and efficient management choices for other facilities, such as pipelines, building and road furniture; that have component parts and many possible interventions during their life time.

Chapter 5: Explores deep learning in civil engineering infrastructure asset management with a special interest in computer vision, an application that has become necessary given challenges such as shortage of labour, safety, need to improve accuracy and a bigger infrastructure stock. Technological advancements have facilitated the change in data type from human-based inspection data to for instance abundant smartphone image data that may require more efficient computer-based techniques for analysis. Human-based data is prone to a number of errors including miss-reporting, omission and/or wrong data entries that compromise analysis results. On the other hand, computer-based techniques are less error prone, cheaper and more efficient. In this chapter, road images from the publically available Road Damage Dataset – 2020 were analyzed by carrying out experiments using simpler image processing techniques (i.e., lazysnapping and region growing from a seed point) and deep learning. The simpler image processing techniques involved the user setting initial Regions of Interest (RoIs) or seed point with the unallocated image pixels allocated as either background or foreground programmatically using a similarity metric. For deep learning, convolutional neural networks (CNNs) using region proposals were applied to train a model to detect and quantify road features and defects in parallel. The deep learning also included an improvement in the setting of the annotation precision and Intersection over Union (IoU) threshold objectively. The simpler segmentation methods were challenged by breakage due to lighting and colour changes, and erroneous allocation of pixels as object whereas, deep learning overcame these challenges and additionally showed more promising and accurate results. A probabilistic road asset management model was developed and the deep learning output was applied as model input to generate information for planning purposes for select roads in Japan. In this chapter, an empirical study was carried out for Japanese roads mainly because of image data unavailability in Uganda. However, the findings in the study are readily applicable to developing countries in future when infrastructure image data is collected. The study showed the possibility of generating intervention proposals for multiple road sections using an efficient and effective method at a lower cost without a huge human dependence, and at comparatively higher accuracy levels. It showed promising

applications and adaptation to regions with less human resources, disaster affected areas, and could be used by practitioners to improve i-construction technologies.

Chapter 6: Concludes the thesis, prescribes policy implications of the studies and investigations in earlier chapters, and gives directions for possible future work.

Contents

List of Figures

List of Tables

Abbreviations

AC – Asphalt Concrete

AHP – Analytic Hierarchy Process

AMS – Asset management System

ANN – Artificial Neural Networks

AP – Average Precision

ASPR – Annual Sector Performance Report

BMS – Bridge Management System

BS – British Standards

CARs – Community Access Roads

CNN – Convolutional Neural Network

CS – Condition State

dTIMS – Deighton's Total Infrastructure Management System

DUCAR – District Urban and Community Access Roads

EBM – Expenditure Budgeting Model

EJEC – Eight Japan Engineering Consultants Inc.

FWD – Falling Weight Deflectometer

GoU – Government of Uganda

GPS – Global Positioning System

HDM-4 – Highway Development Model Four

HMA – hot-mix asphalt

IoU – Intersection over Union

IRI – International Roughness Index

JAF – Joint Assessment Framework

JICA – Japan International Cooperation Agency

KCCA – Kampala Capital City Authority

LCCA – Life Cycle Cost Analysis

mAP – Mean Average Precision

Mask R-CNN – Mask Region Convolutional Neural Network

MCI – Maintenance Control Index

MCMC – Markov Chain Monte Carlo

MH – Metropolis Hastings

MoWT – Ministry of Works and Transport

MTP – Markov Transition Probability

MUSTEM – Multi-State Exponential Markov Hazard Model

NDP – National Development Plan

PCI – Pavement Condition Index

PDCA – Plan-Do-Check-Act

PMS – Pavement Management System

RAMPS – Rehabilitation and Maintenance Planning System

RDD – Road Damage Dataset

RMD – Remaining Duration

RoI – Region of Interest

RUCs – Road User Costs

UNRA – Uganda National Roads Authority

URF – Uganda Road Fund

VCI – Visual Condition Index

WB – World Bank

YOLOv4 – You Only Look Once v4

Notation

Notation used in Chapter 3

A	intervention
k	pavement group
s^k	pavement section in group k
t	time
r	inspection interval
CS	condition state
i	initial condition sate
j	current condition state
J	absorbing condition state
$\underline{i}$	serviceability limit
$\hat{\imath}$	condition a pavement attains after repair
i_{rep}	expression for improvement in pavement condition
π_{ij}	Markov transition probability from condition state i to j
$\boldsymbol{p}$	Markov transition probability matrix
$\boldsymbol{p_{rep}}$	repair (intervention) matrix
$\boldsymbol{p_{trans}}$	transitional probability matrix
$\boldsymbol{r^{s^k}}$	set of inspection intervals for each section
$\boldsymbol{x}^k$	row vector of explanatory variables
$\boldsymbol{\beta}_i$	row vector of unknown parameters
θ_i^k	hazard rate for each group k and condition i
RMD_i^k	remaining duration (life expectancy) for each group k and condition i
φ_A	factor for reduction in life expectancy
C_A	cost of intervention A
$\boldsymbol{m_{A\leftrightarrow i}^{s^k}}$	set of actions performed on each section in correspondence to its condition i
$\boldsymbol{m_p^{s^k}}$	set of maintenance strategies for each section

$\boldsymbol{a}^{t,s^k}$	maintenance history at time t for section s^k
$V_i^{t,s^k}\left(\boldsymbol{a}^{t,s^k}\right)$	agency costs at time t for section s^k with past repair works $\boldsymbol{a}^{t,s^k}$
ρ^r	discount rate
Ω	budget limit

Notation used in Chapter 4

A	intervention
k^g	pavement section k in group g
$\boldsymbol{A}$	set of interventions performed on k^g
a_{k^g}	area of k^g improved
$C^{k^g,A}$	unit cost of intervention on k^g
c^{k^g}	capacity of k^g
$\overline{\boldsymbol{g}}$	group data
i^{k^g}	condition of k^g
$\underline{i^{k^g}}$	safety limit
k^g	pavement section in group g
n	exponent
τ^{k^g}	travel time on k^g
$\tau^{k^g,0}$	free-flow travel time on k^g
v^{k^g}	traffic volume on k^g
W^{k^g}	priority weight
$\boldsymbol{X}^{k^g}$	covariate vector
y	exponent
$\mathbb{R}+$	positive real numbers
θ_1	condition parameter
θ_2	volume:capacity parameter
$\boldsymbol{\Gamma}$	set of all feasible actions
$\boldsymbol{\theta}$	collection of unknown parameters

ω monetary value of one unit of travel time

Ω budget limit

∇ improvement in condition

ξ total social cost

ξ_0 initial total social cost

δ dummy variable

Notation used in Chapter 5

A intervention

d_k^n defect density of class n for section k

$\boldsymbol{d_k}$ vector of defect densities for section k

S_k safety metric

i annotation case

n_i number of annotation cases

e expert

C_k cracking ratio for section k

D_k rutting/ pothole depth for section k

σ_k roughness for section k

MCI_k MCI for section k

MCI_{min}^k minimum MCI for k

MCI_{max}^k maximum MCI for k

p probability of MCI falling within a given range

p_0 probability limit

β_q unknown parameters

$\boldsymbol{\beta}$ vector of unknown parameters

δ_i, $\delta_{k,e}$ dummy variables

Chapter 1

1. Introduction

"A minimum of expense is, of course, highly desirable; but the road which is truly the cheapest is not the one which has cost the least money, but the one which makes the most profitable returns in proportion to the amount spent on it." – W.M. Gillespie, 1847(Bennett and Greenwood, 2002)

1.1 Infrastructure Asset Management

Infrastructure asset management is an evolving field that is highly needed in countries that have developed substantial infrastructure stocks. Developed countries that experienced high economic growth about 60 years ago are deeply engaged in developing efficient asset management systems to delay the total dilapidation of the costly infrastructure including roads, bridges, tunnels and pipelines that facilitate economic growth. Less developed nations have started experiencing similar challenges as their infrastructure stock increases, and so are adapting asset management technologies. The International standard for Asset Management ISO55000 and its sister standards ISO55001 and ISO55002 provide guidance and specify requirements for effective and efficient asset management (British Standards, 2014). The standard defines an asset as:

"An item, thing or entity that has potential or actual value to an organization. The asset value varies between different organizations and can be tangible or intangible, financial or non-financial."

From the above definition of assets, it is in the interest of organizations and/or countries to manage assets well throughout their life and derive maximum value/ benefit from them. The ISO55000 states that asset management supports the realization of asset value while balancing financial, environmental and social costs, risk, quality of service and asset performance. The standard lists improved financial performance, informed asset investment decisions, managed risk, improved

services and outputs, demonstrated social responsibility, demonstrated compliance, enhanced reputation, improved efficiency and effectiveness as some of the benefits of asset management. The Asset Management System (AMS) is related to the organization as shown in Figure 1.1 below.

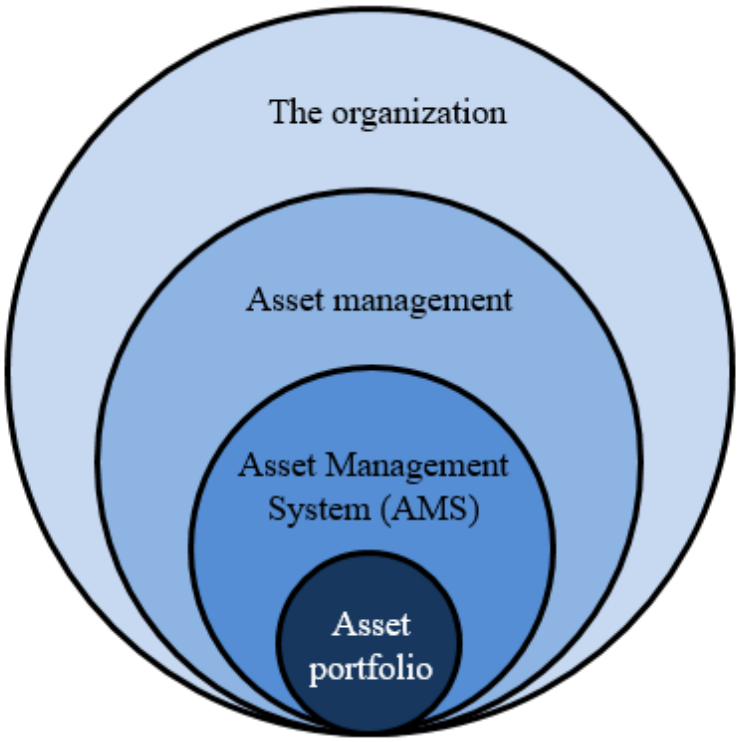

Figure 1.1. Key elements of asset management.

From the above description, Infrastructure Asset Management may be defined as;

"The optimal allocation of scarce budgets between the new arrangement of infrastructure and rehabilitation/maintenance of the existing infrastructure to maximize the value of the stock of infrastructure and to realize the maximum outcomes for the citizens (Kobayashi, 2008)."

The AMS can be viewed as a set of tools, plans and information systems, which are integrated to ensure the delivery of asset management activities. The AMS supports a long-term and sustainable approach to decision making.

1.2 The asset management cycle

The asset management cycle involves activities specified for the infrastructure through its life time until its death where a new development is established. The asset management cycle involves Plan-Do-Check-Act (PDCA) (Figure 1.2). "Plan" involves long, mid and short term planning and design; "Do" contains intervention including minor and major repairs, and construction; "Check" looks at inspection, and estimation of pavement performance; and "Act" involves carrying out rehabilitation, budget policy formulation and evaluation (Kaito 2013). One of the main goals of asset management is to optimize the life cycle costs of an infrastructure system such as a pavement network through Life Cycle Cost Analysis (LCCA). The Highway Development and Management (HDM), developed by the World Bank (WB), and the Kyoto model, developed by Kyoto University Asset Management team, are some of the prominent Pavement Management Systems (PMSs) consistent with ISO55000 in use in the professional world. HDM is the most popular and is arguably regarded as the world standard PMS. The HDM has been improved over the years with HDM-4 as the latest version. The HDM-4 supports decisions on budget planning, condition assessment and road investment evaluation. The HDM-4 requires a rich database with climatic and meteorological data, road condition, pavement age, regional characteristics for full operationalization. On the other hand, the Kyoto model requires only two-time series condition data to estimate pavement deterioration rate and perform budget and road investment planning.

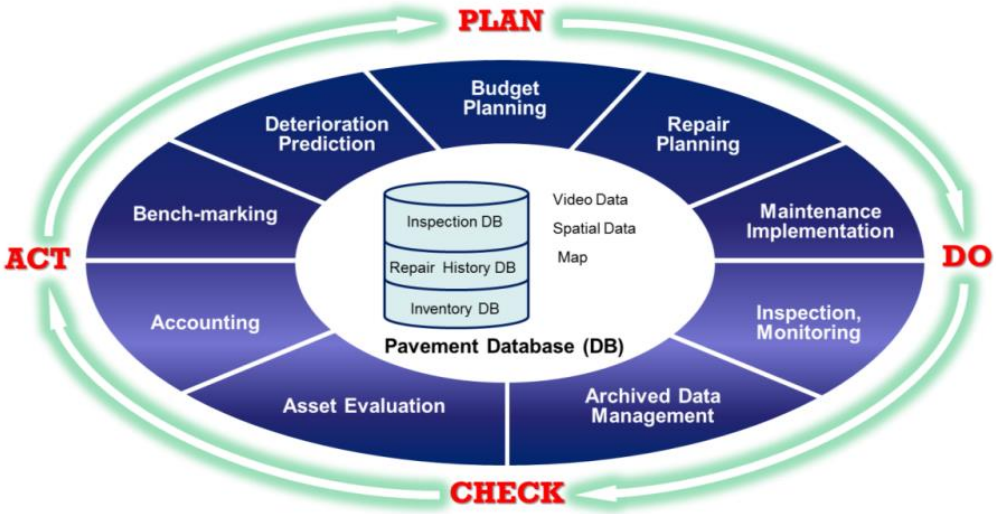

Figure 1.2. PDCA cycle for Infrastructure Asset Management.

1.3 Road Infrastructure Management

Road infrastructure assets comprise of roadways, bridges, tunnels and drainage. Road asset management may require significant amounts of data including condition and repair work history stored in a database that is regularly updated. The data could be used in deterioration prediction models to generate deterioration trends that may be used by road infrastructure managers for intervention planning (AASHTO 2012, Kobayashi et al. 2013). There are a number of prediction models including stochastic, deterministic, Artificial Neural Networks (ANNs) and Bayesian models that can be used for deterioration estimation based on factors such as the nature of infrastructure, data type and management needs of the agency (Uddin 2006, Tsuda et al. 2006, AASHTO 2012). For instance, stochastic models such as the Markov hazard model are ideal for predicting pavement deterioration because of its uncertainty. Deterioration prediction information can then be used to develop management plans and strategies by optimizing life cycle costs (LCC), usage and utility (Kobayashi et al. 2013, Obunguta and Matsushima 2020, Mizutani et al. 2020).

The deterioration of road assets may be influenced by factors including those occurring in the environment such as high impact extreme weather events including floods and gradual changes such as traffic loading and chemicals. These factors may be incorporated in deterioration estimation models as explanatory variables or by creating infrastructure groups (Tsuda et al. 2006, Obunguta and Matsushima 2020). However, some factors that accelerate deterioration may be compounded by deterioration which in turn compounds their effects. A case in point is the compounding of road surface deterioration by the destruction of the subbase layers (Kobayashi and Kaito 2016). As the load bearing capacity of the subbase degrades, the surface deteriorates faster and develops defects including cracks, ruts and potholes which in turn facilitate the further degeneration of the subbase by exposing it to degradation agents such as moisture. Infrastructure attack by chemicals has also been looked at by past studies including Roelfstra et al. (2004), Akiyama et al. (2011), Lethanh et al. (2017) and Cui et al. (2021).

Traffic flow may be delayed due to bottlenecks in the road networks including poor road condition and low capacity of roadways. As a result, road agencies face the challenge of deciding the appropriate intervention choice for multiple road assets mainly due to shortages in budget, shortage of objective decision methods and probably the complexity of these tasks. In the literature, there

have been attempts to model the relationship between condition and travel time (Chandra 2004, Adey et al. 2012, Wang et al. 2014), however, the effect of intervention on multiple road assets on travel times and social cost, that this study explores, hasn't been looked at elaborately.

The need to improve efficiency, accuracy, access to disaster areas and scope of road infrastructure management systems led to the incorporation of image processing and deep learning techniques in data collection (images and videos), analysis and decision making. Studies including Maeda et al. (2018) and Zou et al. (2022) looked at improving the management of civil infrastructure by addressing the shortage of experts leading to less inspection coverage, and the inaccessibility of areas after a disaster, respectively. Deep learning involves important initial steps before model training which include the labor-intensive annotation and setting of model parameters such as the Intersection over Union (IoU) threshold for object detection (Mirikharaji et al. 2021, Greenwald et al. 2022). These important preliminary steps have been determined subjectively which may result in varied results based on the annotator and model inputs including the IoU. This study attempts to make the determination of these initial steps objective by maximizing the probability of correct defect detection, which may be important in ensuring the safety of road users.

1.4 Background and Motivation

A number of developing countries including Uganda have heavily invested in road infrastructure to boost their economic growth. As an example, Uganda has mainly invested in national roads linking cities with the intention of improving the efficiency of transportation of goods and services across the country and region to strengthen the economy through inter and intra national trade links. This ambitious development of transportation infrastructure has been a costly venture similar to the experience of developed nations that had a rapid economic growth period more than 50 years ago. As a result, developing countries are or will inevitably face the challenge of effectively managing the large infrastructure stock. Asset Management has thus become a necessity. Previously, developing countries managed their infrastructure assets in a reactive way with minimal consideration given to the estimation of future condition and without carrying out robust life cycle cost analysis. Management that overlooks proactive intervention and planning results in the faster dilapidation of infrastructure in the developing world despite the huge initial investment costs. Modern infrastructure asset management methods seek to solve key questions such as the

optimum budget allocation, maintenance strategies to optimally manage infrastructure in the long term, the best ways of maximizing infrastructure value, and the optimal balance between new developments verses maintaining existing stocks. These research questions have led to developments including stochastic deterioration hazard models, operations research, and econometric analysis to improve infrastructure performance. These studies generally require large time series data volumes that has also influenced analysis methods such as Bayesian modeling and imputation methods in case of incomplete data, computing techniques for image data, and probabilistic Markov models for a minimum of two-point time series data. Additionally, the differences in environmental exposure between infrastructure may lead to different deterioration trends and hence may require varied approaches.

In Uganda, different agencies are charged with the duty of managing roads. Uganda National Roads Authority (UNRA) manages national roads while local governments manage district roads. In some cases, the line between national and district roads is not so clearly defined; which causes different management decisions by different actors for the same infrastructure. Some of the road projects that have been fully or partly funded by donors require certain management standards after project completion and may involve donors or their agents. The agencies also use separate and incompatible management systems which may not provide avenues for benchmarking. For instance, in Uganda, UNRA uses Deighton's Total Infrastructure Management System (dTIMS) and Highway Development and Management Model (HDM-4) while Ministry of Works and Transport (MoWT) that oversees local governments uses Rehabilitation and Maintenance Planning System (RAMPS). In addition, if donors are involved in the management of roads, an entirely new PMS may be adopted. Each PMS has different data requirements and this introduces incompatibility which affects joint coordination and road management by sister agencies. Furthermore, there is a lack of institutional capacity which makes pavement monitoring and management inconsistent. In these instances, decisions are made based on biased human judgement rather than scientific methods. There is also limited funding for road maintenance because priority has been given to novel construction. Similar inefficient management challenges are common in other developing countries.

The development of asset management systems that include the deterioration rate of infrastructure

condition as opposed to reactive intervention based AMS may improve infrastructure performance. Kobayashi et al. (2013) and Obunguta and Matsushima (2020) have explored condition-dependent infrastructure asset management and showed its advantages such as better performance and cost saving, compared to the time-dependent option, empirically. The challenge of determining the most appropriate intervention for multiple infrastructure assets and its effects on travel time is looked at by Obunguta et al. (2022). These studies attempted to optimize the management of infrastructure using predictive models such as the stochastic Markov hazard model proactively.

This research was motivated by the foreseeable challenges and gaps in planning that could potentially water down all the heavy investment in public infrastructure in developing countries, some of which is donor funded or financed by loans. It was inspired by the need to improve road infrastructure management and planning from reactive to proactive methods that lower LCCs over the long term. To complement current maintenance practice, this study attempted to solve the challenges by introducing management systems that require less input in terms of data and funding but give rich output that is adequate for planning purposes. The cost savings including inspection costs could be used for novel development and maintenance works. The gaps in infrastructure asset management literature including the effect of road condition on travel times also strongly motivated this research so as to contribute to road asset management knowledge. The challenges of inaccessibility of infrastructure damaged after disasters, less coverage due to a shortage of experts and the need to improve management accuracy and decisions also encouraged the futuristic ideas including incorporating the analysis of abundant smartphone image data using image processing techniques and deep learning to improve road infrastructure management systems.

1.5 Research Objectives

The objectives of this study mainly encompass the improvement of infrastructure asset management with a keen focus on the adoption of recent asset management technologies by developing countries. The research extends work by earlier studies including Tsuda et al. (2006), Kobayashi et al. (2013), and Maeda et al. (2018). Specifically, the objectives of this study are;

1) Complement the current infrastructure management practice in developing countries including Uganda by developing AMS with less data requirement but rich output to aid

proactive planning and intervention.

2) Customise earlier AMSs including PMS models based on the needs of developing countries by extending earlier studies to incorporate the aspect of change in deterioration rate due to maintenance history.
3) Develop a social cost model to evaluate effects of road intervention on capacity and durability on travel time for multiple assets concurrently.
4) Build a probabilistic asset management model using deep learning including setting the inputs (i.e., annotation and IoU) objectively so as to support less human dependent AMSs.
5) Test the empirical applicability of the developed models including stochastic Markov models, investigate the effect of preventive maintenance on network condition and the efficiency of the less human dependent computer-based AMSs.

1.6 Expected Contributions

This study is generally expected to contribute to the improvement of asset management and innovatively show possible applications and adaptations of the latest technologies in majorly developing countries following the structure in Figure 1.3. In detail, the expected main contributions are;

1) In Chapter 3, this research encourages a shift to the proactive condition-dependent PMS and preventive maintenance while discouraging the reactive time-dependent PMS. It is expected that this study could be used to support the improvement of PMSs in developing countries.
2) This dissertation expanded the discussion on condition in Chapter 3 to include its effects on traffic flow and the determination of optimum intervention for multiple road sections. The study in Chapter 4 could be applied to optimally decide effective and efficient management choices for other infrastructure including bridges, tunnels, pipelines and buildings; that have component parts and many possible interventions during their life time.
3) Deep learning and computer vision could be adapted to regions with less human resources; disaster affected areas; improve i-construction technologies, infrastructure management efficiency and accuracy. Chapter 5 looks at new computing technologies including deep learning and explores ways to appropriately leverage the merits of technology in the face of modern day challenges including labor shortages. Due to data availability issues, the

empirical application was done for Japanese roads (a developed country); however, the research outcomes show promise and could be applied to developing countries in future when infrastructure image data is available.

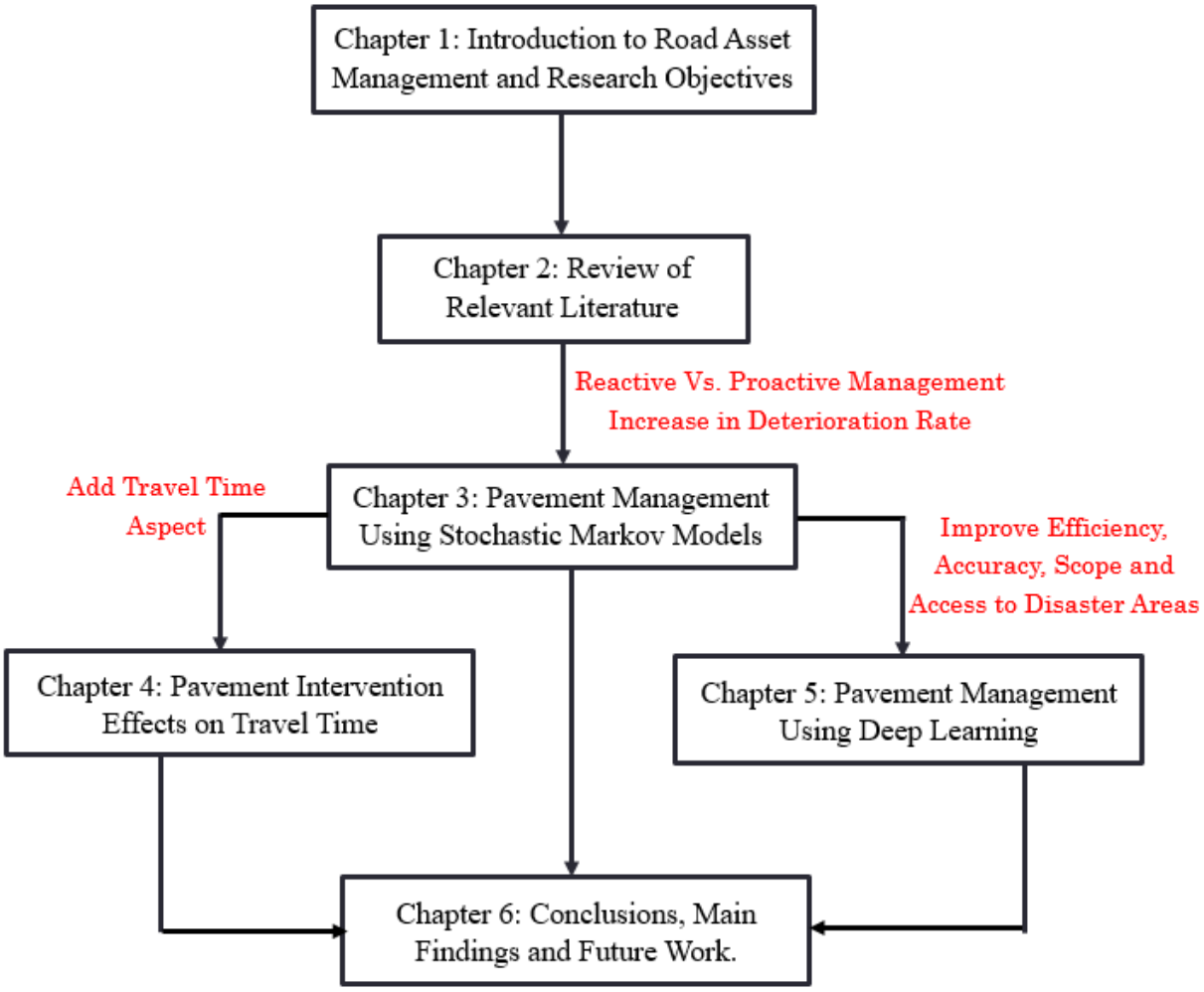

Figure 1.3. Structure of thesis.

Bibliography

AASHTO (American Association of State Highway and Transport Officials), 2012. Pavement Management Guide, 2nd ed. Washington, DC: AASHTO.

Adey, B.T., Hermann, T., Tsafatinos, K., Luking J., Schindele, N., Hajdin, R. 2012. Methodology and base cost models to determine benefits of road preservation interventions in Switzerland, *Structures and Infrastructure Engineering*, 8(7), 639–654 DOI: 10.1080/15732479.2010.491119.

Akiyama, M., Frangopol, D. M., and Matsuzaki, H., 2011. Lifecycle reliability of RC bridge piers under seismic and airborne chloride hazards. *Earthquake Engineering and Structural Dynamics*, 40(15), 1671–1687.

British Standards, 2014. Asset management: Overview, principles and terminology, BS ISO 55000:2014(E).

Chandra, S., 2004. Effect of Road Roughness on Capacity of Two-Lane Roads, *Journal of Transportation Engineering*, 130 (3), 360–364.

Cui, F., Li, H., Dong, X., Wang, B., Li, J., Xue, H., and Qi. M., 2021. Improved time-dependent seismic fragility estimates for deteriorating RC bridge substructures exposed to chloride attack, *Advances in Structural Engineering*, 24(3):437–452, doi:10.1177/1369433220956812.

Greenwald, N.F., Miller, G., Moen, E. et al., 2022. Whole-cell segmentation of tissue images with human-level performance using large-scale data annotation and deep learning, *Nature Biotechnology*, 40, https://doi.org/10.1038/s41587-021-01094-0, pp.555–565.

Kaito, K., 2013. Statistical Deterioration Forecasting Model. *Proceeding of Road Infrastructure Asset Management Summer School 2013*, Kyoto University and University of Transport and Communications.

Kobayashi, K., 2008. Sustainable infrastructure and asset management. In *Proceeding of 3rd The Network of Asian River Basin Organizations (NARBO) Meeting*, Indonesia, February 2008. ADB.

Kobayashi, K., and Kaito, K., 2016. Estimating Composite Hidden Markov Deterioration Models for Pavement Structure with Sample Missing. International Symposium on Infrastructure Asset Management, SIAM 2016, 1–18.

Kobayashi, K., Eguchi, M., Oi, A., Aoki, K., Kaito, K., 2013. The optimal implementation policy for inspecting pavement with deterioration uncertainty. *Journal of Japan Society of Civil Engineers*, 1(1), 551–568.

Lethanh, N., Hackl, J., and Adey, B.T., 2017. Determination of Markov Transition Probabilities to be Used in Bridge Management from Mechanistic-Empirical Models. *Journal of Bridge Engineering,* 2017, 22(10): 04017063, DOI: 10.1061/(ASCE)BE.1943-5592.0001101.

Maeda, H., Sekimoto, Y., Seto, T., Kashiyama, T. and Omata, H., 2018. Road damage detection and classification using deep neural networks with smartphone images, *Journal of Computer-Aided Civil and Infrastructure Engineering*, Vol.33, pp. 1127–1141.

Mirikharaji, Z., Abhishek, K., Izadi, S. and Hamarneh, G., 2021. D-LEMA: Deep Learning Ensembles from Multiple Annotations Application to Skin Lesion Segmentation, *Proceedings of the IEEE/CVF Conference on Computer Vision and Pattern Recognition (CVPR) Workshops*, pp. 1837-1846, Held virtually.

Mizutani, D., Nakazato, Y., and Lee, J., 2020. Network-level synchronized pavement repair and work zone policies: Optimal solution and rule-based approximation, Transportation Research Part C: Emerging Technologies, Vol. 120, https://doi.org/10.1016/j.trc.2020.102797, 102797.

Obunguta, F. and Matsushima, K., 2020. Optimal pavement management strategy development with a stochastic model and its practical application to Ugandan national roads, *International Journal of Pavement Engineering*, Vol.23, No.7, DOI: 10.1080/10298436.2020.1857759, pp. 2405–2419.

Obunguta, F., Matsushima, K. and Bakamwesiga, H., 2022. Social Cost Optimization Model and Empirical Evaluation of Intervention Effects on Ugandan Road Pavements, *Journal of Infrastructure Systems*, Vol.28, No.4, DOI: 10.1061/(ASCE)IS.1943-555X.0000707, 05022005.

Roelfstra, G., Hajdin, R., Adey, B., and Bruhwiler, E., 2004. Condition Evolution in Bridge Management Systems and Corrosion-Induced Deterioration, *Journal of Bridge Engineering,* 2004, 9(3): 268-277, DOI: 10.1061/(ASCE)1084-0702(2004)9:3(268).

Tsuda, T., Kaito, K., Aoki, K. and Kobayashi, K., 2006. Estimating Markovian Transition Probabilities for Bridge Deterioration Forecasting, *Structural Engineering/Earthquake Engineering*, Vol.23, No.2, pp. 241s–256s.

Uddin, W., 2006. Pavement Management Systems. In T. F. Fwa, ed. *The Handbook of Highway Engineering*. Boca Raton, FL, USA: Taylor & Francis.

Wang, T., Harvey, J., Lea, J. and Kim, C., 2014. Impact of Pavement Roughness on Vehicle Free-Flow Speed, *Journal of Transportation Engineering*, 140 (9), 04014039.

Zou, D., Zhang, M., Bai, Z., Liu, T., Zhou, A., Wang, X., Cui, W., and Zhang, S., 2022. Multi-category damage detection and safety assessment of post-earthquake reinforced concrete structures using deep learning, *Journal of Computer-Aided Civil and Infrastructure Engineering*, https://doi.org/10.1111/mice.12815, pp. 1–17.

Chapter 2

2 Review of Relevant Literature

2.1 Introduction

The literature presented in this chapter describes in general terms what is detailed in subsequent chapters. First, literature on infrastructure asset management with a keen interest on road pavements is described followed by transportation mainly the aspect of travel time and the factors that affect it. Next, image processing and deep learning with their applications majorly in transportation and infrastructure asset management research are looked at. This literature review also includes illustrations to emphasize key points raised in the thesis.

2.2 Pavement Infrastructure Asset Management

Infrastructure asset management mainly involves inspection of infrastructure condition, creating an inventory and condition database, modeling infrastructure performance and planning for interventions including minor/ major repairs and reconstruction based on the estimated performance/ deterioration results (Figure 2.1). The database could be updated using subsequent inspection data and repair history information that also informs estimation and future intervention planning (Madanat and Ben-Akiva 1994, AASHTO 2012, Kobayashi et al. 2013, Han et al. 2017, Obunguta and Matsushima 2020).

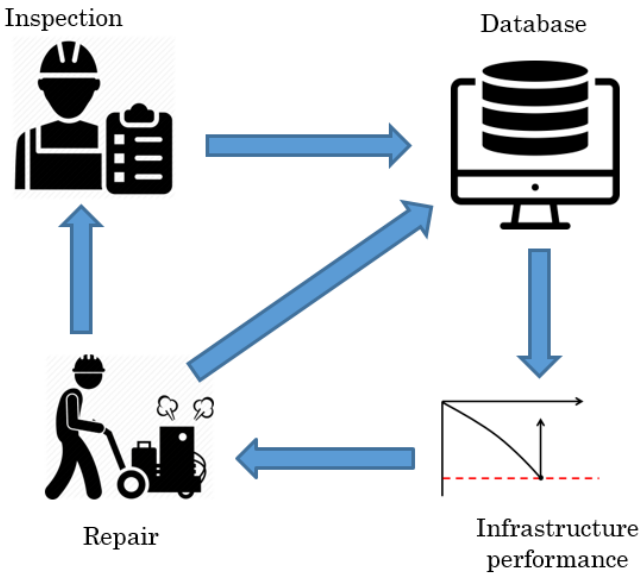

Figure 2.1. Infrastructure Asset Management Process.

Infrastructure performance may be estimated using a number of models for instance deterministic, stochastic or probabilistic, regression, Artificial Neural Networks (ANNs), and subjective or expert-based models (Uddin 2006, Tsuda et al. 2006, AASHTO 2012, Abaza 2016, 2017, Pérez-Acebo et al. 2020). Many of these models require the discretization of infrastructure condition before their application. Discretization involves assigning a representative condition state for a given range of condition data measured using other metrics. The transition of condition states can then be modeled and the estimated outputs used for infrastructure planning purposes. Stochastic models and ANNs have arguably been the most popular because of their practicality in modeling infrastructure deterioration amidst prediction uncertainity (Kobayashi et al. 2013) and increased scope amidst a shortage of experts (Maeda et al. 2018, Pérez-Acebo et al. 2020), respectively. Among the stochastic models, Markov models have been extensively looked at and empirically applied to model deterioration transition for infrastructure including pavements and bridges (Tsuda et al. 2006). The Markov model requires a minimum of two-point data (data collected at two different years for the same infrastructure) to generate deterioration trends. The Figure 2.2 shows possible paths of transition for infrastructure condition state i over time τ that can be modeled probabilistically using stochastic models such as the Multi-State Exponential Markov hazard (MUSTEM) model developed by Tsuda et al. (2006).

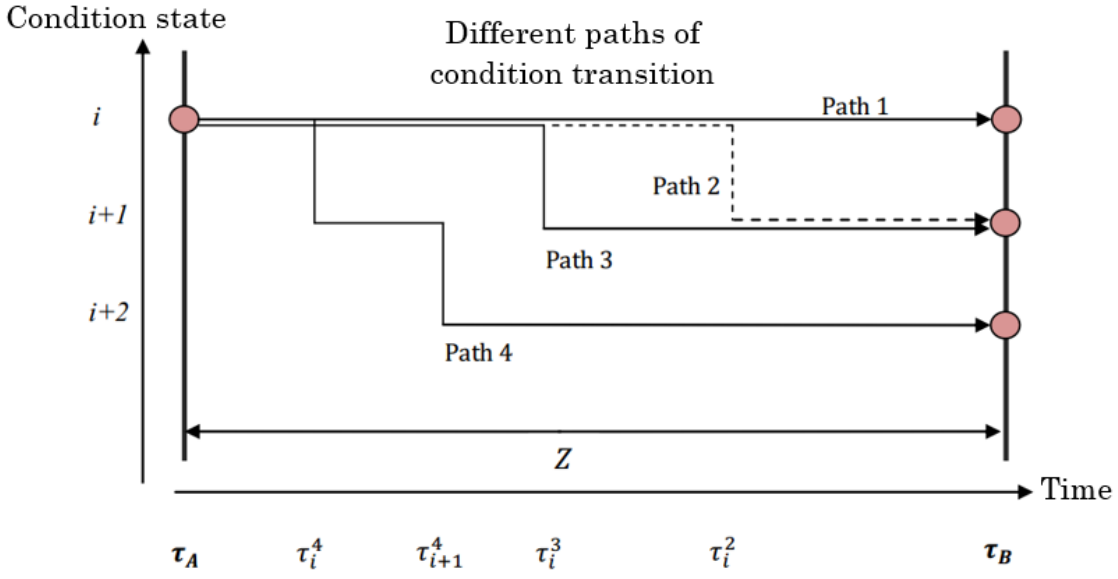

Figure 2.2. Transition of infrastructure condition (Tsuda et al. 2006).

Infrastructure planning is the step that follows infrastructure performance estimation. Planning may be done at either micro level (specific infrastructure) or macro level (infrastructure group). At the macro level, the main goal is to set standards and budgets whereas, at the micro level the goal may be to determine an appropriate repair method for an infrastructure section for example a road junction. For macro level planning, management plans could be drawn based on rules set by the management agency. There are a number of rules applied by agencies in the management of infrastructure that may be broadly grouped into two; i.e., the condition-dependent and the time-dependent rule. The time-dependent policy involves infrastructure interventions after regular intervals regardless of their deteriorated state; whereas, the condition-dependent policy specifies civil infrastructure intervention based on deterioration rates (Kobayashi et al. 2013, Obunguta and Matsushima 2020). The time-dependent policy is ideal for infrastructure such as small lighting, road furniture and buried infrastructure such as pipelines that are costly to inspect. The condition-dependent policy would be more suited for civil infratructure including bridges and road pavements that experience uncertainity in their deterioration. Infrastructure planning also involves the optimization of infrastructure Life Cycle Costs (LCCs) including user, agency and environmental costs; infrastructure usage and utility, for instance, travel time, safety and comfort to determine the most optimum strategies for an infrastructure group (Kobayashi et al. 2013, Obunguta and Matsushima 2020, Mizutani et al. 2020).

Similar to many developing countries, Uganda mainly intervenes on its infrastructure over regular intervals (time-dependent policy) regardless of its deterioration being uncertain (MoWT 2011 – 2017). Past studies haven't made detailed empirical comparisons and shown the advantages of the condition-dependent policy compared to the time-dependent policy for infrastructure including pavements. This thesis builds a model that facilitates the comparison between the time-dependent policy, currently applied by many developing countries, with the condition-dependent policy that is suitable for management of infrastructure with uncertain deterioration; and evaluates the effect of preventive maintenance on pavement condition and LCCs with an empirical application to Ugandan roads.

2.3 Transportation and Asset Management

Transportation, the movement of goods and people from an origin to a destination, is supported by infrastructure such as roads, railways, airports etc. and as such the condition of one affect the other.

For example, narrow dilapitated roads increase transportation costs including travel times, congestion and vehicle operation costs (VOCs); and heavily trafficked roads may deteriorate faster. The Figure 2.3 illustrates this interdependency between road capacity and condition. Road infrastructure systems may require policies that optimize road capacity and condition to improve user utility including travel times. Due to the complexity of infrastructure system intervention decisions, an efficient decision process may be required that for instance evaluates the trade-off between condition improvement and capacity increase choice for multiple road sections concurrently through optimizing social costs including travel, safety, intervention and environmental costs (Obunguta et al. 2022).

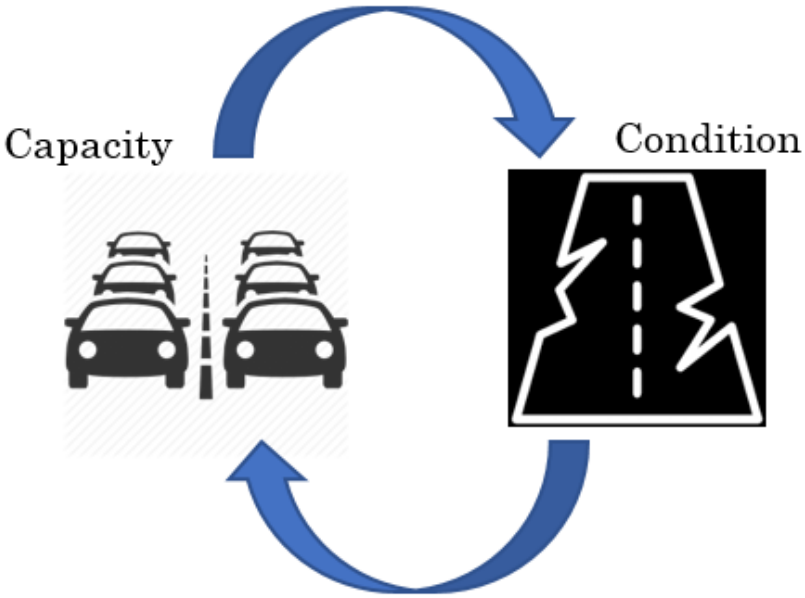

Figure 2.3.Interdependency between road capacity and condition.

Past studies including Watanatada et al. (1987), Bennett and Greenwood (2002), Chandra (2004), Transport Research Board (TRB) (2000, 2010) and Wang et al. (2014) made attempts to model the relationships between the speed, travel time, capacity and road condition with the results showing strong relationships. Adey et al. (2020) listed accident, travel time, vehicle operation, comfort, noise, and particle emissions as important considerations for road service. The calibrated relationships between these variables are important in the evaluation of how the changes in one variable affect the others and vice versa. Generally, wider roads (with higher capacity) and roads in good condition are expected to offer shorter travel times that increases user utility and lowers transportation costs. Additionally, in the optimization of road infastructure costs, it is important to

look at minimizing inspection, maintenance and rehabilitation costs as these directly affect agency costs and user costs mainly VOCs and travel costs (Madanat and Ben-Akiva 1994, Lethanh et al. 2015, Yang et al. 2015).

The novelty of this chapter includes modeling the relationship between pavement condition and capcity and showing how intervention affects travel time not elaborated by earlier studies. This intervention choice (road expansion or repair) decision problem is modeled and includes social cost (user and agency) optimisation. An empirical application using road data from Uganda is shown in the subsequent sections of this thesis.

2.4 Image Processing and Deep Learning for Asset management

Image processing and deep learning are advanced computing fields that can be applied to improve the efficiency and effectiveness of infrastructure asset management. These advancements offer increased coverage in infrastructure monitoring, better access to disaster areas, condition prediction and planning; and improved accuracy especially as the proportionate number of management experts reduces and the infrastructure stock increases (Maeda et al. 2018, Zou et al. 2022). Image processing could involve analysis of images and generating output for infrastructure planning. Deep learning consists of obtaining infrastructure images, annotating (labeling) them, training and validating a program to detect the annotated objects, and the program's application to generate output for a given set of image data (Figure 2.4). The output, for instance, section defect densities could be applied as inputs in infrastructure planning to determine appropriate interventions. Deep learning and image processing seek to accurately detect and segment objects in images. Algorithms built using region proposals and CNNs (R-CNN) including Mask R-CNN algorithm (He et al. 2018) have been the most promising and have shown higher accuracy compared to other algorithms.

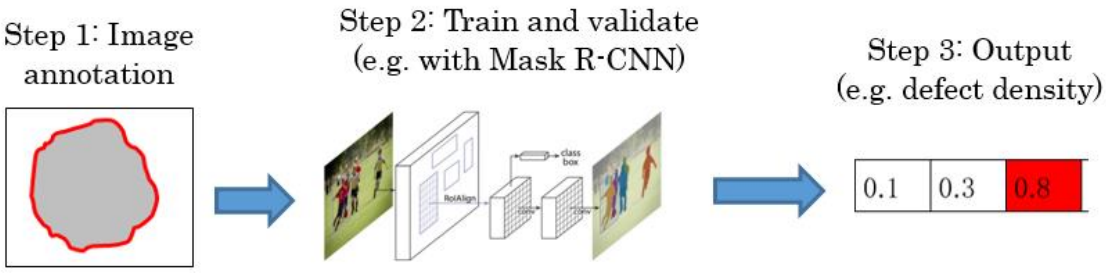

Figure 2.4. Main steps in deep learning.

The vital prerequisite steps to deep learning model training and validation include annotation and the right setting of the Intersection over Union (IoU). These important initial steps are user dependent and affect model training and object detection. The IoU is an important metric that determines whether a right detection of an object can been made (Figure 2.5). Based on the set IoU, a detection in the image may be specified as either true or false and as such IoU should be set carefully. Image annotation is a cumbersome process that requires a lot of labour hours. Very precise annotations may be required for sensitive fields including health and security that require much higher accuracy. Infrastructure performance estimation may not require very high accuracy compared to other more sensitive fields such as health because the damage level need only fall within a specified range for appropriate classification. More precise annotations may increase accuracy, however, they are costly. Therefore, a trade-off may exist between the quality and time cost of annotating images. The accuracy-time cost trade-off may avail practitioners with annotation quality choice for specific purposes (Mirikharaji et al. 2021).

This study seeks to make the determination of annotation quality and IoU objective rather than subjective using probabilistic methods to facilitate efficient choices of these important inputs for specific purposes. As an addition to the discussion in past studies, this study also shows how output from image processing could be applied to determine intervention decisions for infrastructure emprically using Japanese roads as an example.

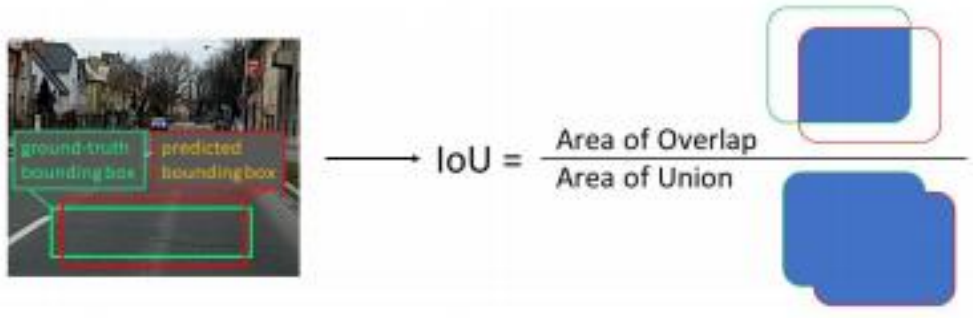

Figure 2.5. Intersection over Union (Arya et al. 2020a).

Bibliography

AASHTO (American Association of State Highway and Transport Officials), 2012. Pavement Management Guide, 2nd ed. Washington, DC: AASHTO.

Abaza, K.A., 2016. Back-calculation of transition probabilities for Markovian-based pavement performance prediction models. *International Journal of Pavement Engineering*, 17(3), 253–264.

Abaza, K.A., 2017. Empirical approach for estimating the pavement transition probabilities used in non-homogenous Markov chains. *International Journal of Pavement Engineering*, 18(2), 128–137.

Adey, B. T., Burkhalter, M., and Martani, C., 2020. Defining road service to facilitate road infrastructure asset management, *Infrastructure Asset Management*, 7(4), 240–255, doi: https://doi.org/10.1680/jinam.18.00045.

Arya, D., Maeda, H., Ghosh, S. K., Toshniwal, D., Mraz, A., Kashiyama, T. and Sekimoto, Y., 2020a. Transfer Learning-based Road Damage Detection for Multiple Countries, arXiv preprint arXiv:2008.13101.

Bennett, C. R. and Greenwood, I. D., 2002. Modelling road user and environmental effects in HDM-4, *The Highway Development and Management Series Collection*, Vol. 4, 44–81, The World Road Association, Paris, France.

Chandra, S., 2004. Effect of Road Roughness on Capacity of Two-Lane Roads, *Journal of Transportation Engineering*, 130 (3), 360–364.

Han, D., Kaito, K., Kobayashi, K., Aoki, K., 2017. Management scheme of road pavements considering heterogeneous multiple life cycles changed by repeated maintenance work. *KSCE Journal of Civil Engineering*, 21(5), 1747–1756.

He, K., Gkioxari, G., Dollar, P. and Girshick, R., 2018. Mask R-CNN, Facebook AI Research (FAIR), arXiv:1703.06870v3.

Kobayashi, K., Eguchi, M., Oi, A., Aoki, K., Kaito, K., 2013. The optimal implementation policy for inspecting pavement with deterioration uncertainty. *Journal of Japan Society of Civil Engineers*, 1(1), 551–568.

Lethanh, N., Adey, B. T. and Fernando, D. N., 2015. Optimal intervention strategies for multiple objects affected by manifest and latent deterioration processes, *Structure and Infrastructure Engineering*, 11(3), 389–401, DOI: 10.1080/15732479.2014.889178.

Madanat, S. and Ben-Akiva, M., 1994. Optimal inspection and repair policies for infrastructure facilities. *Transportation Science*, 28(1), 55–62, doi:10.1287/trsc.28.1.55.

Maeda, H., Sekimoto, Y., Seto, T., Kashiyama, T. and Omata, H., 2018. Road damage detection and classification using deep neural networks with smartphone images, *Journal of Computer-Aided Civil and Infrastructure Engineering*, Vol.33, pp. 1127–1141.

Mirikharaji, Z., Abhishek, K., Izadi, S. and Hamarneh, G., 2021. D-LEMA: Deep Learning Ensembles from Multiple Annotations Application to Skin Lesion Segmentation, *Proceedings of the IEEE/CVF Conference on Computer Vision and Pattern Recognition (CVPR) Workshops*, pp. 1837-1846, Held virtually.

Mizutani, D., Nakazato, Y., and Lee, J., 2020. Network-level synchronized pavement repair and work zone policies: Optimal solution and rule-based approximation, Transportation Research Part C: Emerging Technologies, Vol. 120, https://doi.org/10.1016/j.trc.2020.102797, 102797.

MoWT (Ministry of Works and Transport) – Uganda, 2011–2017. Annual Sector Performance Reports (ASPR); http://www.works.go.ug/document-category/jtsrw/.

Obunguta, F. and Matsushima, K., 2020. Optimal pavement management strategy development with a stochastic model and its practical application to Ugandan national roads, *International Journal of Pavement Engineering*, Vol.23, No.7, DOI: 10.1080/10298436.2020.1857759, pp. 2405–2419.

Obunguta, F., Matsushima, K. and Bakamwesiga, H., 2022. Social Cost Optimization Model and Empirical Evaluation of Intervention Effects on Ugandan Road Pavements, *Journal of Infrastructure Systems*, Vol.28, No.4, DOI: 10.1061/(ASCE)IS.1943-555X.0000707, 05022005.

Pérez-Acebo, H., Linares, A., Roji, E., Gonzalo-Orden, H., 2020. IRI performance models for flexible pavements in two-lane roads until first maintenance and/or rehabilitation work. *Coatings*, 10, 97.

TRB (Transport Research Board), 2000. Highway Capacity Manual. National Research Council, Transportation Research Board, Washington, D.C.

TRB (Transport Research Board), 2010. Highway Capacity Manual. National Research Council, Transportation Research Board, Washington, D.C.

Tsuda, T., Kaito, K., Aoki, K. and Kobayashi, K., 2006. Estimating Markovian Transition Probabilities for Bridge Deterioration Forecasting, *Structural Engineering/Earthquake Engineering*, Vol.23, No.2, pp. 241s–256s.

Uddin, W., 2006. Pavement Management Systems. In T. F. Fwa, ed. *The Handbook of Highway Engineering*. Boca Raton, FL, USA: Taylor & Francis.

Wang, T., Harvey, J., Lea, J. and Kim, C., 2014. Impact of Pavement Roughness on Vehicle Free-Flow Speed, *Journal of Transportation Engineering*, 140 (9), 04014039.

Watanatada, T., Dhareshwar, A. M. and Lima, P. R. S. R., 1987. *Vehicle speeds and operating costs: models for road planning and management*, John Hopkins University Press, Baltimore, MD.

Yang, C., Remenyte-Prescott, R. and Andrews, J., 2015. Road maintenance planning using network flow modelling, *IMA Journal of Management Mathematics*, 2017(28), 387–402, doi:10.1093/imaman/dpv031.

Zou, D., Zhang, M., Bai, Z., Liu, T., Zhou, A., Wang, X., Cui, W., and Zhang, S., 2022. Multi-category damage detection and safety assessment of post-earthquake reinforced concrete structures using deep learning, *Journal of Computer-Aided Civil and Infrastructure Engineering*, https://doi.org/10.1111/mice.12815, pp. 1–17.

Chapter 3

3 Pavement Management Using Stochastic Markov Models

"Investment in infrastructure is a long term requirement for growth and a long term factor that will make growth sustainable." – Chanda Kochhar

3.1 Introduction

In this chapter, a review of relevant pavement management literature was presented including Stochastic models on the estimation of infrastructure (in this case pavements) deterioration rate. The Markov Hazard model was discussed and applied in the estimation of transition probability and life expectancy. Management planning that minimises Life Cycle Costs (LCC) was also presented.

3.2 Pavement Management

Pavement Management Systems (PMSs) contain inventory, condition data obtained after periodical inspections, deterioration prediction models, and rehabilitation and maintenance history (Madanat and Ben-Akiva 1994, AASHTO 2012, Kobayashi et al. 2013, Han et al. 2017). Once inspection is carried out, pavements may be graded based on observed condition according to a discrete scale defining condition states. Typically, road agencies may initially check pavement condition through inspections then carry out detailed tests for example the Falling Weight Deflectometer (FWD) and soil tests for critical sections. However, it should be noted that each road agency has its own specific management procedure. In Uganda, a four-point condition scale is used to categorise pavement condition while a seven-point scale is used in Japan. Saha and Ksaibati (2017) argue that a wider scale compensates for errors made by raters in the field. Pavement deterioration rate can be estimated using deterministic, stochastic (probabilistic), Bayesian, and subjective (expert-based) models (Tsuda et al. 2006, AASHTO 2012). Uddin (2006) classified deterioration prediction

models into regression analysis techniques, Artificial Neural Networks (ANNs), and probabilistic performance models (with Bayesian and Markov models as the main methodologies in this approach). Despite ANNs receiving increasing attention in recent years, deterministic and stochastic models still attract the most attention (Abaza 2016, 2017, Pérez-Acebo et al. 2020).

Pavement management may be handled at either micro level (specific pavement section) or macro level (network). At the macro level, the main goal is to set standards and budgets whereas, at the micro level the goal may be to determine an appropriate repair method for a pavement section. Setting network standards and intervention budgets is heavily reliant on deterioration prediction models. Both deterministic and stochastic models can be used to predict pavement performance at macro level (George 2000, AASHTO 2015, Dalla Rosa et al. 2017); whereas, deterministic models may be preferable at the micro level (Tsuda et al. 2006, Kobayashi et al. 2013). Unlike deterministic models, which predict an exact value for an index, stochastic models estimate the probabilistic distribution of the expected value. Therefore, stochastic models are able to incorporate uncertainty in pavement performance. Because pavement performance is recognised to be probabilistic in nature, some levels of uncertainty are required; hence, stochastic models would be more ideal (Li et al. 1997, Kobayashi et al. 2013, Pérez-Acebo et al. 2019). Among stochastic models, Markov models are the most widely employed to predict pavement deterioration, with many examples in the literature developed by Tsuda et al. (2006), Kobayashi et al. (2010), Lethanh and Adey (2012), and Lethanh et al. (2015). Recent studies have attempted to simplify pavement deterioration prediction requiring only two time-series observations such as Tsuda et al. (2006) whose study was based on Markov models and Mohammadi et al. (2019) who presented both deterministic (based on regression) and probabilistic (based on Markov methods) approaches. Pérez-Acebo et al. (2019) developed a deterioration prediction model considering shorter time intervals (half year cycles) for Moldova. This study showed that intensive data collection over shorter time periods could compensate for inexistent historical data. Performance prediction models based on the Bayesian approach have also been developed (Kobayashi et al. 2012, Tabatabaee and Ziyadi 2013, Han et al. 2014, Pantuso et al. 2019). Once pavement deterioration is estimated, maintenance plans and budgets can be formulated from an informed point of view.

Management plans can be drawn based on either the condition-dependent or the time-dependent policy. The time-dependent policy involves maintenance or renewal of infrastructure after regular

intervals regardless of their deteriorated state; whereas, for the condition-dependent policy civil infrastructure is maintained or replaced based on its deterioration rate (Kobayashi et al. 2013). A condition-dependent management policy would be ideal for pavement infrastructure with uncertain and variable deterioration processes. Kobayashi et al. (2013) determined life cycle costs (LCC) using the Multi-State Exponential Markov hazard (MUSTEM) model (Tsuda et al. 2006) at a specified risk control level for pavements based on the condition-dependent rule and examined the trade-off between risk and LCC. The higher the risk (lower service level), the lower the LCC and vice versa. On the other hand, the time-dependent policy is suitable for smaller systems such as lighting systems and buried civil infrastructure that are costly to inspect. Currently, many developing countries including Uganda have adopted a time-dependent management policy for pavements, neglecting the fact that pavement deterioration is a stochastic process.

In recent years, many developing countries have had a significant increase in their road infrastructure stock due to increased access to finance both locally and internationally. Oxford Economics (2014) forecasts that capital project and infrastructure spending worldwide is expected to total more than US$ 9 trillion (hereafter $ is used) by 2025, up from $ 4 trillion in 2012 with developing countries accounting for nearly half of all infrastructure spending. This poses a new challenge of how to cost-effectively manage the road infrastructure. In the case of Uganda, some donor-funded road projects had specific management standards after completion, hence attempts were made to introduce some PMSs such as the World Bank's HDM-4; however, for the remaining bulk of the network, the time-dependent management policy was still applied. This generated a challenge of incompatibility in pavement network management due to parallel management systems. Additionally, inspection surveys were irregular due to funding shortfalls. Therefore, developing countries need a PMS with less data requirement (two-point data) but which generates a rich output (containing predicted network condition, expected maintenance expenditure and estimated LCC) adequate for planning purposes.

This study empirically shows the advantage of the condition-dependent policy by using the MUSTEM model with Ugandan national road pavement data. As far as is known, no other study investigates the effectiveness of the condition-dependent policy empirically for Ugandan national roads. In addition, this study explicitly considers the acceleration of deterioration due to repeated maintenance following Han et al. (2017).

The rest of this Chapter is organised as follows: the subsequent section discusses the management practice in Uganda and provides the study objectives, followed by the proposed condition-dependent pavement management model and a description of its empirical application. Lastly, the conclusions are presented.

3.3 Deterioration Mechanism of Pavements

3.3.1 Pavement structure and loading

Pavements may be classified into two main groups; i.e., flexible and rigid pavements. Flexible pavements are the most common pavement type because of their lower cost owing to the fact that they require low cost material for the base, subbase and subgrade layers; and a thin surface course. The surface layer is made of Hot-Mix Asphalt (HMA), the base and subbase may contain stabilized (with cement or lime) or unstabilized aggregates, the subgrade is typically a local material. Flexible pavements differ from rigid pavements in their load transfer. When a traffic load is applied at the surface, the load is distributed as shown in Figure 3.1. The load is distributed over a small area at the surface but as depth increases, the same load is distributed over a wider area. Therefore, high quality materials need to be used at the surface due to the high stress and lower quality materials may be used at greater depths. When the load is removed, the localised deformation rebounds (hence the name "Flexible"); however, an infinitesimal amount of deformation could stay and accumulate over time (Mamlouk 2006).

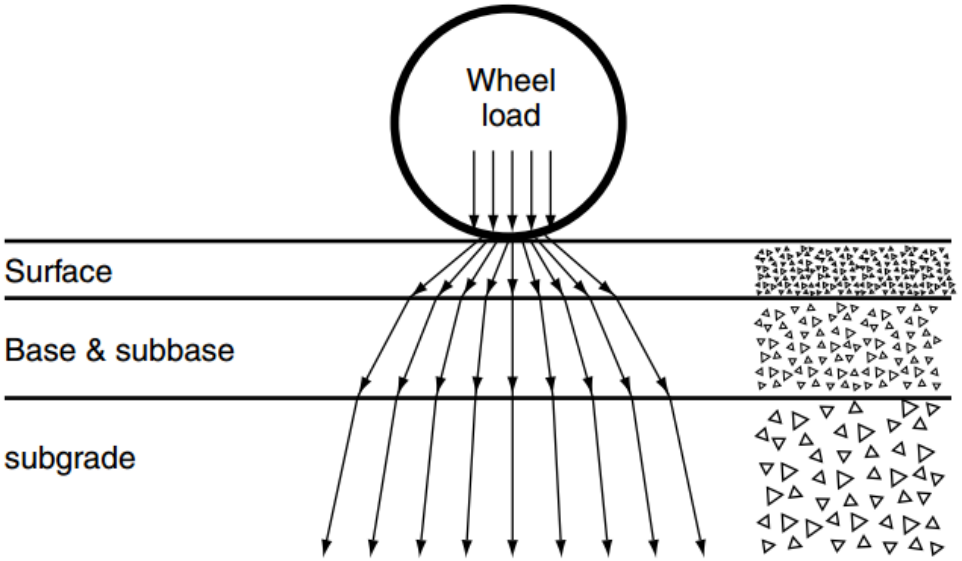

Figure 3.1. Load distribution in flexible pavement (Mamlouk 2006).

3.3.2 Pavement deterioration

Flexible pavements have unique properties including repeated and variable loading cycles, change in material properties with environment and fast deterioration, unlike other structures that are safe for an extended period of time if the maximum possible design load is not exceeded. Typically, flexible pavement life may average about 10 to 15 years before reaching a failed state (Mamlouk 2006). Common pavement distresses include fatigue cracking, rutting, roughness, thermal cracking, shoving, bleeding, raveling, polished aggregates, and reflection cracking. Pavement failure occurs when one or more of the distresses reach an unacceptable level (Figure 3.2). The deterioration process of pavement can be discretized into condition states in order to model the deterioration trends using stochastic Markov hazard models (Tsuda et al. 2006).

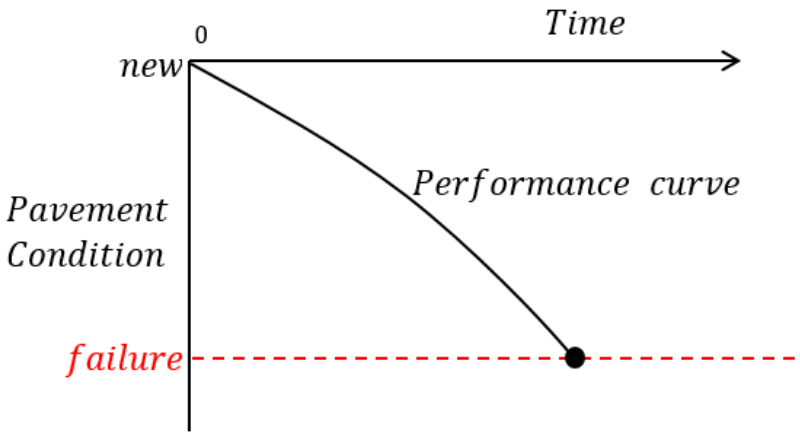

Figure 3.2. Deterioration of pavement condition over time.

3.4 Management practice in Uganda

3.4.1 Road management in Uganda

In Uganda, 96.5 % of freight traffic and 95.0 % of passengers travel by road. In 2017, the road network in Uganda consisted of 20,544 km of national roads (4,551 km paved and 15,993 km unpaved), 124,241 km of district, urban and community access roads of which 5,389 km were paved (JICA 2015, MoWT 2011 – 2017).

Different agencies are charged with the duty of managing roads in Uganda. The Uganda National Roads Authority (UNRA) manages national roads while local governments, under the Ministry of Works and Transport (MoWT), manage district roads. As discussed earlier, Uganda adopted the time-dependent management policy for pavements and, in a number of cases, planning is based on

human judgement. This time-dependent policy does not involve regular inspections and maintenance actions are performed after specified intervals. Intervention actions are also done after complaints from road users about bad road condition.

Road management finance in Uganda is provided by the Government of Uganda and partners through the Uganda Road Fund which dispatches funds based on needs of each road management agency, with consideration given to national plans. The funds cater for monitoring, administrative, and actual maintenance costs (MoWT 2011 – 2017). As a measure to improve maintenance planning, MoWT categorises areas by priority for maintenance (e.g. close proximity to schools or hospitals and in disaster zones) as shown in Figure 3.3. The road rehabilitation prioritisation grid gives priority to pavements with a critical state (worst first), neglecting those with fast deterioration. The grid is based on the following factors, with the percentage in brackets showing contribution to priority (MoWT 2015):

1) Land cover (30%) – urban areas, agricultural, natural terrestrial vegetation and bare lands.
2) Population distribution (30%).
3) Public facilities (30%) – health facilities (1/2) and schools (1/2).
4) Hazards (10%) – floods (7/10) and landslides (3/10).

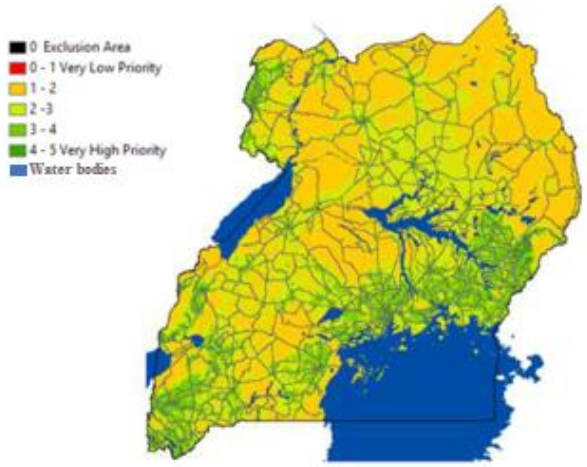

Figure 3.3. Road rehabilitation prioritisation grid for Uganda (MoWT 2015).

3.4.2 Study objectives

This study builds on earlier studies to develop a PMS suitable for developing countries. The objectives of this study are;

1) Complement the current network management practice in developing countries such as Uganda by introducing a PMS with less data requirement but rich output.
2) Customise earlier PMS models based on the needs of developing countries by adding an extension to the study of Kobayashi et al. (2013) to include the aspect of change in deterioration rate due to maintenance history and generalising pavement interventions (Figure 3.4).
3) Test the applicability of the model in Uganda by comparing the current time-dependent policy to the proposed condition-dependent policy and investigate the effect of preventive maintenance on network condition.

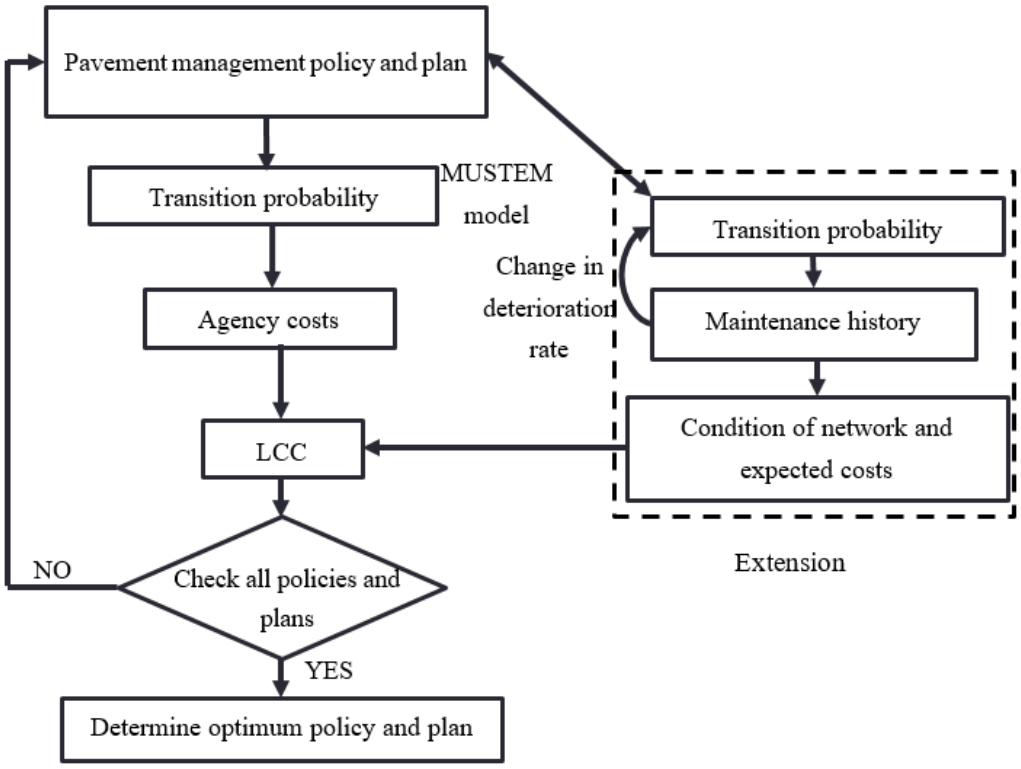

Figure 3.4. Extension to earlier PMS model.

3.5 Pavement management model

3.5.1 Model framework

Road agencies are responsible for management of roads. Specifically, road agencies formulate management plans, sets standards and budgets, carry out inspections, maintain databases, and perform maintenance works periodically. Inspection and repair works are done per pavement section defined by the road agency according to, for instance, length and type. In this model,

pavement condition is considered to be graded into condition states according to a discrete scale after inspection. Pavement condition is represented by discrete condition states $i(i = 1, \dots, J)$ with condition J as the absorbing (final) state. For user safety and comfort, a serviceability limit, $\underline{i}$, at which road pavements reach the minimum standard is set by the road agency. It is the goal of the agency to determine an optimum maintenance strategy from a set ($\boldsymbol{m_p}$) by defining inspection intervals (r), maintenance actions ($\boldsymbol{A}$), and minimum service levels ($\underline{i}$) in a given discrete service time t. A finite planning period (from $t = 0$ to $t = T$) is considered. The optimum strategy is one that minimises LCC with the highest standard and, maintains more roads in better and fewer in worse condition. The LCC is considered to contain agency costs (inspection and maintenance). Although pavement maintenance works generate social costs such as user and environmental costs, these are not considered in this study. User safety and comfort is considered by setting an appropriate serviceability limit.

With at least two time-series data sets (e.g. at $t = 0$ and $t = r$) shown in Figure 3.5, it is possible to predict the future deteriorated condition of pavement infrastructure despite the uncertainty of transition of condition states. A continuous distribution of life expectancy, the time a pavement remains in a specific condition state, can be defined. Uncertainty in predicting future pavement condition, with a life cycle characterised by deterioration and repair, increases as shown by the shaded probability area below the distribution in Figure 3.5. With more accurate data and better analysis methods, it is possible to reduce uncertainty levels. It is considered that within a pavement's service time (from $t = 0$ to $t = T$), n number of discrete inspection surveys are carried out. Maintenance actions, denoted by $\boldsymbol{A}(A_0, A_1, A_2, \dots, A_{i-1})$, are performed on pavements in correspondence to observed condition i after inspection. Maintenance is done based on the time-dependent or condition-dependent rule. At time T, reconstruction (A_{J-1}) is carried out for all sections. An example of correspondence between observed condition and action is shown in Table 3.1. In some cases, preventive maintenance actions can be performed on pavements even before they reach $\underline{i}$, ($\underline{i} = 2, \dots, J-1$). Expected expenditure that is necessary for planning purposes can be estimated from the maintenance plans.

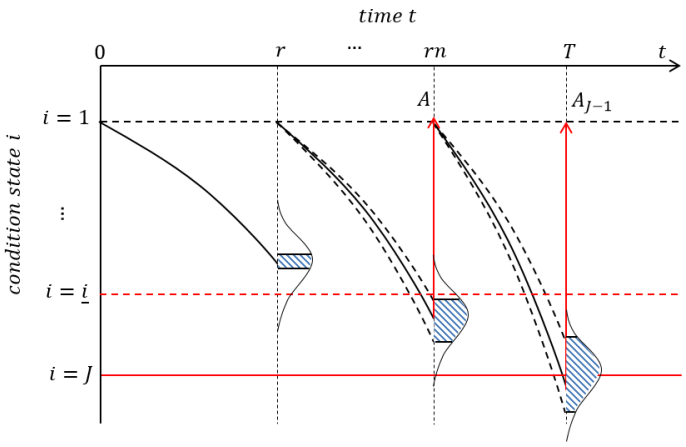

Figure 3.5. Uncertain deterioration considering repair.

It is necessary to estimate pavement condition i before action A can be specified. Deterioration rate can be estimated using Markov hazard models. In the estimation of deterioration rate, the mixed MUSTEM model (Tsuda et al. 2006, Kaito et al. 2015) was adopted.

3.5.2 Maintenance strategy

A pavement structure will deteriorate over time t due to usage (traffic loads) and environmental agents (e.g. temperature and moisture). Considering the discrete time axis ($t = 0,1,2, \dots$) and that pavements are regularly inspected after specified discrete intervals r ($r = 1,2,3, \dots$), n number of road inspections are carried out as defined by the discrete time axis as $t = rn$ ($n = 0,1,2, \dots$). At a given inspection time rn, road inspectors observe pavement condition $h(rn) = i (i = 1, \dots, J)$. Actions $\boldsymbol{A}(A_0, A_1, A_2, \dots, A_{J-1})$ are performed on pavements in correspondence to observed condition i after inspection. Once action is taken, pavement condition i is assumed to improve to a better condition $\hat{\imath}$. This improvement in pavement condition can be expressed using i_{rep}, the better condition of a pavement section following repair:

$$i_{rep} = \begin{cases} i & if \quad A_0 \ (No\ action) \\ \hat{\imath} & otherwise \quad (A_1, A_2, \dots, A_{J-1}) \end{cases} \qquad (3.1)$$
$$(i = 1, \dots, J)$$

Inspected pavement sections can be grouped based on such factors as traffic loading and environment. Consider that in each $k (k = 1, \dots, K)$ pavement group, there are $s^k (s^k = 1, \dots, S^k)$

road sections in total. The road agency sets maintenance strategy $\boldsymbol{m_p^{s^k}}$ per pavement section; $\boldsymbol{m_p^{s^k}}$ is a set of strategies $\boldsymbol{m_p^{s^k}}(\boldsymbol{m_{A\leftrightarrow i}^{s^k}}, \boldsymbol{r^{s^k}})$, $\boldsymbol{r^{s^k}} = (r_1^{s^k}, \dots, r_T^{s^k})$ is a row vector of inspection intervals, and $\boldsymbol{m_{A\leftrightarrow i}^{s^k}} = (A_0^{s^k} \leftrightarrow 1, \dots, A_{i-1}^{s^k} \leftrightarrow i)$ is a set of actions performed on each section depending on observed condition i. Precise processes on setting strategies and actions are outside the scope of this study. Table 3.1 shows an example of actions set by the road agency, their associated costs and attained condition after repair. The repair actions are set, considering a trade-off between cost and repair frequency. It was assumed that patching improved condition by one step while overlay improved condition by two steps. Reconstruction (A_{J-1}) is only done at the end of pavement service life. The inspection and repair cost C_{i-1} is an increasing monotone function with action A and satisfies constraints in ($C_{A_0} = 0$):

$$C_{A_0} \leq C_{A_1} \leq C_{A_2} \leq \cdots \leq C_{A_{J-1}} \tag{3.2}$$

Table 3.1**.** Action taken for roads based on observed condition.

Condition state, i	Costs	Repair actions	Condition after repair, $\hat{\imath}$
1	C_{A_0}	A_0	1
2	C_{A_0}	A_0	2
	C_{A_1}	A_1 e.g. patching	1
	C_{A_2}	A_2 e. g. overlay	1
3	C_{A_0}	A_0	3
	C_{A_1}	A_1	2
	C_{A_2}	A_2	1
…	…	…	…
J	C_{A_0}	A_0	J
	C_{A_1}	A_1	$J-1$
	C_{A_2}	A_2	$J-2$
	…	…	…
	$C_{A_{J-1}}$	A_{J-1}	1

3.5.3 Estimation of Markov Transition Probability (MTP)

The MTP, given a condition state $h(rn) = i$ observed at discrete time rn, defines the probability that the condition state at a future time will change to $h(rn + r) = j$.

$$Prob[h(rn+r)=j|h(rn)=i]=\pi_{ij} \tag{3.3}$$

The MTP from condition i to j given that there was no repair can be expressed as (Tsuda et al. 2006):

$$\pi_{ij}=\sum_{\tilde{k}=i}^{j}\prod_{\tilde{m}=i}^{\tilde{k}-1}\frac{\theta_{\tilde{m}}}{\theta_{\tilde{m}}-\theta_{\tilde{k}}}\prod_{\tilde{m}=\tilde{k}}^{j-1}\frac{\theta_{\tilde{m}}}{\theta_{\tilde{m}+1}-\theta_{\tilde{k}}}exp(-\theta_{\tilde{k}}r) \tag{3.4}$$

$$i\le\tilde{k}\le\tilde{m}\le j$$

where θ_i is the hazard rate and, $\tilde{k}$ and $\tilde{m}$ are indices.

For a set of condition states $(i=1,\dots,J)$, the matrix of MTP can be defined by using transition probabilities between each pair of condition states (i,j):

$$\boldsymbol{p}=\begin{bmatrix}\pi_{11} & \cdots & \pi_{1J}\\ \vdots & \ddots & \vdots\\ 0 & \cdots & \pi_{JJ}\end{bmatrix} \tag{3.5}$$

As properties of MTP and nature of pavement deterioration considering no repair, all of conditions below must be satisfied:

$$\left.\begin{aligned}&\pi_{ij}\ge 0\\ &\pi_{ij}=0\ (when\ i>j)\\ &\sum_{j=1}^{J}\pi_{ij}=1\end{aligned}\right\} \tag{3.6}$$

The Markov prediction model is a stochastic process that follows three restrictions (Ortiz-García et al. 2006, Pérez-Acebo et al. 2018) as follow:

(1) The process should be discrete in time.

(2) The process should have a finite state space.

(3) The process should verify Markov property (Isaacson and Madsen 1976). This property states that any future state of the process depends on its present state and not on the past states (Hillier and Lieberman 1990). Pavement deterioration has been proven to follow

Markov property (Kerali and Snaith 1992).

Therefore, MTP does not depend on earlier history, hence Markov processes are memoryless. The transition probability from time rn to $rn + r$ depends only on the condition state $h(rn)$. In the prediction of future pavement condition, it is possible to estimate the probability distribution of pavement condition. The deterioration process at time $rn + r$ can be expressed by MTP:

$$\boldsymbol{p}(r) = \boldsymbol{p}^r \tag{3.7}$$

The hazard rate for each group k and condition i can be expressed in exponential form:

$$\theta_i^k = exp(\boldsymbol{x}^k \boldsymbol{\beta}_i') \quad (i = 1, \dots, J-1) \tag{3.8}$$

where $\boldsymbol{\beta}_i = (\boldsymbol{\beta}_{i,1}, \dots, \boldsymbol{\beta}_{i,M})$ is a row vector of unknown parameters with symbol [′] showing that it is transposed and $\boldsymbol{x}^k$ is a row vector of explanatory variables.

The log-likelihood function can be expressed as:

$$ln[\boldsymbol{L}(\boldsymbol{\beta})] = ln\left[\prod_{i=1}^{J-1}\prod_{j=i}^{J}\prod_{k=1}^{K}\left\{\pi_{ij}(\bar{r}^k, \bar{\boldsymbol{x}}^k : \boldsymbol{\beta})\right\}^{\delta_{ij}^k}\right] = \sum_{i=1}^{J-1}\sum_{j=i}^{J}\sum_{k=1}^{K}\delta_{ij}^k ln[\pi_{ij}(\bar{r}^k, \bar{\boldsymbol{x}}^k : \boldsymbol{\beta})] \tag{3.9}$$

$$\delta_{ij}^k = \begin{cases} 1 & when\ h(rn)^k = i\ and\ h(rn+r)^k = j \\ 0 & otherwise \end{cases}$$

where δ_{ij}^k is a dummy variable and the symbol [¯] signifies a measured quantity.

The unknown parameters $\boldsymbol{\beta}_i$ can be obtained by maximising the log-likelihood function in (3.9) using Newton's method (Tsuda et al. 2006) or by using Bayesian methods such as Markov Chain

Monte Carlo (MCMC) using the Metropolis-Hastings (MH) algorithm (Hastings 1970, Gilks et al. 1995, Kobayashi et al. 2010, 2011, 2012, Han et al. 2016). MCMC samples $\boldsymbol{\beta}_i$ values from a probability distribution until equilibrium where the Markov chain converges. The MH algorithm is used to randomly sample $\boldsymbol{\beta}_i$ values from the probability distribution.

The life expectancy (RMD_i^k) for a given pavement group k is then given by (Lancaster 1990):

$$RMD_i^k = \frac{1}{\theta_i^k} \tag{3.10}$$

The average life expectancy $ET_j^k (j = 2, \dots, J)$ is obtained by summing up life expectancies from condition state $i = 1$ at the start of the pavement life cycle:

$$ET_j^k = \sum_{i=1}^{j} \frac{1}{\theta_i^k} \tag{3.11}$$

In reality it is difficult to have a homogeneous infrastructure group; consequently, models that incorporate mixing mechanisms are ideal. The aspect of heterogeneity is introduced to pavement groups. The heterogeneity factor of an individual group is denoted ε^k. If $\varepsilon^k > 1$, this pavement group undergoes faster deterioration; if $\varepsilon^k < 1$, the pavement group has longer life than the benchmark. The hazard rate can be expressed in mixture form (Kaito et al. 2015) as follows;

$$\theta_i^k = \varepsilon^k \, \tilde{\theta}_i^k \tag{3.12}$$
$$(i = 1, \dots, J-1; k = 1, \dots, K)$$

where $\tilde{\theta}_i^k$ is the average hazard rate for group k and condition i.

3.5.4 Mixture Markov Hazard Model

In reality it is difficult to have a homogeneous infrastructure group. Due to this, models that incorporate mixing mechanisms are ideal. The aspect of heterogeneity is introduced to pavement groups. The heterogeneity factor of an individual group is denoted as ε^k. If $\varepsilon^k > 1$, this pavement group undergoes faster deterioration, if $\varepsilon^k < 1$, the pavement group has longer life. The hazard rate can be expressed in mixture form as;

$$\lambda_i^{s_k} = \tilde{\lambda}_i^{s_k} \varepsilon^k \tag{3.13}$$
$$(i = 1, \dots, J-1; k = 1, \dots, K; s_k = 1, \dots, S_k)$$

where $\tilde{\lambda}_i^{s_k}$ is the average hazard rate for group k and condition i

The Markov transition probability can then be expressed as;

$$\pi_{ij}^k(z^k : \bar{\varepsilon}^k) = \sum_{l=i}^{j} \prod_{m=i,\neq l}^{j-1} \frac{\tilde{\lambda}_m^k}{\tilde{\lambda}_m^k - \tilde{\lambda}_l^k} exp\left(-\tilde{\lambda}_l \bar{\varepsilon}^k z^k\right) \tag{3.14}$$
$$= \sum_{l=i}^{j} \psi_{ij}^l \left(\tilde{\boldsymbol{\lambda}}^k\right) exp\left(-\tilde{\lambda}_l \bar{\varepsilon}^k z^k\right)$$
$$(i = 1, \dots, I-1; j = i+1, \dots, I; k = 1, \dots, K),$$

where

$$\psi_{ij}^l\left(\tilde{\boldsymbol{\lambda}}^k\right) = \prod_{m=i,\neq l}^{j-1} \frac{\tilde{\lambda}_m^k}{\tilde{\lambda}_m^k - \tilde{\lambda}_l^k}$$

3.5.5 Markov Chain Monte Carlo (MCMC) Methods

MCMC methods have been widely covered in earlier literature. Here we give a snapshot of this estimation method using the Metropolis-Hastings Algorithm. Let X denote observed data (variables) and β denote unknown parameters. The joint distribution;

$$p(X, \beta) = \quad p(X|\beta)p(\beta) \tag{3.15}$$

Where $p(\beta)$ is the prior distribution and $p(X|\beta)$ is the likelihood

By Bayes theorem, the posterior distribution of β conditional on observed data X is;

$$p(\beta|X) = \frac{p(\beta)p(X|\beta)}{\int p(\beta)p(X|\beta)d\beta} \tag{3.16}$$

Suppose $E[f(\beta)]$ is the expectation of given quantity of β given observed data. MCMC estimates $E[f(\beta)]$ by drawing samples β_t $(t = 1, \dots, n)$ from the posterior distribution. The expectation is approximated by;

$$E[f(\beta)] = \frac{1}{n}\sum_{t=1}^{n} f(\beta_t) \tag{3.17}$$

For a Markov chain, the next state β_{t+1} depends only on the current state β_t, not on the history of the chain $(\beta_0, \beta_1, \dots, \beta_{t-1})$, i.e., is memoryless. In some cases, especially where the Markov chain takes long to converge, burn-in (discarded samples) are considered to eliminate the error due to the initial estimate of β. Consider that b burn-in samples are eliminated; the ergodic average will be;

$$f^e = \frac{1}{n-b}\sum_{t=b+1}^{n} f(\beta_t) \tag{3.18}$$

3.5.6 Metropolis-Hastings Algorithm

The Metropolis-Hastings (MH) algorithm is a tool for accepting or rejecting a move to the next state. For each time point t, the next state β_{t+1} is chosen by sampling a candidate point ρ from a proposal distribution $q(.|\beta_t)$. The candidate point is accepted with probability $\alpha(\beta_t, \rho)$ where;

$$\alpha(\beta, \rho) = \min\left(1, \quad \frac{P.D(\rho)q(\beta|\rho)}{P.D(\beta)q(\rho|\beta)}\right) \tag{3.19}$$

Where $P.D$ stands for posterior distribution

If the proposed candidate point is accepted, the next state becomes $\beta_{t+1} = \rho$ and if rejected the

chain does not move ($\beta_{t+1} = \beta_t$).

3.5.7 Change in deterioration rate

When maintenance actions $\boldsymbol{A}(A_0, A_1, A_2, \dots, A_{J-1})$ are carried out, an inventory of the number of past maintenance works, $\boldsymbol{a^{t,s^k}}(a_0^t, a_1^t, a_2^t \dots, a_{J-1}^t)$ for each pavement section $s^k(s^k = 1, \dots, S^k)$ in each pavement group $k(k = 1, \dots, K)$ is recorded. As discussed by Han et al. (2017), past maintenance works may increase pavement deterioration. The increase could be due to the difference in exposure to deterioration agents such as moisture (e.g. through patching joints) for a maintained pavement section compared to a new one. Consider that pavement sections $s^k = 1$ and $s^k = 2$ have maintenance history $\boldsymbol{a^{t,1}}$ and $\boldsymbol{a^{t,2}}$ respectively with the number of works $\boldsymbol{a^{t,2}}$ significantly greater than $\boldsymbol{a^{t,1}}$ at time t. It can be expected that pavement section two would deteriorate faster than one as discussed above (Figure 3.6). If both pavement sections are inspected and are observed to have reached or exceeded the service limit $\underline{i}$, different corrective actions A should be taken despite the fact that they could be in the same deteriorated state. Pavement section two, with faster deterioration should be maintained with stronger and thicker materials and superior designs compared to one with slower deterioration.

To account for an increased deterioration rate, it is considered that pavement service life is shortened due to past maintenance works $\boldsymbol{a^{t,s^k}}$. The remaining duration $RMD_i^{s^k}$ reduces by a factor φ_A and hazard rate $\theta_i^{s^k}$ increases. The MTP $\pi_{ij}(\theta_i^{s^k})$ is transformed, which in turn affects estimated LCC.

$$RMD_i^{s^k(rn+r)} = (1 - \varphi_{A_0})^{a_0^{rn+r}} * \dots * (1 - \varphi_{A_{J-1}})^{a_{J-1}^{rn+r}} * RMD_i^{s^k(rn)} \qquad (3.20)$$

$$\boldsymbol{a^{(rn+r),s^k}}(a_0^{rn+r}, a_1^{rn+r}, a_2^{rn+r} \dots, a_{J-1}^{rn+r}), (i = 1, \dots, J-1)$$

Once reconstruction is done for a pavement section in the absorbing state J, it is considered to recover to the original state without any accelerated deterioration ($\boldsymbol{a^{t,s^k}} = \boldsymbol{0}$). Faster pavement deterioration to J attracts a renewal cost $C_{J-1} \approx \infty$, which is prohibitive and so it is desirable to prevent pavement deterioration to J between $t = 0$ *and* $t = T$.

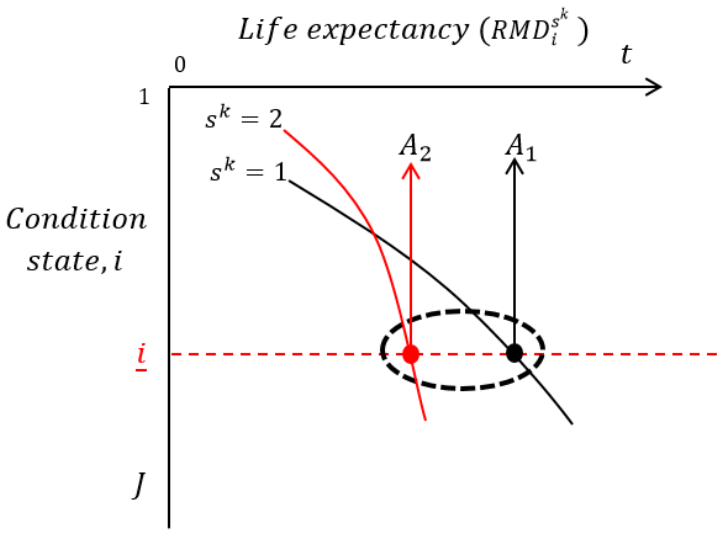

Figure 3.6. Increase in deterioration rate due to past repair works.

3.5.8 Transition probability considering repair

When a pavement undergoes repair, the transition probability will be modified because the pavement system has become newer. The MTP matrix will be multiplied with a repair matrix $\boldsymbol{p_{rep}}$. The elements of the $J \times J$ repair matrix are denoted as π_{ij}^{rep} $(i = 1, \dots J), (j = 1, \dots, J)$. Once no repair (A_0) is done to a pavement, we expect the pavement to undergo deterioration and so the MTP matrix will remain unchanged. In this case, the repair matrix will be an identity matrix $\boldsymbol{p_{rep}} = \boldsymbol{I}$. This is the default state of the repair matrix with all values in the major diagonal being 1 and all other matrix elements being 0.

$$\boldsymbol{p_{rep}} = \begin{bmatrix} 1 & 0 & 0 & 0 & 0 \\ 0 & 1 & 0 & 0 & 0 \\ 0 & 0 & \ddots & 0 & 0 \\ 0 & 0 & 0 & 1 & 0 \\ 0 & 0 & 0 & 0 & 1 \end{bmatrix} \tag{3.21}$$

For all repair matrices, the values of π_{ij}^{rep} above the major diagonal must be 0 because it is not expected that any repair action will worsen pavement condition. The values on the major diagonal or below it can take the value of either 1 or 0. The condition $\sum_{j=1}^{J} \pi_{ij}^{rep} = 1$ must be met within $\boldsymbol{p_{rep}}$. The repair probability π_{ij}^{rep} is defined by:

$$\pi_{ij}^{rep} = \begin{cases} 1 & if \ \ i_{rep} = \hat{\imath} \\ 0 & otherwise \end{cases} \quad (i = 1, \dots, J) \tag{3.22}$$

The transitional probability matrix $\boldsymbol{p_{trans}}$ is a matrix with elements $\pi_{ij}^{trans}(i = 1, \dots J), (j = 1, \dots, J)$: $\boldsymbol{p_{trans}}$ is obtained according to:

$$\boldsymbol{p_{trans}} = \boldsymbol{p}(r) * \boldsymbol{p_{rep}} \tag{3.23}$$

3.5.9 Maintenance optimisation

3.5.9.1 Agency costs (inspection and repair)

In the optimisation model, the maintenance strategy $\boldsymbol{m_p^{s^k}}$ is set by road managers. A finite horizon $(t = T)$ is considered and so there is need to estimate pavement salvage value (Tsunokawa and Schofer 1994, Li and Madanat 2002). The inspection and repair costs of each pavement section can be expressed using a value function:

$$V_i^{t,s^k}\left(\boldsymbol{a^{t,s^k}}\right) = C_i^{t,s^k} + ex\,p\left(-\rho^r(t+r)\right)\sum_{j=1}^{J}\left\{\left(\pi_{ij}^{trans} * E\left(V_j^{t,s^k}\left(\boldsymbol{a^{t,s^k}}\right)\right)\right\} \tag{3.24}$$

$$i(i = 1, \dots, J)\ (\ t = 0, \dots, T)$$

$$E\left(V_j^{t,s^k}\left(a^{t,s^k}\right)\right) = \sum_{A=1}^{N_A}\left(p_A^t * V_j^{(t+r),s^k}\left(a^{(t+r),s^k}\right)\right)$$

$$C_i^{t,s^k} = \delta_1 c^{t,s^k} + C_{A\leftrightarrow i}^{t,s^k}$$

$$(j = 1, \dots, J)$$

$$\delta_1 = \begin{cases} 1 & if\ t = rn\ (n = 0,1,2, \dots) \\ 0 & otherwise \end{cases}$$

where

$V_i^{t,s^k}\left(\boldsymbol{a^{t,s^k}}\right)$ are agency costs at time t for section s^k with past repair works $\boldsymbol{a^{t,s^k}}$

$C_{A\leftrightarrow i}^{t,s^k}$ is repair cost at time t and condition i for section s^k

c^{t,s^k} is cost of inspecting a pavement section

δ_1 is a dummy variable

ρ^r is the discount rate

π_{ij}^{trans} is transitional probability

$E\left(V_j^{t,s^k}\left(\boldsymbol{a}^{t,s^k}\right)\right)$ is the expectation of inspection and repair costs for section s^k

T is the duration between reconstruction times

p_A^t is the probability of taking action A at time t

N_A is the total number of possible repair actions A

3.5.9.2 Optimisation problem

For each strategy, $\boldsymbol{m_p^{s^k}}$ the LCC can be obtained by summing up all agency costs for all pavement sections $s^k(s^k = 1, \dots, S^k)$ within pavement reconstruction time T. Due to a finite time horizon, the pavement section will have a salvage value $C_v^{s^k}$. It is assumed that $C_v^{s^k} = 0$ at T.

$$LCC = \sum_{s^k=1}^{S^k} (V_i^0)^{s^k} \tag{3.25}$$

The optimisation problem can then be expressed by:

$$\begin{gathered} min\ LCC \\ \boldsymbol{m_{A\leftrightarrow i}^{s^k}, r^{s^k}} \\ subject\ to \\ \sum_{k=1}^{K} \sum_{s^k=1}^{S^k} C_i^{t,s^k} \in \Omega \end{gathered} \tag{3.26}$$

where Ω is the budget limit

To obtain LCC, unknowns $V_i^{t,s^k}\left(\boldsymbol{a}^{t,s^k}\right)$ need to be solved first; $V_i^{t,s^k}\left(\boldsymbol{a}^{t,s^k}\right)$ forms a dynamic programming problem that can be solved by backwards induction starting at time T (Sundaram

1999). As shown in Figure 3.7, for a given section s^k at time rn, set $V_i^T = 0 \ \forall i$ we obtain the following:

$$V_i^{rn} = C_i^{rn} \quad \forall i$$

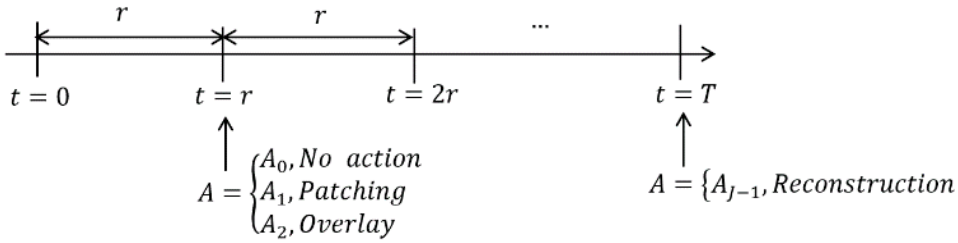

Figure 3.7**.** Pavement inspection and maintenance timeline.

Since we have a solution at time rn, we can obtain subsequent solutions of V_i^t by backwards induction from $t = r(n-1)$ to $t = 0$, which is of interest. These are compounded and at $t = 0$ we obtain the following:

$$V_i^0 = C_i^0 + exp(-\rho^r r)\left[\sum_{j=1}^{J}\left(\pi_{ij}^{trans} * \left(\sum_{A=1}^{N_A} p_A^0\right) * V_j^r\right)\right] \quad \forall i \tag{3.27}$$

$$\sum_{A=1}^{N_A} p_A^0 = 1$$

An algorithm showing the solution procedure is shown in Figure 3.8. The steps to the solution are detailed below:

1) Define strategy $\boldsymbol{m_p^{s^k}}$.
2) Calculate $(V_i^0)^{s^k}$ by backwards induction.
3) Calculate LCC.
4) Check that all strategies $\boldsymbol{m_p^{s^k}}$ have been evaluated and constraints satisfied.
5) Determine optimal strategy $\boldsymbol{m_p^{s^k*}}(\boldsymbol{m_{A\leftrightarrow i}^{s^k*}}, \boldsymbol{r^{s^k*}})$.

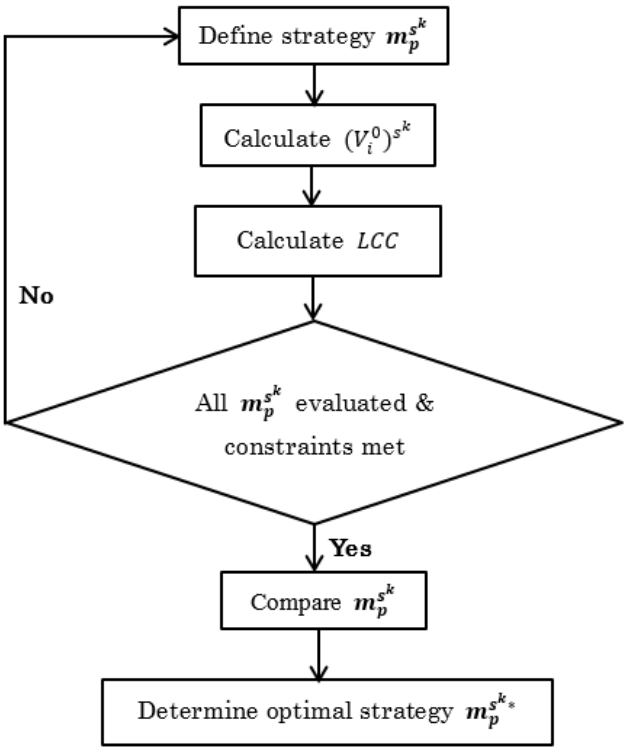

Figure 3.8. Solution to optimisation problem.

In reality, the maintenance works can only be done within the allocated budget each financial year. If the repair cost exceeds budget limits, works could be deferred for low priority sections or less costly preventive actions performed. The decision on selection of sections for repair is complex and involves a balancing of pavement condition, economic, political and other considerations associated with the road section. In this study we simplify this complex problem to a knapsack problem with sections selected using a greedy algorithm (GA) (Rinnooy Kan et al. 1993). The budget limit is represented by the knapsack and the sections to be maintained are selected based on fastest deterioration rate first (condition-dependent policy) or worst condition first (time-dependent policy) at any intervention time. The GA may generate solutions approximate to optimal solutions.

3.5.10 Estimated condition of network

To further aid the decision process on selection of optimum maintenance strategy, it is important to add a third parameter, condition of network, which is derived from set service level $\underline{i}$ and selected maintenance strategy based on repair in correspondence to observed condition after

inspection ($A_{i-1}^{s^k} \leftrightarrow i$). The length of network in each condition state (CS) at discrete time $rn + r$ is determined as follows:

$$\boldsymbol{CS}_{rn+r} = \boldsymbol{p}(r) * \boldsymbol{CS}_{rn} \quad (n = 0,1,2,3, \dots) \tag{3.28}$$

where $\boldsymbol{CS}_{rn}$ is a $1 \times J$ matrix of number of road sections per condition state and $\boldsymbol{p}(r)$ is a $J \times J$ MTP matrix at time rn.

Knowing the percentage of network in each condition state at a specified descrete time will aid decisions on selecting the optimum maintenance strategy especially in the case where the $\boldsymbol{m}_{\boldsymbol{p}}^{\boldsymbol{s^k}}$ pool is small.

3.6 Empirical study

3.6.1 Uganda national roads network

The Uganda national roads database consists of paved and unpaved roads, road structural type, daily traffic volume, average speed, and pavement condition for 1-km sections for survey years 2009 – 2019 (UNRA 2019). Data for 41 paved national roads collected in November and December of 2017 and 2018 (two-point data), which was complete, was selected. This data consisted of 2,425 sections that were additionally sorted to eliminate sections that erroneously showed improvement in condition despite there being no repair, leaving a total of 1,993 sections. Out of the 1,993 sections, 24 sections for road A001 were rigid pavements and the rest were flexible. Roads were categorised by condition (Table 3.2). Road condition measured in form of International Roughness Index (IRI) using a test vehicle by UNRA was categorised into condition states (Table 3.3). The IRI estimates the roughness of a road obtained by measuring longitudinal road profiles. Pavement condition in the Uganda national roads database was also measured using another index, the Visual Condition Index (VCI). There was no major difference in estimation results (shown later on) considering VCI or IRI data. Surveyed Ugandan pavements deteriorated between 2017 and 2018, with deterioration being attributed to agents such as traffic loading and environmental conditions (e.g. moisture and temperature). As pavement condition worsened, average speed reduced, therefore speed may be an indicator of pavement condition (Table 3.2). The increase in speed on

pavements in condition 2 could be due to other factors such as road geometry and driver behaviour. To estimate deterioration rate, pavement sections were grouped based on traffic on specific roads (Table 3.5). The road group names were listed in Table 3.11 in the Appendix. Pavements may also be grouped based on administrative area, environmental zone etc. Grouping based on traffic, a major deterioration agent, was selected because it was the most practical for this study. It made intervention actions more specific and hence more effective.

Table 3.2. Road surface condition.

Road Surface Condition	Category	No. of sections		Average speed (km/h)		Description
		2017	2018	2017	2018	
	1 – Good	1,284	981	52.70	55.07	Good shape, smooth running surface
	2 – Fair	648	727	58.05	56.80	Reasonable shape, corrugations and potholes up to 10 cm deep
	3 – Poor	59	224	49.69	50.15	Poor shape, frequent depressions, rutting and potholes >10 cm deep
	4 – Bad	2	61	18.50	27.84	Bad shape, deep depressions and potholes, serious rutting, dry weather only

Table 3.3. Categorisation of condition states for paved roads (MoWT, 2011–17).

Categorisation	1. Good	2. Fair	3. Poor	4. Bad
IRI (mm/m)	0 – 3.50	3.51 – 5.00	5.01 – 6.50	>6.50

3.6.2 Estimation of deterioration rate

Estimation of deterioration rate was done for pavement sections grouped based on road traffic. Equation (3.12) can specifically be written as:

$$\theta_i = exp\left(\beta_{0,i} + \beta_{1,i}x_1 + \beta_{2,i}x_2 + \beta_{3,i}x_3\right) \tag{3.29}$$

where x_1 is traffic loading in Equivalent Standard Axle Loads (ESALs), x_2 is average speed (km/h), and x_3 is a dummy variable based on road type (i.e., rigid and flexible pavements):

$$x_3 = \begin{cases} 1 & for\ CC \\ 0 & for\ AC, SD\ and\ PB \end{cases} \tag{3.30}$$

where AC is asphalt concrete, SD is surface dressed, PB is permeable base, and CC is cement concrete; CC pavements are rigid and the rest are flexible.

The vehicle traffic load was converted to ESALs (Table 3.12 and Table 3.13 in the Appendix) using the load equivalency factor for each vehicle type (MoWT 2010, FHWA 2014). Average speed was used as an explanatory variable despite the fact that speed may be affected by road geometry and driver behaviour. Other explanatory variables such as environmental factors (e.g. temperature and moisture) and, pavement structural strength (e.g. layer thickness) would have improved estimation results for hazard rate and life expectancy but these were not used due to the data limitation in the current Uganda national roads database.

Estimation was carried out using MCMC methods with the MH algorithm. The MATLAB programming language was used to solve for the unknown parameters. The MCMC methods were used because the formulated log-likelihood function was conditional on many unknown parameters and the merits of shorter computation time. The unknown β parameters converged as shown in Table 3.4. By the central limit theorem, as the number of samples increases, the sample mean will tend towards the population mean and the normal distribution curve will be more bell shaped. Burn-in values up to the 100th iteration were eliminated for a 1000 run because the initial estimate was off the convergence value. Some β values were excluded due to sign restrictions. The β values indicated that traffic loading had a significant impact on deterioration rate in condition state 2. Higher traffic loading leads to faster deterioration rates. Faster average speeds can be achieved on smoother pavements despite the fact that road geometry and driver behaviour significantly influence speed, and sections of stronger pavement type (rigid) have longer life hence the negative β values for both explanatory variables. *Geweke* diagnostic values for all β values should fall within the [1.96, –1.96] limits to test chain convergence. A *Geweke* value of 0 means perfect convergence. Table 3.5 and Figure 3.9 show estimated life expectancy for surveyed Ugandan national roads. Generally, the surveyed roads exhibit shorter life spans than their expected design life of about 20 years (MoWT 2010). The short life is probably due to heavier traffic loading and lower strength construction materials. For instance, despite both roads A001 and A003 having high average daily traffic (17.44 and 16.93 thousand ESALs in 2018 respectively), road A001 has longer life expectancy because it is constructed with stronger materials (A001 has 24 CC sections).

Table 3.4. Estimated β values.

Condition state, i	Absolute	Traffic loading	Average speed	Pavement type
	β_0	β_1	β_2	β_3
1	– 0.6399 (– 0.0040)	-	– 1.2325 (0.1322)	– 0.1583 (– 0.0415)
2	– 0.1094 (– 0.0367)	0.3020 (– 0.0700)	– 2.0156 (0.0806)	– 1.3499 (– 0.0261)
3	0.3948 (– 0.0806)	-	– 2.8973 (0.0181)	– 1.3938 (0.0751)

**Values in parentheses are the Geweke diagnostic for β.*

Table 3.5. Life expectancy for surveyed Ugandan national roads.

k	Road section group	Actual road length (km)	No. of surveyed sections	Average daily traffic (thousand ESALs)		$*\varepsilon^k$	Life expectancy (years) Condition state			
				2017	2018		1	2	3	Total
0	BM**	3,377.74	1,993	3.95	3.64	1.00	3.78	3.24	3.67	10.69
1	A001	224.52	87	19.13	17.44	1.03	3.20	3.02	4.41	10.64
2	A002	421.32	355	8.50	6.18	1.13	3.64	2.60	3.35	9.60
3	A003	47.29	11	28.33	16.93	1.98	3.09	1.07	2.20	6.36
4	A004	88.90	77	1.21	1.23	0.88	4.09	3.81	4.18	12.08
5	A005	418.38	94	2.09	2.48	0.84	4.22	3.91	4.53	12.66
6	A006	433.62	348	3.70	4.55	0.95	3.95	3.40	3.92	11.27
7	A007	342.99	93	3.88	3.88	0.93	4.01	3.42	4.02	11.45
8	A008	310.85	235	1.61	1.78	0.94	3.96	3.56	3.86	11.38
9	B100	33.50	23	4.77	5.24	1.55	2.98	2.05	2.04	7.07
10	B103	10.11	9	0.30	0.84	1.15	3.44	2.99	2.90	9.33
11	B150	174.00	77	0.63	0.74	0.85	4.19	4.01	4.37	12.57
12	B151	59.18	41	0.51	1.08	1.27	3.23	2.69	2.53	8.46
13	B152	123.54	49	0.51	0.96	0.96	3.84	3.55	3.73	11.13
14	B153	87.87	77	0.51	1.20	1.07	3.61	3.20	3.21	10.02
15	B200	43.26	41	0.43	0.43	0.85	4.20	4.04	4.37	12.61
16	B300	146.41	63	0.23	0.30	0.86	4.14	3.99	4.28	12.41
17	B303	8.00	8	0.46	0.42	2.08	2.49	1.73	1.29	5.51
18	B307	55.79	55	1.70	1.72	1.17	3.44	2.87	2.90	9.21
19	B308	16.91	17	2.81	2.81	1.04	3.69	3.12	3.44	10.25
20	C004	21.48	19	2.75	0.97	1.42	3.12	2.33	2.22	7.67
21	C157	3.37	3	0.97	0.97	2.32	2.36	1.55	1.12	5.03
22	C158	1.52	1	0.97	0.97	2.30	2.37	1.56	1.14	5.06
23	C170	2.05	2	0.97	0.97	1.63	2.86	2.13	1.80	6.80
24	C198	3.72	3	0.97	0.97	1.85	2.66	1.90	1.52	6.08
25	C199	1.48	1	0.97	0.97	2.46	2.28	1.47	1.04	4.79
26	C210	5.40	1	0.18	0.18	2.24	2.40	1.63	1.17	5.19
27	C232	1.33	1	0.11	0.11	2.34	2.34	1.57	1.10	5.01
28	C308	12.76	11	0.17	0.17	0.93	3.93	3.69	3.82	11.44
29	C309	6.70	7	0.17	0.17	1.35	3.16	2.58	2.29	8.03

30	C350	54.30	52	0.63	0.83	1.04	3.68	3.27	3.29	10.24
31	C354	2.72	2	0.33	0.33	1.16	3.46	2.98	2.85	9.28
32	C356	32.43	14	0.18	0.49	1.02	3.71	3.36	3.36	10.44
33	C410	34.54	17	0.61	0.83	1.08	3.56	3.16	3.23	9.95
34	C412	9.89	10	0.033	0.14	0.99	3.79	3.50	3.55	10.84
35	C420	2.90	2	0.069	0.069	2.18	2.43	1.67	1.20	5.30
36	C457	5.10	4	0.033	0.033	1.25	3.27	2.77	2.56	8.61
37	C511	11.73	9	0.068	0.068	1.12	3.46	3.07	3.02	9.55
38	C517	0.76	1	0.068	0.068	2.18	2.43	1.67	1.20	5.30
39	C540	103.61	63	0.25	0.25	1.07	3.61	3.22	3.21	10.03
40	C684	4.10	4	0.55	0.55	1.66	2.82	2.11	1.74	6.67
41	C744	9.41	6	0.69	0.69	1.01	3.75	3.36	3.44	10.55

*$*\varepsilon^k$ is the heterogeneity parameter, **Benchmark (BM) is the total of all sections in the network.*

Note: The hazard rate is obtained as shown in Equation (3.10).

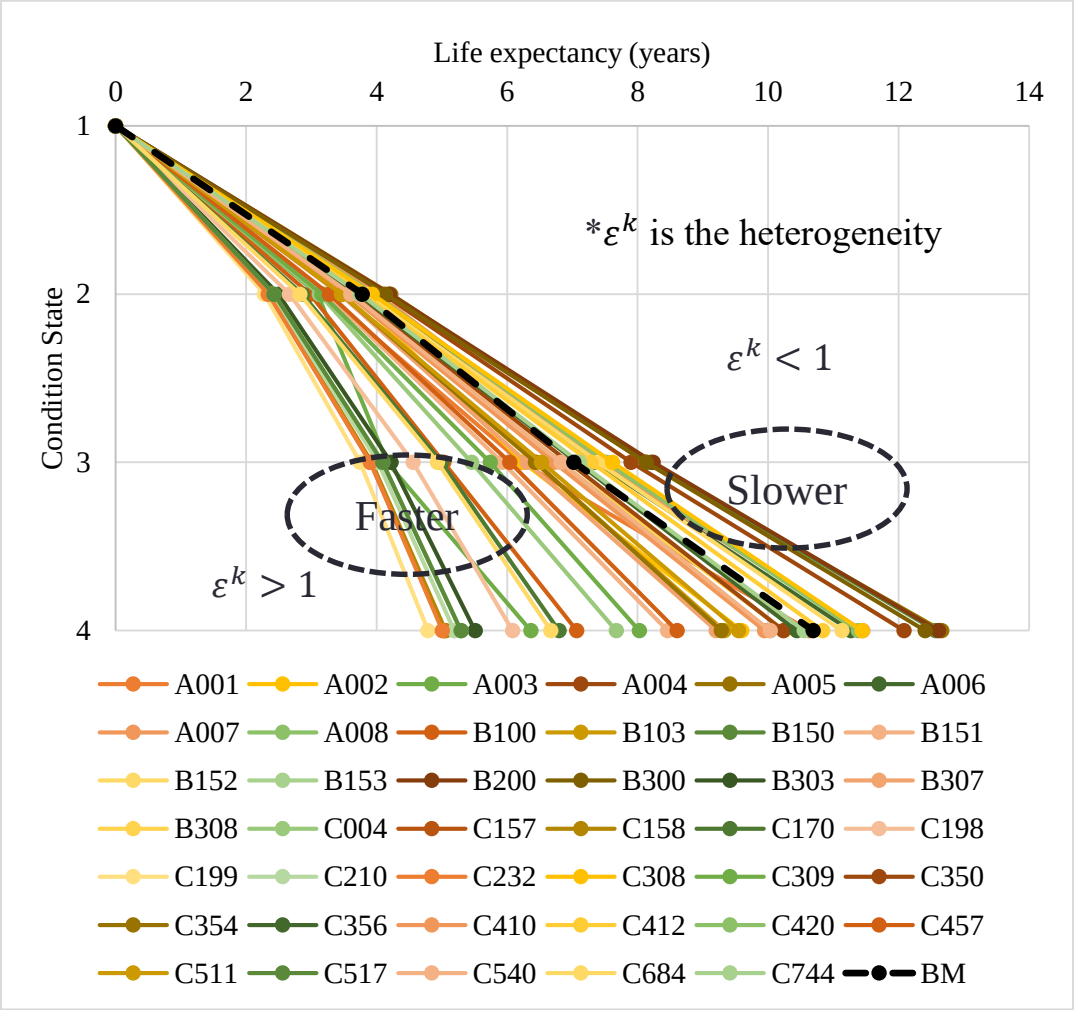

Figure 3.9. Life expectancy of Ugandan national roads.

3.7 Management strategy ideal for Uganda

3.7.1 Management policy setting

The current time-dependent policy and the proposed condition-dependent policy were compared considering a basic plan and a fixed budget. The basic plan involves laying overlays when a pavement deteriorates to condition 3 or 4. The comparison was based on surveyed network condition and LCC at end of analysis period per policy. The Ugandan road maintenance budget was $138.3, $145.2, $118.8, and $166.1 million in Financial Year (FY) 2013/14, FY 2014/15, FY 2015/16 and FY 2016/17 respectively (MoWT 2011 – 2017). This averaged at about $142.1 million each year for the entire 4,551 km network. For the surveyed 1,993 km network, the equivalent budget was about $62.2 million and this was used as a fixed annual budget. Sections for repair were selected using a GA basing on worst condition first (time-dependent policy) or fastest deterioration first (condition-dependent policy) as weights in the selection process. The LCC options used in this study are shown in Table 3.6. Repair cost was presented as a range due to different traffic volumes. It was assumed that some technological advancements kept the overlay cost at lower bound (C_{A_2} = 280,000 $/km). For patching, average cost (C_{A_1} = 12,950 $/km) and an inspection cost of 1,000 $/km were considered.

Intervention actions, i.e., patching (A_1) and overlay (A_2), were set in correspondence to pavement condition. It was considered that the same action was performed throughout the lifecycle of a pavement after it was specified. Absorbing state J was avoided by carrying out more inspections for the case of the condition-dependent policy and making more effective interventions for the case of the time-dependent policy due to prohibitive renewal costs. Each action was considered to cause an acceleration of pavement deterioration (reduction in service life) with A_2 which is more costly causing less reduction in service life and the reverse for less costly A_1. Han et al. (2017) showed that repeated maintenance accelerated pavement deterioration by up to about 30% in South Korea. Due to the absence of maintenance history data in Uganda, it was assumed that $\varphi_{A_1} = 20\%$ and $\varphi_{A_2} = 10\%$ as factors for reduction in pavement service life due to actions A_1 and A_2, respectively. Other φ_A values were considered but there was no significant difference in results. The analysis period was fixed as $T = 15$ years and the inspection interval was fixed as $r = 1$ year.

Table 3.6. LCC analysis options.

Option	Details	Source
Number of sections	1,993 out of about 4,551	Uganda national paved road network database
Life expectancy	Obtained probabilistically by MCMC methods in case of condition-dependent policy, unknown for time-dependent policy	
Unit costs (for two-lane roads)	C_{A_0} (0) C_{A_1} (8.4 – 17.5)* C_{A_2} (280 – 497.5)* Discount rate ρ^r (10%)	MoWT (2011 – 2017), Bank of Uganda (2018)

**Value in 1,000 $/km (in 2017). Range shows value for low and high traffic roads.*

The MTP is affected by φ_A due to maintenance history $\boldsymbol{a}^{t,s^k}$. As shown in the empirical study, MTP is important in estimating agency costs and subsequently LCC. Without any past repair works, the MTP matrix for the surveyed Ugandan network is shown in Equation (3.31). With increased maintenance works, the probability values above the major diagonal are expected to increase signifying faster pavement deterioration as shown in Equation (3.32) at year 15 (end of the analysis period).

$$\boldsymbol{p}_{\boldsymbol{year\ 1}} = \begin{bmatrix} 0.7676 & 0.1986 & 0.0308 & 0.0030 \\ 0 & 0.7346 & 0.2307 & 0.0347 \\ 0 & 0 & 0.7614 & 0.2386 \\ 0 & 0 & 0 & 1 \end{bmatrix} \tag{3.31}$$

$$\boldsymbol{p}_{\boldsymbol{year\ 15}} = \begin{bmatrix} 0.5974 & 0.2949 & 0.0894 & 0.0183 \\ 0 & 0.5483 & 0.3413 & 0.1104 \\ 0 & 0 & 0.5880 & 0.4120 \\ 0 & 0 & 0 & 1 \end{bmatrix} \tag{3.32}$$

Considering a fixed annual budget of $62.2 million, the LCC and surveyed network condition, which are the criteria for comparison, are shown in Table 3.7, Figure 3.10, and Figure 3.11 per policy; there was no difference in LCC because the annual budget was fully utilised in both cases. A shift from the current time-dependent policy to the proposed condition-dependent policy could lead to an improvement in network condition by increasing percentages of the surveyed network in good and fair condition by 8.6% and 2.5%, respectively, and reducing percentages in poor and

bad condition by 8.5% and 2.6%, respectively, at the current budget level.

Table 3.7. Condition of surveyed Ugandan roads and LCC at end of the analysis period based on adopted management policy.

Policy	LCC ($ million)	Percentage (%) of surveyed network in condition state			
		1	2	3	4
Initially*	-	49.2	36.5	11.2	3.1
Time-dependent	538.43	0.5	15.8	27.4	56.3
Condition-dependent	538.43	9.1	18.3	18.9	53.7

**Percentages shown are at start of the analysis period.*

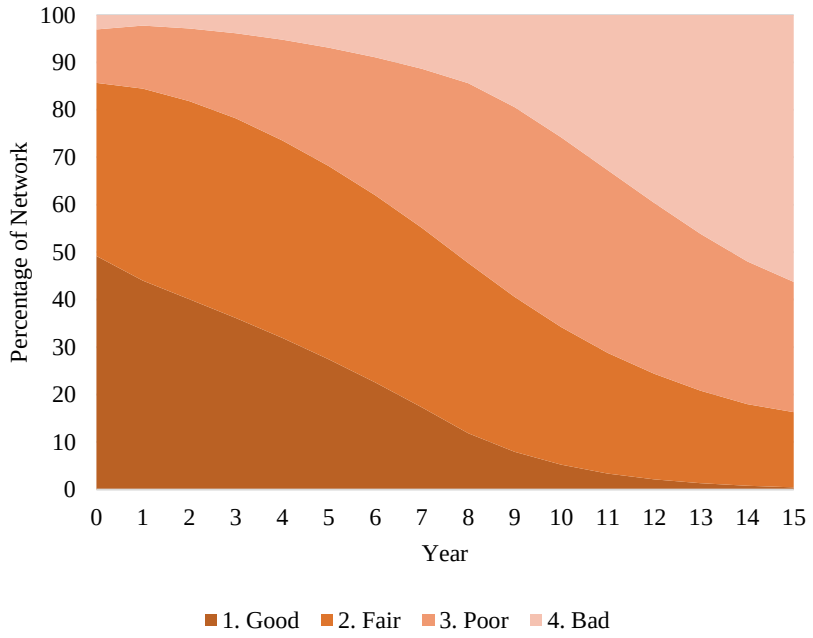

Figure 3.10. Condition of surveyed network considering time-dependent policy.

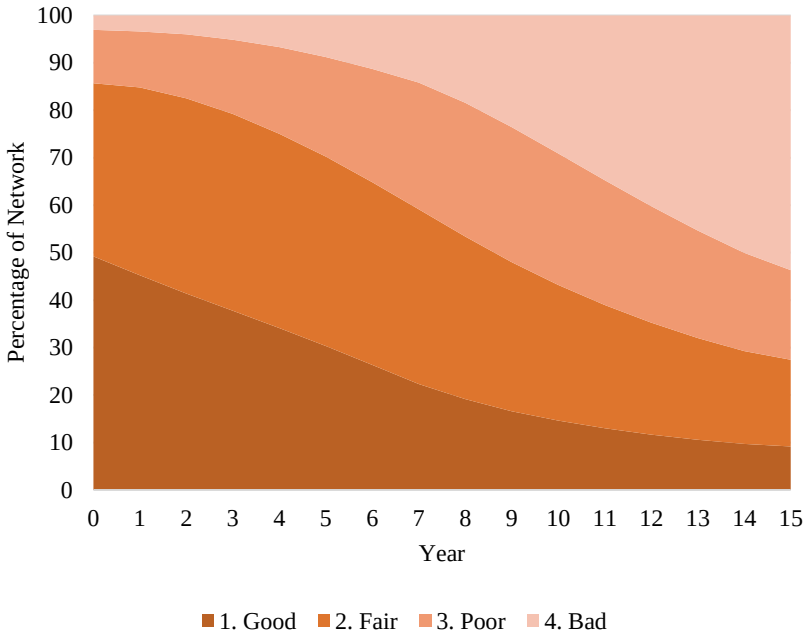

Figure 3.11. Condition of surveyed network considering condition-dependent policy.

At the current budget level, more than 50% of the pavement sections would deteriorate beyond the service level ($\underline{i}$ = 3). In order to maintain the service level 3, an annual budget of about $100.2 million is required. This results in improved network condition, with only 6.2% of the network deteriorating to the worst condition at the end of the analysis period with a 15-year LCC of $839.05 million (Table 3.8).

Table 3.8. Condition of surveyed Ugandan roads and LCC at end of the analysis period considering that service level 3 is strictly maintained.

LCC ($ million)	$\underline{i}$	Percentage (%) of road network in condition state			
		1	2	3	4
839.05	3	31.2	41.6	21.0	6.2

3.7.2 Maintenance plan setting

Three maintenance plans including the do-nothing plan, were investigated by varying serviceability limit $\underline{i}$ and actions in correspondence to observed condition after inspection ($A \leftrightarrow i$) were compared (Table 3.9). Plan 1 involves preventive maintenance works done when pavements reach condition 2. A similar analysis period, inspection interval, and criteria were used for

comparison as in the previous subsection, and a condition-dependent policy was assumed. The budget level was set at $100.2 million annually.

Table 3.9. Proposed maintenance plans.

Plan	$\underline{i}$	Condition state (i)		
		1	2	3 and 4
$\boldsymbol{m_{p,0}}$	-	A_0	A_0	A_0
$\boldsymbol{m_{p,1}}$	2	A_0	A_1	A_2
$\boldsymbol{m_{p,2}}$	3	A_0	A_0	A_2

Table 3.10 shows surveyed network condition and LCC at end of the analysis period per plan. Plan 1 had the best condition, with LCC falling within limits (Figure 3.12, Figure 3.13 and Table 3.10) making it optimum. Plan 1 with preventive maintenance intervention led to a further improvement in network condition by increasing percentage of the surveyed network in good condition by 27.4% and reducing percentages in poor and bad condition by 11.6% and 4.2%, respectively, with a 53.5% LCC reduction compared to plan 2. This result shows the effectiveness of preventive maintenance with the same budget constraint. The budget was not fully utilised for plan 1 because the road agency was restricted to carry out inspection and intervention only once in a year. The lower percentage of sections in condition 2 for plan 1 is because preventive works maintained the sections in condition 1. If nothing was done, 87% of the network would deteriorate to the worst condition (Figure 3.14 and Table 3.10).

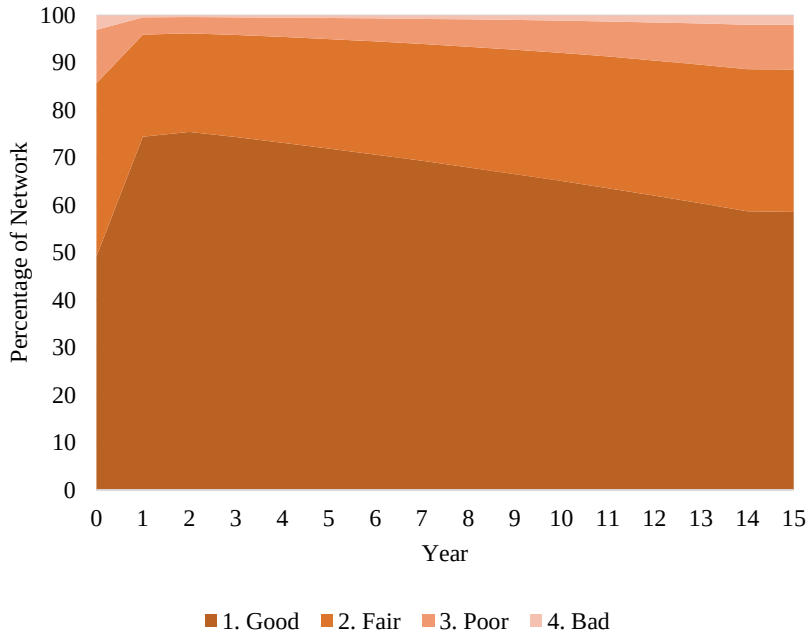

Figure 3.12. Condition of surveyed network with plan 1, fixed budget and condition-dependent policy.

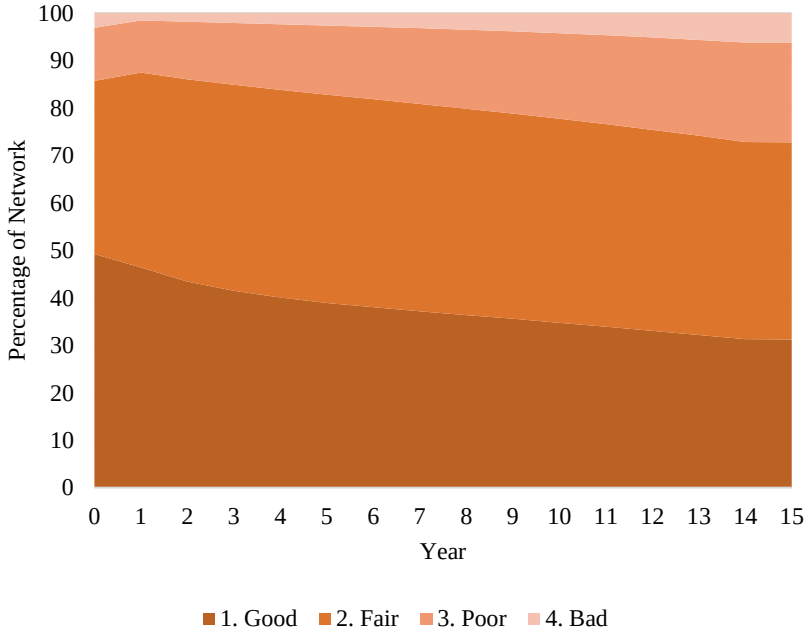

Figure 3.13. Condition of surveyed network with plan 2, fixed budget and condition-dependent policy.

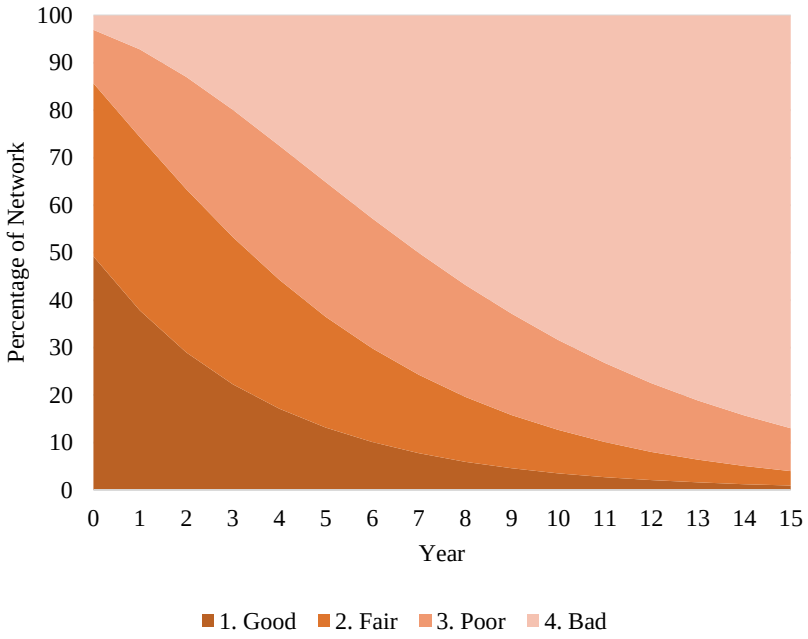

Figure 3.14. Condition of surveyed network considering doing nothing.

Table 3.10. Condition of surveyed Ugandan roads and LCC at end of the analysis period per plan.

Plan	LCC ($ million)	Budget utilisation (%)	Percentage (%) of road network in condition state			
			1	2	3	4
$\boldsymbol{m_{p,0}}$	-	-	0.9	3.1	9.0	87.0
$\boldsymbol{m_{p,1}}$	390.55	46.5	58.6	30.0	9.4	2.0
$\boldsymbol{m_{p,2}}$	839.05	100	31.2	41.6	21.0	6.2

3.8 Discussion of main results

The MUSTEM model adopted to estimate deterioration rate requires a minimum of two-point data which is manageable for developing countries such as Uganda. Life expectancy of surveyed Ugandan roads was about 10.69 years (benchmark). This estimated pavement life of the surveyed roads was noted to be shorter than the expected design life of about 20 years attributable to heavier traffic loading and lower strength construction materials. The estimation results could be improved with better data such as temperature and layer thickness as explanatory variables.

A shift from time-dependent to condition-dependent management policy resulted in a significant improvement in network condition by increasing percentages of the surveyed network in good and

fair condition by 8.6% and 2.5%, respectively, and reducing percentage, in poor and bad condition by 8.5% and 2.6%, respectively. By prioritising repair for pavement sections with fast deterioration instead of those in worse condition, the road agency slowed the deterioration rate of sections to worse condition, in effect preserving the entire network in better condition for a longer time.

Preventive maintenance works further improved road network condition by increasing percentage of the surveyed network in good condition by 27.4% and reducing percentages in poor and bad condition by 11.6% and 4.2%, respectively, with a 53.5% reduction in LCC. Due to the low cost of preventive works, they can be done at higher frequencies (repair cost and frequency trade-off). In addition, preventive works limit exposure of the pavement to deterioration agents such as moisture, hence slowing deterioration.

The budget was not fully utilised for plan 1 because the road agency was restricted to carry out inspection and intervention only once in a year. It would be impractical for the road agency to carry out inspection and intervention actions over much smaller intervals of less than a year. Additionally, this could generate other costs due to disruption of road traffic and noise pollution during the numerous repairs.

3.9 Conclusions and recommendations

This study attempted to introduce planning for pavement maintenance based on the condition-dependent instead of the time-dependent policy commonly used in developing countries such as Uganda. A shift from time-dependent to condition-dependent policy was studied considering a fixed budget. Also, maintenance planning with and without preventive maintenance was investigated considering a limited budget. A management policy shift to condition-dependent policy resulted in a significant improvement in pavement condition. Preventive maintenance works further improved road network condition. This study therefore supports a pavement management policy shift to the condition-dependent policy and maintenance planning with preventive maintenance works to be adopted in developing countries such as Uganda. There is also a need to analyse the relationship between the pavement design and estimated life expectancy in order to empirically show the effectiveness of increasing design life in future research.

The extension to include effect of maintenance works and generalisation of repair interventions made the model more practical. Additionally, due to the low data requirement of this PMS, it could

easily be adapted to network systems in developing countries. With a few adjustments, it may be applied to other infrastructure systems such as bridges.

The study faced a number of limitations including the following:

1) Incomplete data: deterioration of road pavements is also affected by environmental conditions such as temperature and moisture. Average speed was used as an explanatory variable in the estimation of the hazard rate and life expectancy despite the fact that average speed is affected by other factors such as road geometry and driver behaviour not only pavement condition. Average speed was used because it was an indicator of road condition and also due to scarcity of data in the current database.
2) Solution procedure: the solution procedure was cumbersome for a bigger pool of suggested plans.

Despite the practicality of this study, a few areas of improvement were identified. The following are recommended:

1) Data collection: the sectioning of Ugandan roads at about 1 km per section was probably due to limited resources and labour for data collection. Pavement quality over a distance of 1 km varies and it could be erroneous to report a uniform pavement condition. Pavement section length could be reduced to a maximum of 100 m per section and marked according to how critical they are, for instance bridge and intersection approach sections, for better management. More pavement data such as temperature and layer thickness could be collected to improve estimation and planning.
2) Solution method: plans were considered to be set by the road agency. Selection of an optimum plan could be a cumbersome process in the case of a bigger pool. A more efficient solution method is therefore required.

A.1 Appendix

Table 3.11 shows the names of the surveyed Ugandan road groups. The roads were named based on the cities and towns they connect.

Table 3.11. Names of surveyed Ugandan national roads.

Road section group	Road name
A001	Kampala - Mukono - Lugazi - Njeru - Jinja - Kakira - Iganga - Nakalama - Bugiri - Namutere - Tororo - Malaba (Uganda/Kenya border)
A002	Kampala - Kibuye - Natete - Busega - Mpigi - Buwama - Lukaya - Masaka - Lyantonde - Mbarara - Ntungamo - Rubaale - Muhanga - Kabale - Katuna (Uganda/Rwanda border)
A003	Kibuye - Zana - Entebbe Airport
A004	Masaka - Kyotera - Mutukula (Uganda/Tanzania border)
A005	Busega - Bujuuko - Mityana - Naama - Myanzi - Kiganda - Kitenga - Mubende - Lusalira - Nabingoola - Lubaale - Kyegegwa - Kakabala - Kyenjojo - Rugombe - Fortportal - Rwimi - Hima - Mubuku - Kasese - Kikorongo - Bwera - Mpondwe (Uganda/Congo border)
A006	Kampala - Kawempe - Matuga - Wobulenzi - Kasana - Luweero - Nakasongola - Kafu - Kigumba - Karuma - Kamdini - Minakulu - Bobi - Gulu - Atiak - Nimule (Uganda/South Sudan border)
A007	Malaba (Uganda/Kenya border) - Tororo - Magodes - Nabumali - Mbale - Namunsi - Kumi - Soroti - Dokolo - Agwata - Lira - Ayer - Kamdini
A008	Karuma - Olwiyo - Packwach - Nebbi - Eruba - Arua - Manibe - Maracha - Koboko - Oraba (Uganda/South Sudan border)
B100	Kubiri - Gayaza - Kalagi
B103	Nyendo - Villa Maria - Sembabule - Lwemiyaga - Nkonge - Kibula - Magege - Kasambya - Lusalira
B150	Ishanyu - Bwizibwera - Ibanda - Muziza - Kamwenge - Fortportal
B151	Mbarara - Ishanyu - Kabwohe - Ishaka
B152	Ntungamo - Kagamba - Ishaka - Buhinda - Rugazi - Katunguru - Kikorongo
B153	Kabale - Ikumba - Muko - Nyakabande - Kisoro – Bunagana (Uganda/Congo border)
B200	Kafu - Masindi
B300	Namunsi - Sironko - Muyembe - Namalu - Chosan - Lokapel - Ariamoi - Moroto
B303	Soroti - Arapai - Katakwi - Iriri - Ariamoi - Nadunget
B307	Jinja - Buwenge - Kamuli - Nawantale - Bukungu
B308	Namutere - Busia
C004	Namboole - Gayaza road - Hoima road - Busega
C157	Entebbe - Nakiwogo
C158	Nakiwogo Statehouse road
C170	Namboole access road
C198	Budo - Nakasozi
C199	Nabbingo access road
C210	Nyendo - Masaka
C232	Lyantonde - High Street
C308	Nakasongola loop
C309	Nakasongola - Airbase
C350	Katete - Isingiro
C354	Kikagati - Murungo bridge
C356	Ibanda - Kanoni - Kazo

C410	Kagamba - Kebisoni - Rukugiri
C412	Kisoro - Kyanika (Uganda/Rwanda border)
C420	Kabale access road
C457	Kisoro - Muganzi - Chahi
C511	Kasese - Kilembe mines
C517	Kasese Railway station road
C540	Fortportal - Kichwamba - Karugutu - Bundibugyo - Lamia (Uganda/Congo border)
C684	Gulu Airport road
C744	Eruba - Vurra (Uganda/Congo border)

Table 3.12 and Table 3.13 show load conversion to ESALs for each vehicle type.

Table 3.12. Vehicle weight and equivalent ESALs factor (MoWT 2010, FHWA 2014).

Vehicle type	Min – Max weight (kN)*	ESALs**
Motorcycles and scooters	0.044 - 13.34	-
Saloon cars and taxis	4.45 - 35.54	0.06
Light Goods	4.45 - 35.54	0.06
Small Buses	88.92 >	1.59
Medium Buses	88.92 >	1.59
Large Buses	133.45 >	6.92
Light Trucks	88.92 -133.45	1.59
Medium Trucks	88.92 >	1.59
Truck trailer/ semi-trailer	133.45 >	6.92
Bicycles	NA	-
Carts	NA	-

**Maximum weight was considered following normal practice of designing for the worst case.*

*** ESALs can be obtained from MoWT (2010) (*Table 3.13*) considering a commonly applied relative damage exponent ($\dot{n}$=4) or by simply calculating ESALs=*$[axel\ load/80]^{\dot{n}}$ *for loads in kN.*

Table 3.13. Load equivalency factors for different axel load groups in ESALs (MoWT 2010).

Axle Loads Measured in kg				Axle Loads Measured in kN			
Axle Load Range (kg)	$\dot{n} = 3$	$\dot{n} = 4$	$\dot{n} = 4.5$	Axle Load Range (kN)	$\dot{n} = 3$	$\dot{n} = 4$	$\dot{n} = 4.5$
Less than 1500	-	-	-	Less than 15	-	-	-
1500-2499	.02	-	-	15-24	.02	-	-
2500-3499	.05	.02	.01	25-34	.05	.02	.01
3500-4499	.12	.06	.05	35-44	.13	.06	.05
4500-5499	.24	.15	.12	45-54	.24	.15	.12
5500-6499	.41	.30	.26	55-64	.42	.32	.28
6500-7499	.64	.56	.52	65-74	.66	.58	.55
7500-8499	.95	.95	.94	75-84	.99	.99	1.00
8500-9499	1.35	1.51	1.59	85-94	1.41	1.59	1.69
9500-10499	1.85	2.29	2.55	95-104	1.94	2.42	2.71
10500-11499	2.46	3.34	3.90	105-114	2.58	3.55	4.16
11500-12499	3.20	4.72	5.75	115-124	3.35	5.02	6.15
12500-13499	4.06	6.50	8.22	125-134	4.26	6.92	8.82
13500-14499	5.07	8.73	11.46	135-144	5.32	9.3	12.31
14500-15499	6.23	11.49	15.61	145-154	6.54	12.26	16.79
15500-16499	7.56	14.87	20.85	155-164	7.94	15.88	22.45
16500-17499	9.06	18.93	27.37	165-174	9.53	20.24	29.50
17500-18499	10.76	23.78	35.37	175-184	11.32	25.44	38.15
18500-19499	12.65	29.51	45.09	185-194	13.31	31.59	48.67
19500-20499	14.75	36.22	56.77	195-204	15.53	38.79	61.32

Derivation of MTP

Consider that the condition state of one pavement section at time τ_i or time point y_i is assumed to increase from i to $i+1$. The period length in which the condition state remains in i is represented by stochastic variable $\zeta_i = \tau_i - \tau_{i-1} = y_i$. ζ_i is the life expectancy of a condition state i with probability density function $f_i(\zeta_i)$ and distribution function $F_i(\zeta_i)$ (Lancaster, 1990).

$$F_i(y_i) = \int_0^{y_i} f_i\ (\zeta_i) d\xi_i \tag{3.33}$$

The probability $\widetilde{F_i}\ (y_i)$ of a transition in the condition state i during the time point interval $y_i = 0$ to $y_i \in [0, \infty]$ is;

$$Prob\{\zeta_i \geq y_i\} = \widetilde{F_i}(y_i) = 1 - F_i(y_i) \tag{3.34}$$

The conditional probability that the condition state of one pavement section at time y_i advances from i to $i+1$ during the time interval $[\ y_i, y_i + \ \Delta y_i]$ is defined as;

$$\lambda_i(y_i)\Delta y_i = \frac{f_i\ (y_i)\Delta y_i}{\widetilde{F_i}(y_i)} \tag{3.35}$$

The probability density $\lambda_i(y_i)$is the hazard function and can be defined with independence from time as;

$$\lambda_i(y_i) = \theta_i \tag{3.36}$$

Differentiating both sides of (3.34) with respect to y_i we obtain

$$\frac{d\widetilde{F_i}(y_i)}{dy_i} = -f_i(y_i) \tag{3.37}$$

(3.35) then reduces to

$$\lambda_i(y_i) = \frac{f_i\,(y_i)}{\widetilde{F}_i(y_i)} = -\frac{\frac{d\widetilde{F}_i(y_i)}{dy_i}}{\widetilde{F}_i(y_i)} = \frac{d}{d(y_i)}\left(-\log \widetilde{F}_i(y_i)\right) \tag{3.38}$$

Integrating equation (3.38)

$$\int_0^{y_i} \lambda_i(u)du = [-\log \widetilde{F}_i(u)]_0^{y_i} = -\log \widetilde{F}_i(y_i) \tag{3.39}$$

$$\widetilde{F}_i(0) = 1 - F_i(0) = 1$$

Substituting (3.36), probability $\widetilde{F}_i(y_i)$ that life expectancy of condition state i becomes longer than y_i is;

$$\widetilde{F}_i(y_i) = exp\left[-\int_0^{y_i} \lambda_i(u)du\right] = exp(-\theta_i y_i) \tag{3.40}$$

According to (3.37)

$$f_i(\zeta_i) = \theta_i exp(-\theta_i \zeta_i) \tag{3.41}$$

Now consider that the condition state has changed to i at the time τ_{i-1}, and remains constant until the inspection time τ_A(time point y_A). The probability that the condition state i remains constant in a subsequent time $z_i(\geq 0)$ measured from y_A is;

$$\widetilde{F}_i(y_A + z_i|\zeta_i \geq y_A) = Prob\{\zeta_i \geq y_A + z_i|\zeta_i \geq y_A\} \tag{3.42}$$

Dividing both sides by $\widetilde{F}_i(y_i)$ in (3.34)

$$\frac{Prob\{\zeta_i \geq y_A + z_i\}}{Prob\{\zeta_i \geq y_A\}} = \frac{\widetilde{F}_i(y_A + z_i)}{\widetilde{F}_i(y_A)} \tag{3.43}$$

Using (3.40) on the right side of (3.42);

$$\frac{\widetilde{F}_i(y_A + z_i)}{\widetilde{F}_i(y_A)} = \frac{exp\{-\theta_i(y_A + z_i)\}}{exp(-\theta_i y_A)} = exp(-\theta_i z_i) \tag{3.44}$$

Therefore the transition probability;

$$Prob[h(y_B) = i | h(y_A) = i] = exp(-\theta_i Z) \tag{3.45}$$

where Z is the interval between two inspection times y_A and y_B.

(For derivation of other MTPs refer to Tsuda et al. 2006)

Photo Gallery

Figure 3.15. Categorization of road condition for Uganda (MoWT, 2014)

Figure 3.16. Inspection vehicle (Shimizu Corporation et al., 2021).

Figure 3.17. Sensor mounted on car wheel (Shimizu Corporation et al., 2021).

Figure 3.18. Road images from Uganda (Shimizu Corporation et al., 2021).

Figure 3.19. Inspected road condition for select routes in 2017 (Using UNRA 2019 data).

Figure 3.20. Inspected road condition for select routes in 2018 (Using UNRA 2019 data).

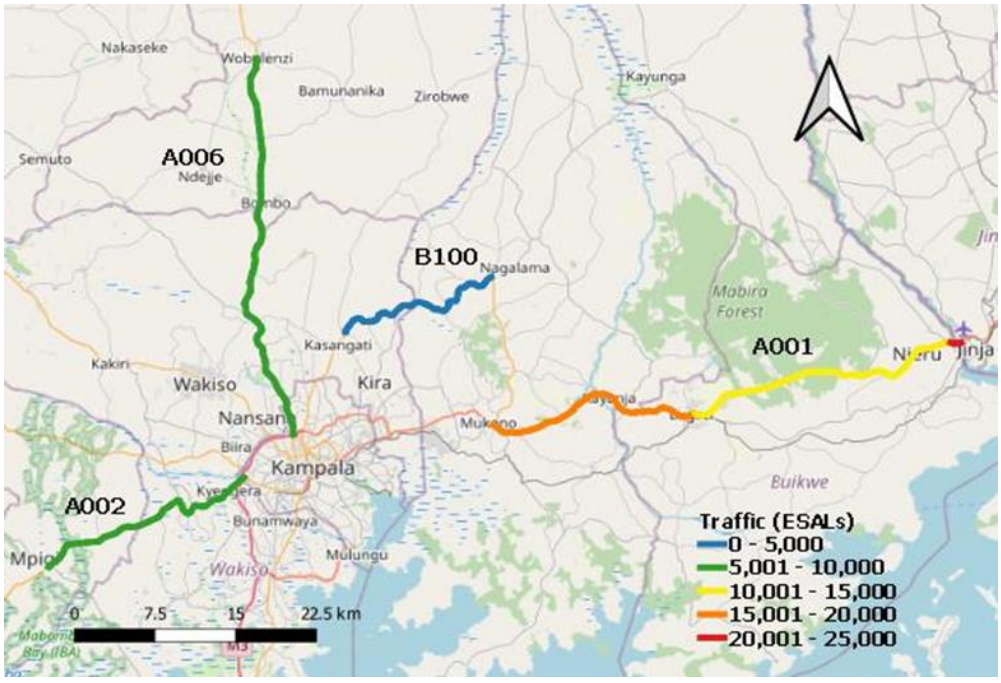

Figure 3.21. Traffic level on select routes in 2017 (Using UNRA 2019 data).

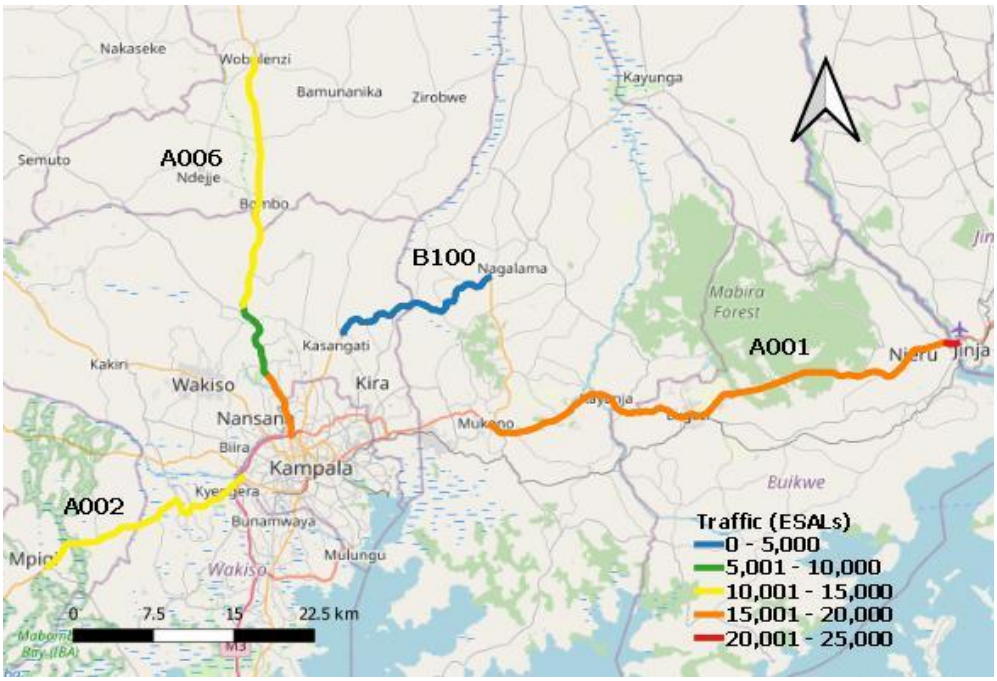

Figure 3.22. Traffic level on select routes in 2018 (Using UNRA 2019 data).

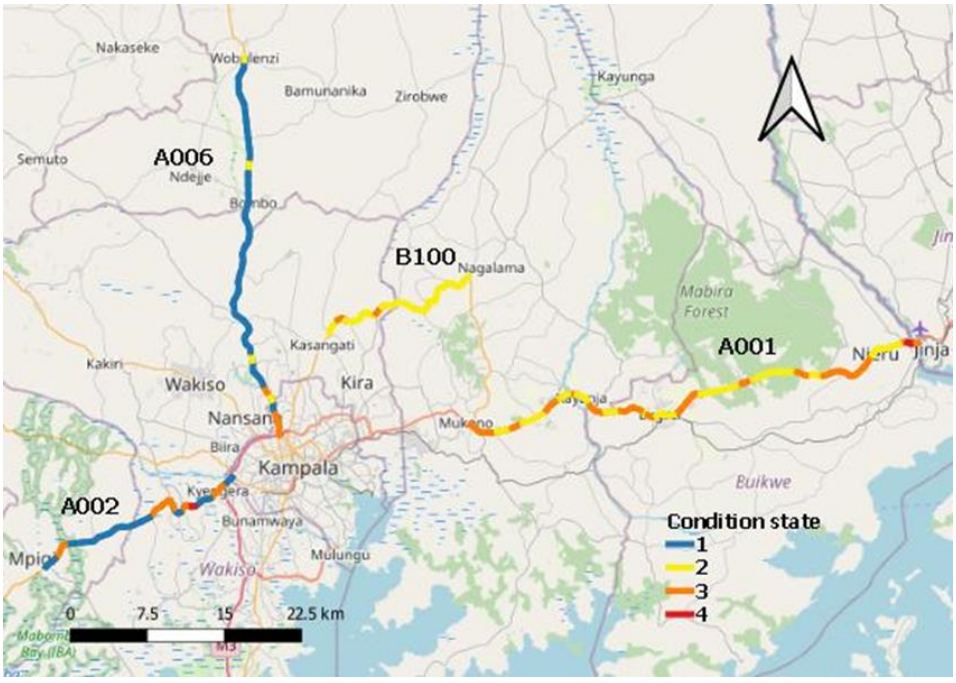

Figure 3.23. Estimated road pavement condition in 2021.

Bibliography

AASHTO (American Association of State Highway and Transport Officials), 2012. Pavement Management Guide, 2nd ed. Washington, DC: AASHTO.

AASHTO (American Association of State Highway and Transport Officials), 2015. *Mechanistic-empirical pavement design guide: a manual of practice*. Washington, DC AASHTO.

Abaza, K.A., 2016. Back-calculation of transition probabilities for Markovian-based pavement performance prediction models. *International Journal of Pavement Engineering*, 17(3), 253–264.

Abaza, K.A., 2017. Empirical approach for estimating the pavement transition probabilities used in non-homogenous Markov chains. *International Journal of Pavement Engineering*, 18(2), 128–137.

Bank of Uganda, 2018. Annual Report; https://www.bou.or.ug/bou/bouwebsite/bouwebsitecontent/publications/Annual_Reports/All/Bank-of-Uganda-Annual-Report-2018.pdf.

Dalla Rosa, F., Liu, L., Gharaibeh, N.G., 2017. IRI prediction model for use in network-level pavement management systems. *Journal of Transportation Engineering, Part B: Pavement*, 143, 04017001.

FHWA (Federal Highway Administration), USDoT (US Department of Transportation), 2014. Vehicle Classification Manual; FHWA-HRT-13-091.

George, K.P., 2000. *MDOT Pavement Management System: Prediction models and feedback systems*. Jackson, MS, USA: Mississippi Department of Transportation, Report Number FHWA/MS-DOT-RD-00-119.

Gilks, W.R., Richardson, S., Spiegelhalter, D., 1995. *Markov Chain Monte Carlo in Practice*. Chapman & Hall/CRC Interdisciplinary Statistics.

Han, D., Kaito, K., Kobayashi, K., 2014. Application of Bayesian estimation method with Markov hazard model to improve deterioration forecasts for infrastructure asset management. *KSCE Journal of Civil Engineering*, 18(7), 210 –2119.

Han, D., Kaito, K., Kobayashi, K., Aoki, K., 2016. Performance evaluation of advanced pavement materials by Bayesian Markov mixture hazard model. *KSCE Journal of Civil Engineering*, 20(2), 729–737.

Han, D., Kaito, K., Kobayashi, K., Aoki, K., 2017. Management scheme of road pavements considering heterogeneous multiple life cycles changed by repeated maintenance work. *KSCE Journal of Civil Engineering*, 21(5), 1747–1756.

Hastings, W.K., 1970. Monte Carlo sampling methods using Markov chains and their applications. *Biometrika*, 57(1), 97.

Hillier, F.S. and Lieberman, G.J., 1990. *Introduction to operations research*. 5th ed. New York: MacGraw-Hill.

Isaacson, D.L., Madsen, R.W., 1976. *Markov chains: theory and applications*. New York: Wiley.

JICA (Japan International Cooperation Agency), 2015. *District and Urban Roads (DUR) Mapping and Roads Database Project in the Republic of Uganda: Project Completion Report.*

Kaito, K., Sakai, Y., Tsukamoto, S., Mizutani, D., Kobayashi, K., 2015. A Multi-hierarchical mixed Markov deterioration hazard model: application for deterioration speed evaluation for joint members. *Journal of Japan Society of Civil Engineers*, 71(1), 1–18.

Kerali, H. R. and Snaith, M. S., 1992. NETCOM: the TRL visual condition model for road networks, Crowthorne, UK: Transport Research Laboratory, Contractor Report No. 921.

Kobayashi, K., Do, M. and Han, D., 2010. Estimation of Markovian transition probabilities for pavement deterioration forecasting, *KSCE Journal of Civil Engineering*, Vol.14, No.3, pp. 343–351.

Kobayashi, K., Eguchi, M., Oi, A., Aoki, K., Kaito, K., 2013. The optimal implementation policy for inspecting pavement with deterioration uncertainty. *Journal of Japan Society of Civil Engineers*, 1(1), 551–568.

Kobayashi, K., Kaito, K. and Lethanh, N., 2011. A Statistical deterioration forecasting method using hidden Markov model for infrastructure management. *Transportation Research Part B: Methodological*, 46(4), 544–561.

Kobayashi, K., Kaito, K. and Lethanh, N., 2012. A Bayesian estimation method to improve deterioration prediction for infrastructure system with Markov chain model, *International Journal of Architecture, Engineering and Construction*, Vol.1, No.1, doi:10.7492/IJAEC.2012.001, pp. 1–13.

Lancaster, T., 1990. *The Econometric Analysis of Transition Data*, Cambridge University Press.

Lethanh, N., Adey, B.T., 2012. A hidden Markov model for modeling pavement deterioration under incomplete monitoring data. *International Journal of Civil and Environmental Engineering*, 6(1), 7–14.

Lethanh, N., Kaito, K., Kobayashi, K., 2015. Infrastructure deterioration prediction with a Poisson hidden Markov model on time series data. *Journal of Infrastructure Systems*, 21(3) 04014051.

Li, N.Y., Haas, R., Xie, W.C., 1997. Development of a new asphalt pavement performance prediction model. *Canadian Journal of Civil Engineering*, 24, 547–559.

Li, Y., Madanat, S., 2002. A steady-state solution for the optimal pavement resurfacing problem. *Transportation Research Part A* 36, 525–89.

Madanat, S. and Ben-Akiva, M., 1994. Optimal inspection and repair policies for infrastructure facilities. *Transportation Science*, 28(1), 55–62, doi:10.1287/trsc.28.1.55.

Mamlouk, M. S., 2006. Pavement Management Systems. In T. F. Fwa, ed. *The Handbook of Highway Engineering*. Boca Raton, FL, USA: Taylor & Francis.

Mohammadi, A., Amador-Jimenez, L., Elsaid, F., 2019. Simplified pavement performance modeling with only two-time series observations: a case study of Montreal Island. *Journal of Transportation Engineering, Part B: Pavements*, 145(4), 05019004.

MoWT (Ministry of Works and Transport) – Uganda, 2010. *Road Design Manual, Volume 1 Geometric Design Manual, Volume 3: Pavement Design; Part I: Flexible Pavements*. Kampala, Uganda: MoWT.

MoWT (Ministry of Works and Transport) – Uganda, 2011–2017. Annual Sector Performance Reports (ASPR); http://www.works.go.ug/document-category/jtsrw/.

MoWT (Ministry of Works and Transport) – Uganda, 2015. *Road Inventory Survey Manual*. Kampala, Uganda: MoWT.

Ortiz-García, J.J., Costello, S.B., Snaith, M.S., 2006. Derivation of transition probability matrices for pavement deterioration modeling. *Journal of Transportation Engineering*, 132 (2), 141–161.

Oxford Economics, 2014. Capital project and infrastructure spending Outlook to 2025; https://www.pwc.com/gx/en/capital-projects-infrastructure/publications/cpi-outlook/assets/cpi-outlook-to-2025.pdf.

Pantuso, A., Flintsch, G.W., Katicha, S.W., Loprencipe, G., 2019. Development of network-level pavement deterioration curves using the linear empirical Bayes approach. *International Journal of Pavement Engineering*, doi: 10.1080/10298436.2019.1646912.

Pérez-Acebo, H., Bejan, S., Gonzalo-Orden, H., 2018. Transition probability matrices for flexible pavement deterioration models with half-year cycle time. *International Journal of Civil Engineering*, 16, 1045–1056.

Pérez-Acebo, H., Linares, A., Roji, E., Gonzalo-Orden, H., 2020. IRI performance models for flexible pavements in two-lane roads until first maintenance and/or rehabilitation work. *Coatings*, 10, 97.

Pérez-Acebo, H., Mindrab, N., Railean, A. and Rojí, E., 2019. Rigid pavement performance models by means of Markov Chains with half-year step time*, International Journal of Pavement Engineering,* Vol.20, pp. 830–843. doi:10.1080/10298436. 2017.1353390.

Rinnooy Kan, A. H. G., Stougie, L. and Vercellis, C., 1993. A class of generalized greedy algorithms for the multi-knapsack problem, *Discrete Applied Mathematics,* 42, 279–290.

Saha, P., Ksaibati, K., 2017. Developing an optimization model to manage unpaved roads. *Journal of Advanced Transportation*, 2017, 9474838.

Shimizu Corporation, Eight Japan Engineering Consultants Inc. (EJEC), and Kyoto University, 2021. Basic study for Problem solution on Road maintenance in African countries (BPRA) Report.

Sundaram, R.K., 1999. *A first course in optimization theory*. Cambridge University Press.

Tabatabaee, N. and Ziyadi, M., 2013. Bayesian approach to updating Markov-based models for predicting pavement performance, *Transportation Research Record: Journal of the Transportation Research Board*, Vol.2366, No.1, doi:10.3141/2366-04, pp. 34–42.

Tsuda, T., Kaito, K., Aoki, K. and Kobayashi, K., 2006. Estimating Markovian Transition Probabilities for Bridge Deterioration Forecasting, *Structural Engineering/Earthquake Engineering*, Vol.23, No.2, pp. 241s–256s.

Tsunokawa, K., Schofer, J.L., 1994. Trend curve optimal control model for highway pavement maintenance: case study and evaluation. *Transport Research*, 28A, 151–166.

Uddin, W., 2006. Pavement Management Systems. In T. F. Fwa, ed. *The Handbook of Highway Engineering*. Boca Raton, FL, USA: Taylor & Francis.

UNRA (Uganda National Roads Authority), 2019. Database (Available on request from UNRA).

Chapter 4

4 Pavement Intervention Effects on Travel Time

"Adding car lanes to deal with traffic congestion is like loosening your belt to cure obesity." – Lewis Mumford (1955)

4.1 Introduction

Efficient transportation systems are an important prerequisite for economic growth since they facilitate the efficient and safe delivery of goods and services. In many developing countries, the most popular delivery mode for goods is road transportation. Because of the poor condition and congestion on some roads, a significant amount of productive time is lost during travel; a huge cost that hinders economic development. For instance, in Kampala, Uganda, an estimated 40% of rush-hour journeys are spent at a standstill due to narrow dilapidated roads. In addition, pavement management has been fragmented with uncoordinated decisions taken for interlinked road aspects; for example, the inadequacy in road capacity (congestion) has been managed separately by planners, whereas durability (structural failure) has been handled by engineers despite the close links between these aspects. This study looks at three fundamental considerations for road travel; i.e., safety, condition, and capacity. The study builds a social cost model to evaluate intervention (condition improvement and capacity increase) choice for multiple road sections simultaneously by optimizing social costs after setting safety limits. The social cost model contains a travel time function that incorporates a condition term in the original Bureau of Public Roads function. The model defines social cost as a summation of travel and intervention costs incurred by the society, and proposes an evaluation framework that combines both capacity and durability aspects. To show the applicability of the model, an empirical study was carried out on Ugandan road pavements.

4.2 Pavement Management

Pavement management policies could be formulated to deal with the inadequacies in road capacity (congestion) and durability (structural failure). The fragmentation of pavement management where uncoordinated decisions are taken for interlinked road aspects is a recurring challenge that has led to, for instance, planners dealing only with congestion and leaving pavement failure to engineers. A case in point is in Uganda where some roads are managed by both the Uganda National Roads Authority (UNRA) and local authorities at different times with often varying maintenance and expansion decisions yet both are under the Ministry of Works and Transport (MoWT 2011–2017). As a result, pavement intervention does not always fully meet the required maintenance and improvement needs. Furthermore, this disjointed management is exacerbated by the current problem of rapidly aging or deteriorating infrastructure that has led to the widening gap between maintenance needs and finance allocation. For example, in Uganda, the national road maintenance budget catered for only 26%, 48%, and 34.8% of the total needs in 2013, 2014, and 2015, respectively (MoWT 2011–2017). This underscores the challenges faced by road administrators in providing efficient road service.

The efficient transportation of goods and services is an important prerequisite for economic growth in any country. In Uganda, about 96.5% of freight and 95.0% of passengers travel by road, confirming the popularity of road transport compared to other modes (rail, water, and air). In Kampala, Uganda, an estimated 40% of rush-hour journeys are spent at a standstill due to such reasons as narrow roads in poor condition (MoWT 2011–2017; Bird and Venables 2020). This lost time is a huge social cost that slows down economic development. It is therefore in the interest of any public road administrator to improve the effectiveness and efficiency of road service, a challenge this study attempts to solve.

This study proposes a social cost model with an evaluation framework that combines both capacity and durability aspects and looks at three fundamental considerations for road travel; i.e., safety, condition and capacity by incorporating a condition term in the original Bureau of Public Roads (BPR 1964) travel time function and evaluates the trade-off between intervention (condition improvement and capacity increase) choice for multiple road sections concurrently by optimizing

social costs after setting safety limits. There exist more considerations for road travel including noise, comfort and particle emission (Adey et al. 2020). Some of these items could be sub components or outcomes of the three fundamental considerations; for instance, comfort may be a sub component of safety and poor condition may lead to particle (dust) emission. Social cost was defined as a summation of travel and intervention costs incurred by the society. To show the applicability of the model, an empirical study was carried out on Ugandan road pavements. As far as is known, no past study builds a model that can be applied to empirically evaluate intervention effects for multiple sections simultaneously. The objectives of this study are:

1) Develop a social cost model to evaluate effects of road intervention on capacity and durability for multiple sections concurrently.
2) Empirically apply the model to Ugandan road pavements.

The rest of this chapter is organized as follows. The next section presents a review of relevant literature; followed by a summary of Ugandan road data, based on which a social cost optimization model is developed. The subsequent section contains the model application. Finally, conclusions from the results and suggestions for future work are made.

4.3 Literature Review

Models consist of functions defining relationships between dependent and independent variables. These functions may include parametric and non-parametric forms. Parametric functions involve a prior selection of the functional form, whereas for non-parametric methods, functions and patterns are generated by linking independent short linear segments. In the literature, parametric models in the pavement infrastructure management field such as regression models (e.g., TRB 2000, 2010; Chandra 2004; and Wang et al. 2014) and non-parametric models (e.g., Richmond et al. 2021) have been developed. Non-parametric forms give room for the data to generate a shape from which representative functional forms can be derived, whereas parametric methods enable reference to past literature for similar functional forms and therefore could be useful for comparative studies. Additionally, functional forms may be linear or non-linear. Generally, non-linear functional forms are more appropriate than linear forms because they can account for scale economies or diseconomies (Sinha and Labi 2007).

A number of studies have attempted to develop relationships between the speed, travel time, capacity, and road condition. Wang et al. (2014) developed an empirical model for Californian freeways showing the relationship between the pavement roughness and Free-Flow Speed (FFS), the speed achieved by a single vehicle when no other vehicles are on a corridor (road section). The number of lanes, days of the week, gasoline price, and pavement roughness were used as explanatory variables. It was shown that the roughness had a small impact on the FFS given the good state of Californian roads (90% of the surveyed roads had a roughness level of 3 mm/m or lower). A study by Chandra (2004) investigated the effect of road roughness on the capacity of two-lane roads in India taking into consideration the effect of lane indiscipline on Passenger Car Unit (PCU) equivalents. A regression model was built empirically and it showed that for every 1,000 mm/km increase in surface unevenness, the capacity of two-lane roads decreased by 300 PCUs per hour.

The Transport Research Board (TRB) also developed linear models to estimate the FFS for US roads using the lane width and lateral clearance, total number of lanes, interchange density, and road horizontal and vertical alignment as the main factors affecting the speed (TRB 2000, 2010). The TRB models did not include the road surface condition as an explanatory variable, probably because of its insignificant effect on FFS for US roads. For roads with high roughness levels (approximately > 6 mm/m), Bennett and Greenwood (2002) developed a limiting speed model.

An empirical study in Brazil by the World Bank showed that the travel time function vs. condition was expected to follow the trend as shown in Figure 4.1. Shorter travel times could be achieved before a road section deteriorated to a critical condition. In the case of Brazilian roads, the significant condition level, where condition has an effect on travel time, was determined as 6 mm/m (Watanatada et al. 1987). The slightly increasing trend line, highlighted in red color, could occur due to traffic congestion on pavements in good condition. Additionally, according to the Bureau of Public Roads (BPR, 1964), the travel time function vs. volume:capacity ratio was expected to follow the trend as shown in Figure 4.2. Travel time reduction could be achieved by making improvements on a section (e.g., condition improvement and capacity increase). These ideas on travel time, condition and volume:capacity relationships are followed later on in the

calibration of the travel time function and to evaluate the trade-off between condition improvement and capacity increase that was not considered by earlier studies.

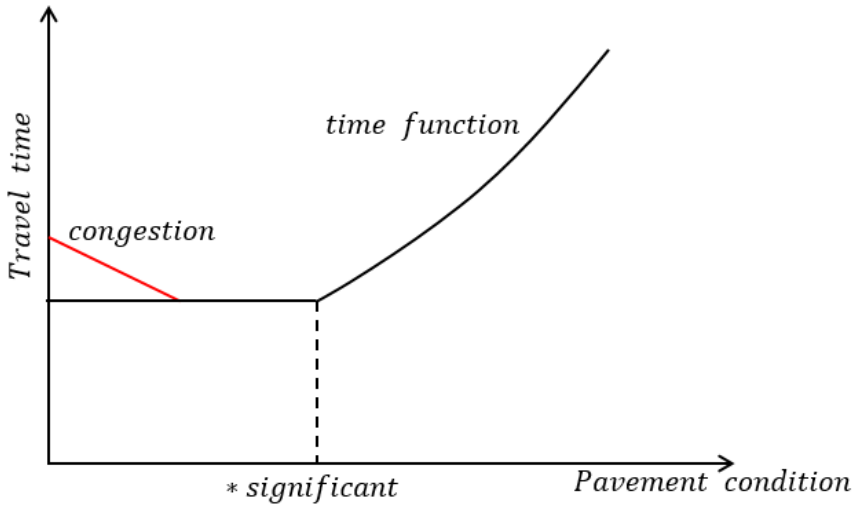

Figure 4.1. Expected trend of travel time function.

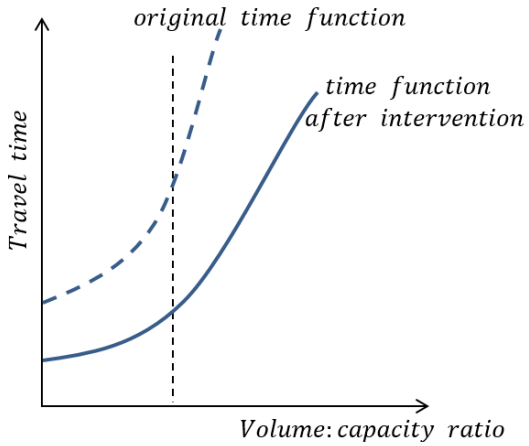

Figure 4.2. Time function before and after intervention.

Sinha and Labi (2007) detailed the decision making process for transportation systems. Transportation systems can be evaluated using costs consisting of agency costs (incurred by the road service provider) including facility maintenance costs; user costs (incurred by the road users), for example, travel time costs; and secondary costs or externalities such as congestion. When evaluating improvement strategies for transportation systems, interventions can be compared to a base alternative, typically the do-nothing option; and comparisons of the level of transportation

cost saving/ reduction can be made, and the cost optimizing alternative selected. In the evaluation process, the analyst may exclude costs that may not vary across alternatives such as initial planning, and right of way; and the costing of interventions may be done in an aggregate or disaggregate manner. Aggregate costing may involve using an average rate; for instance, cost per lane-kilometer, whereas disaggregate costing may be more detailed with costing done using prices of individual intervention items. The costs may be adjusted for temporal (e.g., inflation) and spatial variations based on the location of the project, economies of scale accrued due to handling more project units, and they may also incorporate uncertainties brought about by disasters.

Specifically, in the asset management field, Adey (2019) looked at the road infrastructure asset management process in its entirety with the goal of improving efficiency and effectiveness. Adey et al. (2020) defined impact types for users and the public and listed accident, travel time, vehicle operation, comfort, noise, and particle emissions as important considerations for road service. Adey et al. (2012) built models to evaluate total benefits of road preservation in Switzerland and showed how the relationship between benefits to road condition through pavement condition indicators, such as surface friction, surface damage and the longitudinal unevenness, and road type could be used to determine optimal intervention strategies. Adey's (2012) study built different models to evaluate intervention strategies on Swiss roads but did not develop a framework to evaluate varied interventions for multiple sections concurrently.

Madanat and Ben-Akiva (1994) developed a Latent Markov Decision Process (LMDP) for optimal inspection and repair of facilities by minimizing the sum of inspection, maintenance and rehabilitation costs. Smilowitz and Madanat (2000) extended the LMDP to include network level constraints by using randomized policies. Adey et al. (2014) built an optimization model to determine the optimal intervention strategy for a road link composed of multiple objects and investigated the use of impact hierarchy in a case study in the Netherlands. Lethanh et al. (2015) developed a model to optimize intervention strategies for multiple assets using Markov models and empirically demonstrated the model using a road link comprising one road section and one bridge. Kobayashi et al. (2013) formulated optimal policies for inspecting pavements with deterioration uncertainty by minimizing life cycle costs. These studies gave less attention to the evaluation of intervention effects on multiple sections.

The Analytic Hierarchy Process (AHP) has been used by earlier researchers to determine the priority of pavement sections for repair work. For instance, Moazami et al. (2011) and Dabous et al. (2019) used the AHP framework to prioritize pavement maintenance using the pavement condition, type, and traffic volume as the alternative options at different decision levels.

Yang et al. (2015) investigated the trade-off between road user costs and agency costs (maintenance) by balancing maintenance operations during peak and non-peak traffic hours (at night) when road user costs were low but the time was unsafe for workers and agency costs were higher. Yang et al. (2015) optimized the start time and duration of maintenance work with minimal impact on the total costs (user and agency) in the road network.

Other studies in the literature also attempted to improve the efficiency of the pavement network by suggesting different management policies. Small and Winston (1988), Newbery (1988, 1989), and Small et al. (1989) investigated specific road cost recovery policies considering road damage costs and congestion costs. They examined whether congestion and durability charges recovered costs due to road damage attributed to vehicle loading (especially by trucks) and weather, congestion, and other non-traffic related costs such as policing and lighting. Verhoef and Small (2004), and Small and Yan (2001) investigated road pricing considering differentiated products to maximize the benefits of tolling considering heterogeneous users and applied Wardrop's equilibrium for congested networks (Wardrop 1952). Liu and Wang (2016) used the stochastic user equilibrium approach based on the logit model to determine appropriate extensions to road networks by minimizing the total network travel time. Lin and Lin (2011) developed a pavement maintenance strategy for Kaohsiung, Taiwan by using pavement roughness data, traffic volume, and expert advice as the criteria to support the pavement maintenance decision process. A study by Volovski et al. (2017) empirically suggested that maintenance expenditure exhibited significant spatial and temporal variations for maintenance done at different locations and years.

As shown in the literature review, the bulk of the past studies suggest policies and models to improve efficiency and effectiveness of road maintenance to achieve acceptable road service but do not specifically build a joint framework to evaluate intervention effects on capacity and

durability. This study attempts to narrow this gap in the literature by contributing to the development of a framework to evaluate the effect of intervention on road capacity and durability for multiple sections simultaneously and shows its application through an empirical study on actual road sections.

4.4 Travel time vs. condition and capacity relationships for Ugandan roads

4.4.1 Database

Ugandan national roads are managed by UNRA under the supervision of the MoWT. As of 2017, the entire national road network in Uganda consisted of 20,544 km (4,551 km paved and 15,993 km unpaved). Road data for the year 2018 consisting of traffic volume, speed, pavement condition and type, location, and other inventory data such as the section length and width were obtained from the UNRA database (UNRA 2019). The data covered both paved and unpaved sections with the pavement condition measured using the International Roughness Index (IRI). The IRI estimates the roughness of a road obtained by measuring longitudinal road profiles using a test vehicle. UNRA engineers used a bump integrator to measure the IRI. A road section in perfectly good condition has an IRI of about 0 to 2.00 mm/m, whereas one in worse condition has an IRI of 8.00 mm/m or more (MoWT 2011–2017). The IRI was obtained mainly for paved sections at 1 km intervals, probably due to limited manpower and equipment. The traffic volume was measured in terms of the average annual daily traffic per road link using manual road counts at specific locations following the American Association of State Highway and Transportation Officials (AASHTO) average of averages method (FHWA 2018). The speed on a road section was measured using a radar gun. Sections with unknown travel speed, traffic volume, or condition (all unpaved) were cleaned out. The remaining data sample consisted of 2,425 sections each with a length of 1 km, which were reduced to 2,404 sections after further cleaning. A summary of the data is presented in the following subsections. Data was also available for 2017, but it showed similar trends to those of the 2018 data.

4.4.2 Data summary

The data summary presents the pavement condition, travel time, and volume:capacity ratio for the surveyed paved Ugandan road network. The daily traffic on Ugandan roads was heterogeneous; hence, it was converted to a homogeneous equivalent, passenger car units (PCUs), based on the PCU factor for each vehicle type according to Table 4.1. Then, the daily traffic volume was

multiplied by the thirtieth hourly volume factor of 0.15 to convert it to an hourly volume so as to compute the volume:capacity (v/c) ratio for each section (MoWT 2010). The road section capacity, the flow that produces the minimum acceptable journey speed, could be approximated from the measured width within the database. Most of the national roads were typically two-lane (with section width ranging from 6 to 11 m for all sections). The sections with a narrower width had no shoulders. The road capacity was set at the typical value of 2,200 PCU/h for two-lane roads (TRB 2000, 2010; Chandra 2004).

Table 4.1. PCU factors (MoWT 2010 and FHWA 2014)

Vehicle type	Terrain	
	Rolling	Mountainous
Motorcycles and scooters	1.0	1.5
Saloon cars and taxis	1.0	1.5
Light goods	1.5	3.0
Small buses	1.5	3.0
Medium buses	4.0	6.0
Large buses	4.0	6.0
Light trucks	1.5	3.0
Medium trucks	5.0	10.0
Truck trailer/semi-trailer	8.0	20.0
Bicycles	0.5	NA*
Carts	1.0	NA

** NA stands for not applicable.*

Histograms were developed to show the distribution of the measured travel time, roughness, and volume:capacity ratio across the surveyed sections (Figure 4.3). The histograms showed that most of the sections had a measured time falling between 50 and 100 s, most sections were uncongested ($v/c < 1$) because they are interurban center national roads, and most sections were in good to fair condition with an IRI of 5.00 mm/m and below.

Figure 4.3. Histograms for 2018 data.

Travel time τ vs. IRI scatter plots per section were generated but did not show a clear trend. A clearer trend could be seen when the plots were averaged (grouped) (Table 4.2 and Figure 4.4). It can be deduced that the condition effect was experienced from an IRI of about 4.00 mm/m and above (worse condition), shown by the exponential increase in the travel time for IRI > 4.00 mm/m, whereas the congestion effect was experienced from an IRI of about 3.00 mm/m and below (better condition), shown by the slight increase in the travel time for IRI < 3.00 mm/m.

Table 4.2. Average travel time (τ) and volume:capacity (v/c) ratio per IRI group for 2018

IRI group (mm/m)	No.	τ (s)	*v/c*
0.00–2.00	181	64.35 (22.50)	0.67 (0.34)
2.01–3.00	679	76.67** (38.40)	0.62 (0.75)
3.01–4.00	837	68.84 (35.55)	0.45 (0.58)
4.01–5.00	426	73.66 (40.44)	0.46 (0.46)
5.01–6.00	189	90.18* (61.37)	0.51 (0.63)
6.01–7.00	49	114.37* (79.02)	0.38 (0.42)
7.01–	43	172.98* (72.94)	0.73 (1.15)

Note: Values in parentheses are the standard deviations.

** Condition effect, ** congestion effect.*

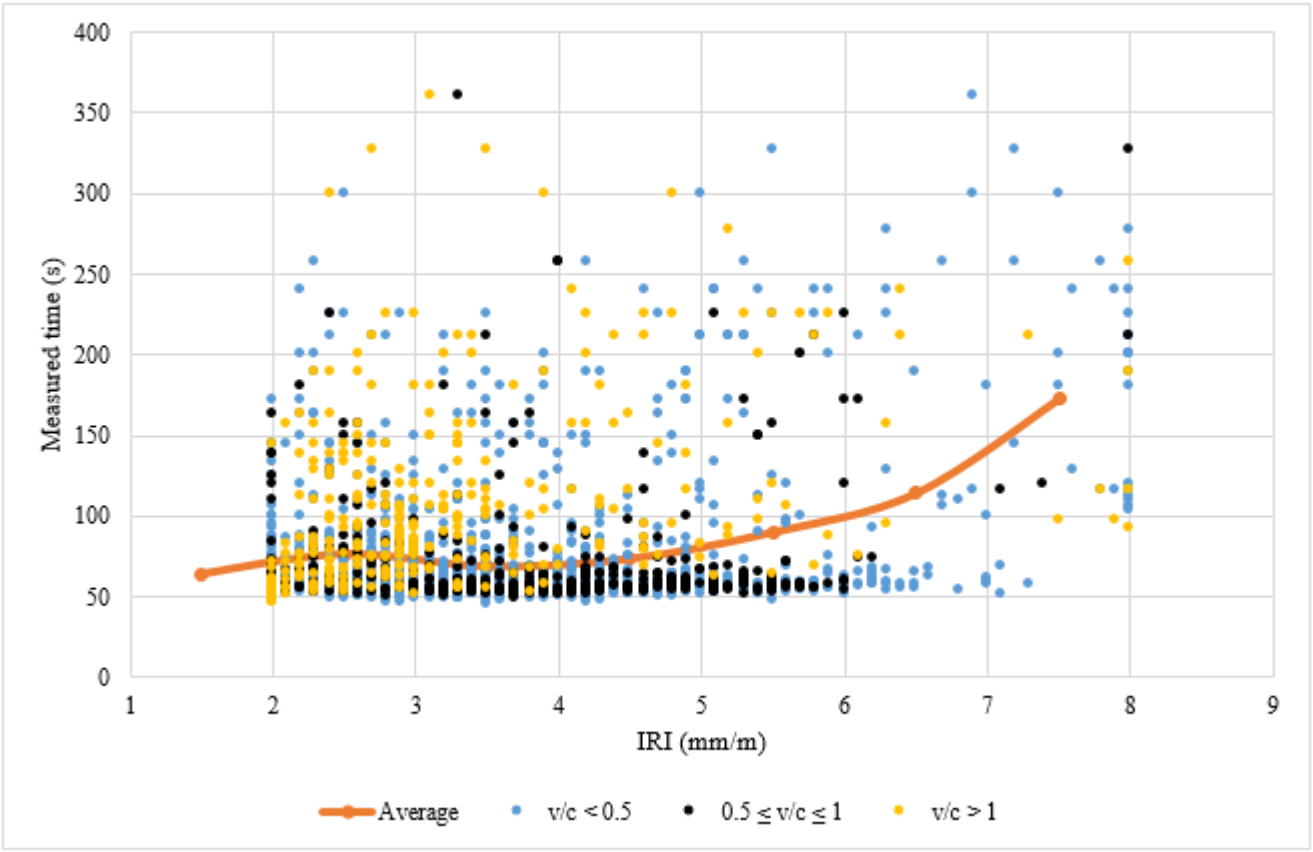

Figure 4.4. Measured time vs. IRI for 2018.

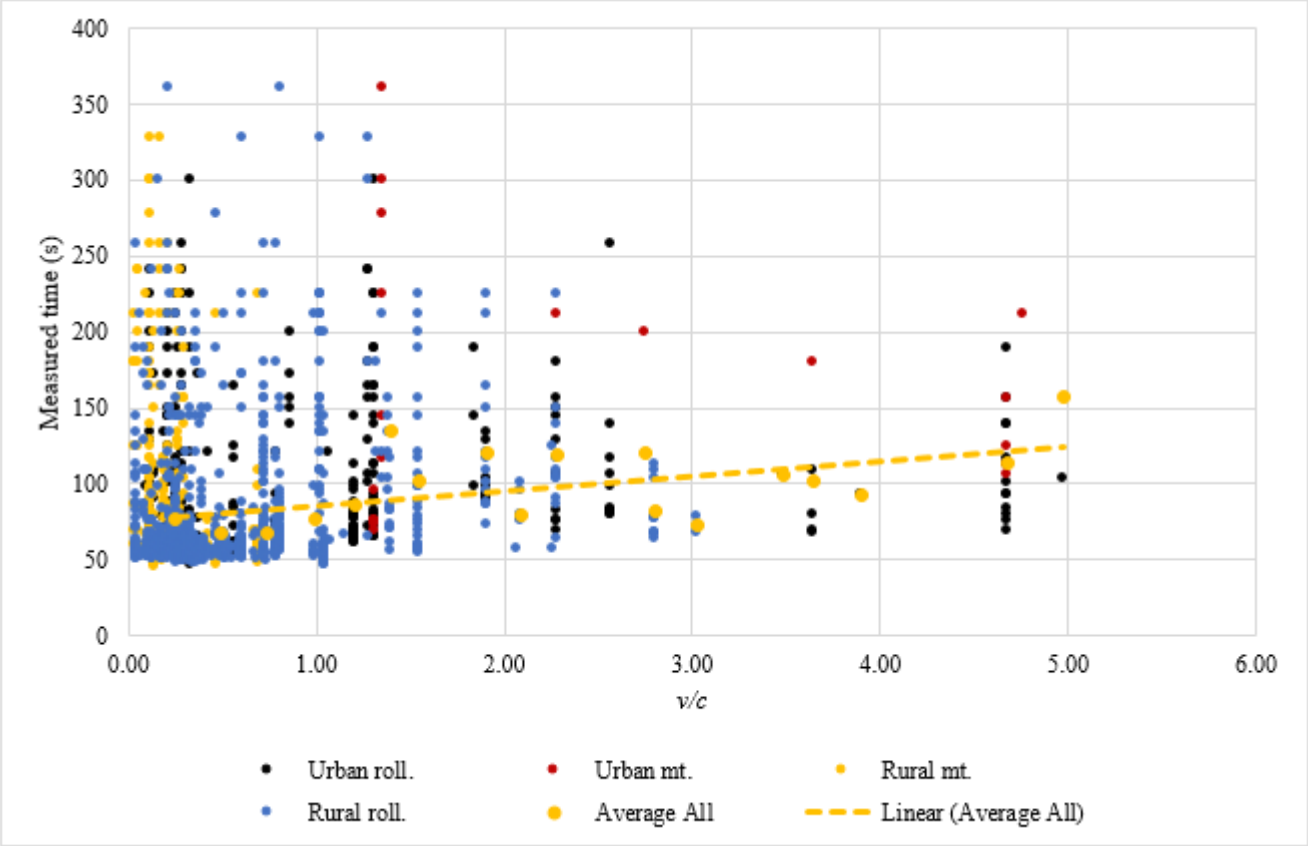

Figure 4.5. Measured time vs. v/c for 2018.

Travel time vs. volume:capacity scatter plots were also generated but, again, these plots did not clearly show that the travel time increased with an increase in the volume:capacity ratio. Hence, the sections were classified based on the location (urban or rural) and terrain (rolling or mountainous) as shown in Table 4.3. This classification showed that urban roads were more congested than rural roads and that roads in mountainous areas were less congested compared to those in rolling terrain. The vertical lines of the plotted points, which represent roads, showed that one road may crisscross from one region to another; e.g., from rural-rolling to rural-mountainous (Figure 4.5). Therefore, the sections were grouped into 45 road groups based on the location and terrain (Table 4.3). When grouped, the worst condition, average volume:capacity ratio, and average travel time within the group were obtained. The worst condition was considered for safety reasons and the average travel time and volume:capacity ratio were considered because national roads are not as heavily trafficked as urban roads. The travel time vs. volume:capacity trend became clearer with the travel time being stagnant when $v/c \leq 0.5$ and then increased when

$v/c > 0.5$ (Figure 4.6). It was also shown that roads in urban mountainous areas had longer travel times. The histograms developed for the 45 road groups showed a similar distribution for the measured travel time and volume:capacity ratio as for the case of individual sections. For the roughness, the proportion in a worse condition showed a slight increase for groups (Figure 4.7).

Table 4.3. Number of road sections and groups for 2018 data

Region	Sections	Groups
Urban mountainous	20	6
Urban rolling	436	13
Rural mountainous	434	13
Rural rolling	1,514	13
Total	2,404	45

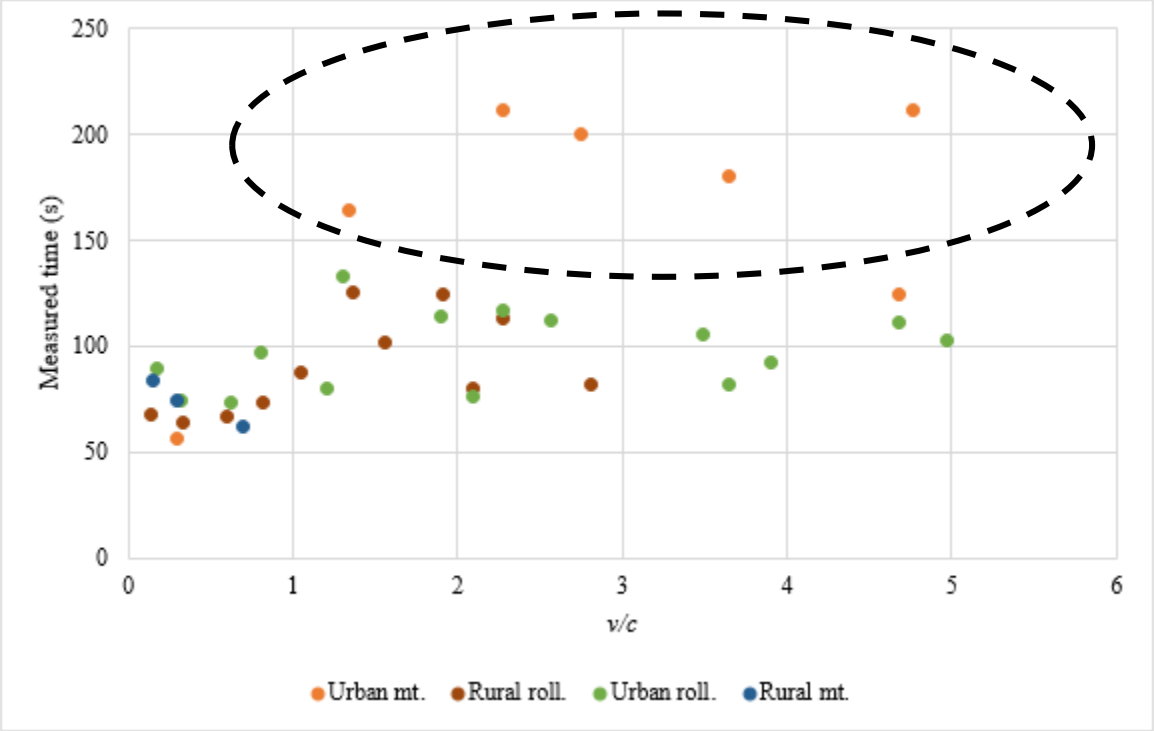

Figure 4.6. Average measured time vs. v/c per group for 2018.

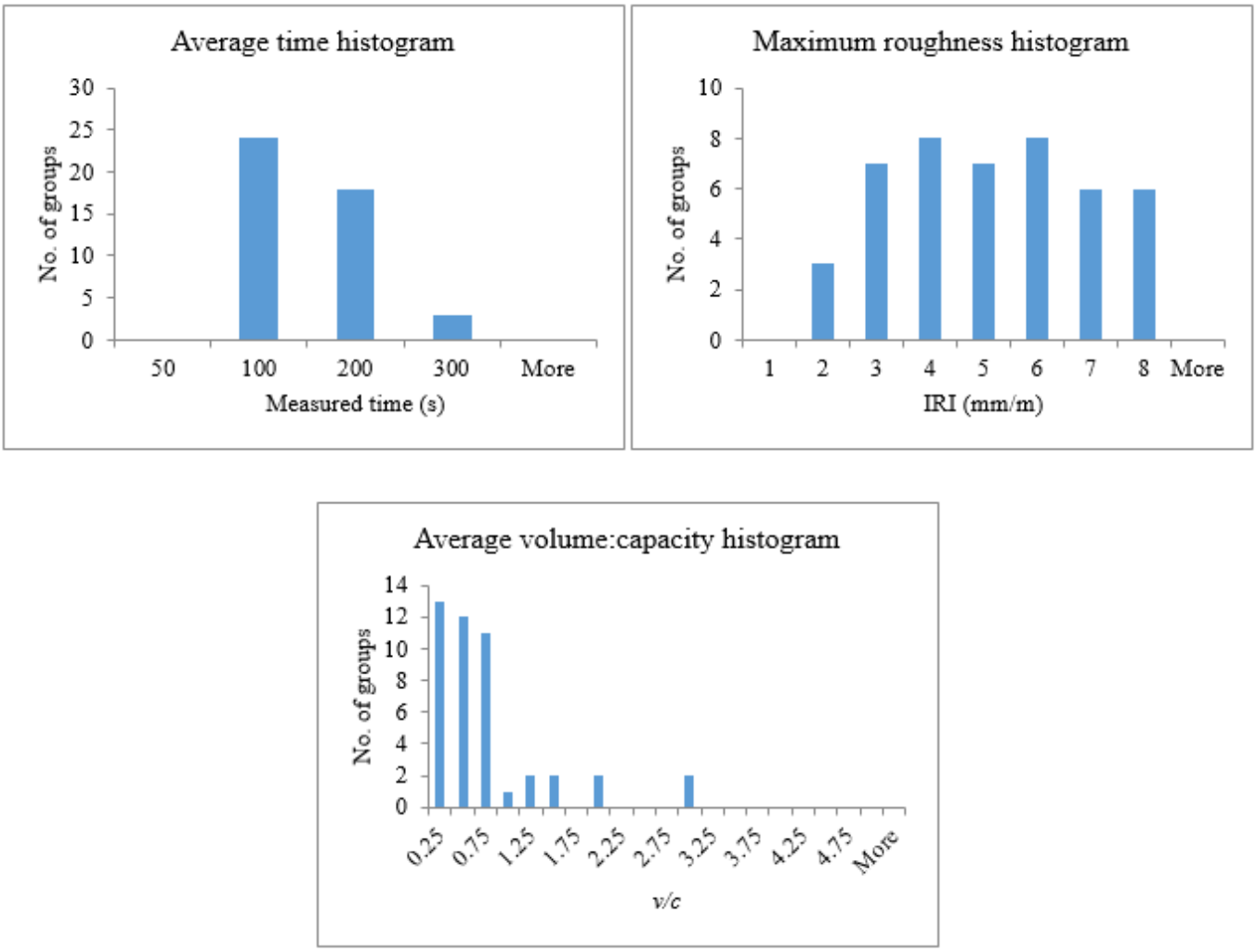

Figure 4.7. Histograms for groups for 2018.

Based on the data summary, it was shown that grouping the road sections produced the expected trend as shown in the literature and thus could generate better model estimates compared to using individual sections. This can be explained by the fact that road sections on the same link or interlinked sections interact and the condition of one section may affect the travel time on other sections.

4.5 Model

4.5.1 Model Framework and Notation

Road networks consist of origins and destinations joined by links comprising sections and nodes. Nodes are often seen as junctions or points representing changes in the link characteristics; e.g.,

travel speed, capacity, etc. (Luis 2008). In the model, a road network is subdivided into individual (discrete) pavement sections because the identification of poor network sections may be more targeted which could make intervention more effective. Based on the data summary as shown in Figure 4.4 and Table 4.2; the BPR function, a regression model, may be suitable to represent the relationship between travel time, condition and volume:capacity ratio on paved Ugandan roads. Consider a road network with a population of K^g road sections with $k^g = 1^g, \dots, k^g$ each belonging to a group $g = 1, \dots, G$. Each road section k^g has a covariate vector $\boldsymbol{X}^{k^g} \in \mathbb{R}^q +$, and requires travel time $\tau^{k^g} \in \mathbb{R} +$ to traverse. The scalar q is defined as $q(q = 1,2,3, \dots)$. The travel time on each section τ^{k^g} can be defined as a regression model:

$$\tau^{k^g} = \theta_1 (X_1^{k^g})^n + \cdots + \theta_q \left(X_q^{k^g}\right)^{n'} \tag{4.1}$$

where

$\theta_1, \dots, \theta_q$ are unknowns collected in the parameter $\boldsymbol{\theta}$;

$n(n = 1,2,3, \dots)$ is an index; and

$\mathbb{R} +$ denotes positive real numbers.

The notation $n^{'}$ is used to avoid confusion that may arise because index n may vary for each covariate. The covariate vector may include covariates: the pavement condition $i^{k^g} = X_1^{k^g}$, and the traffic volume:capacity $(v^{k^g}/c^{k^g}) = X_2^{k^g}$ following the parametric BPR power function (BPR 1964) with the pavement condition as an additional explanatory variable.

The society, including road users, may face the travel time and intervention costs. The benefits of product differentiation for the case of heterogeneous users as discussed by Small and Yan (2001) were not considered. Intervention costs were assumed to have no spatial variations. Also, discount rates considering multiple interventions at the same time (economies of scale) were fixed and discounts considering the time value of money were not considered because the interventions for all candidate sections were assumed to be done at once. Additionally, for this study, even if we considered such discounts, there may be no significant change in the results. In the actual road network, users may shift to a route with a lower travel cost or stop travel altogether. For simplicity,

it was assumed that there was no incentive (i.e., free-flow conditions or no charges) for road users to change their route (section) or to stop travel; hence, the traffic volume v^{k^g} was assumed to remain constant on each section k^g.

Pavement durability may be affected by traffic loading, moisture penetration to sublayers, and significant temperature variations (i.e., loading and weather). Pavement durability was included in the model using the variable pavement condition. Congestion is one of the major indicators of the level of service of a road network. Inadequacy in road capacity was included in the model by considering the volume:capacity (v^{k^g}/c^{k^g}) ratio on a road section.

Whereas other studies (e.g., Small and Yan 2001; Lui and Wang 2016) have approached network design problems by using Wardrop's equilibrium (Wardrop 1952), the present study optimized the social cost considering action on each individual section because of the generally lower traffic levels (uncongested) for intercity national roads following optimization frameworks; e.g., Yang et al. (2015), Smilowitz and Madanat (2000). This was because equilibrium may be difficult to achieve for uncongested roads within practical time limits contrary to Wardrop's consideration of congested networks. Optimum intervention strategies were obtained by minimizing the social cost ξ. The social cost was defined as a summation of travel and intervention costs, incurred by the society, for all road sections.

4.5.2 Travel Time Function

As shown in the data summary, it was more likely that regression on groups could generate better results compared to regression on individual sections. The adopted travel time function was general; i.e., it could be applied to groups or individual sections. Comparisons could then be made for regression results considering groups or individual sections to determine the better model fit.

The travel time $\tau^{k^g}\left(i^{k^g}, v^{k^g}, c^{k^g}\right)$ was defined as a function of the pavement condition i^{k^g}, traffic volume v^{k^g}, and section capacity c^{k^g} as shown by the modified BPR function in Equation (4.2) with the unknown parameter vector $\boldsymbol{\theta}$ and index n. The modified BPR function was more promising because Ugandan road data showed an exponential increase in the travel time after the significant condition i^{k^g*} and significant volume:capacity ratio $(v^{k^g}/c^{k^g})^*$. The original BPR

function has a power of $n = 4$ and $\theta_2 = 0.15$, and does not include the condition term. Whereas other studies have used linear functions with explanatory variables to define the travel speed (TRB 2000, 2010; Chandra 2004; Vlahogianni 2007; Wang et al. 2014; Ravi Sekhar et al. 2016) or the travel time (Iryo et al. 2005), this study defined travel time using the nonlinear function:

$$\tau^{k^g} = \tau^{k^g,0}\left[\left\{1 + \theta_1 f(i^{k^g})\right\}\left\{1 + \theta_2\left(f(v^{k^g}/c^{k^g})\right)^n\right\}\right] \tag{4.2}$$

$$f(i^{k^g}) = \begin{cases} 0 & if\ \ IRI^{k^g} \le i^{k^g*} \\ (i^{k^g} - i^{k^g*})^y & if\ \ IRI^{k^g} > i^{k^g*} \end{cases}$$

$$f(v^{k^g}/c^{k^g}) = \begin{cases} 0 & if\ \ (v^{k^g}/c^{k^g}) \le (v^{k^g}/c^{k^g})^* \\ (v^{k^g}/c^{k^g}) - (v^{k^g}/c^{k^g})^* & if\ \ (v^{k^g}/c^{k^g}) > (v^{k^g}/c^{k^g})^* \end{cases}$$

where

θ_1 and θ_2 are unknowns collected in parameter $\boldsymbol{\theta}$;

$\tau^{k^g,0}$ is free-flow travel time on section k^g when traveling at the FFS;

IRI^{k^g} is the IRI of section k^g;

$f(i^{k^g})$ and $f(v^{k^g}/c^{k^g})$ are the condition and volume:capacity functions, respectively;

y is an index; and

i^{k^g*} and $(v^{k^g}/c^{k^g})^*$ are the condition and volume:capacity significant values.

During free flow, $\theta_2 = 0$ and at full capacity ($v^{k^g} = c^{k^g}$), the critical speed is reached, where operations are unstable and any slight disturbance to the network causes traffic flow breakdown (FHWA 2018).

Road users may prefer a specific section leading to negative impacts, such as congestion. Oversized vehicles and junctions (in urban settings) are the main contributors to congestion (Lu et al. 2016; Luis 2008). In this study, the congestion externality was captured in the volume:capacity ratio (delay cost) term in Equation (4.2).

The modified BPR function can be calibrated as a nonlinear least squares problem by minimizing the loss function $L(\tau^{k^g}, \boldsymbol{X}^{k^g}; \boldsymbol{\theta}, n)$. The loss function was defined as the sum of squared deviations

between the predicted travel time and the actual measured travel time for all road groups. The objective function can be expressed as:

$$\min_{\boldsymbol{\theta}, n} L = \sum_{k^g=1}^{K^g} \left(\tau_{model}^{k^g} - \tau_{measured}^{k^g}\right)^2 \tag{4.3}$$

For regression on individual sections, exact section values can be used. When regression is done based on groups, group data $\overline{\boldsymbol{g}}(\overline{\tau^{k^g}}, \overline{(v^{k^g}/c^{k^g})}, \overline{\imath^{k^g}})$ may be defined as:

$$\overline{\tau^{k^g}} = \frac{1}{k^g} * \sum_{k^g=1^g}^{k^g} \tau^{k^g} \qquad \forall g \tag{4.4}$$

$$\overline{(v^{k^g}/c^{k^g})} = \frac{1}{k^g} * \sum_{k^g=1^g}^{k^g} (v^{k^g}/c^{k^g}) \qquad \forall g \tag{4.5}$$

$$\overline{\imath^{k^g}} = \underset{i^{k^g}}{argmax} f\left(i^{k^g}\right) \qquad i^{k^g} \in g \ \ \forall g \tag{4.6}$$

4.5.3 Calibration of the Modified BPR Function

The modified BPR function was calibrated using the data for 2018, and then the model was applied to the entire surveyed paved Ugandan national road network. The significant values $i^{k^{g*}}$ and $(v^{k^g}/c^{k^g})^*$ were fixed at 4.00 mm/m IRI and 0.5, respectively based on the surveyed Ugandan pavement data summary. Other significant values did not generate majorly different results. Also, model calibration considering individual sections did not generate better results compared to calibration considering groups. In the calibration, the following considerations were made:

1) The FFS was set according to Figure 4.8 and Table 4.4.
2) Higher travel speeds can be achieved in rural areas and for rolling terrain. The free-flow travel time was obtained from the FFS by dividing it by the section length.

3) The data was aggregated into groups based on the terrain and location. For aggregate data, the worst condition value, average time, and average volume:capacity ratio were used as a representative section for a group in the estimation.
4) The index y was fixed to 1 because the use of other values did not improve the results.

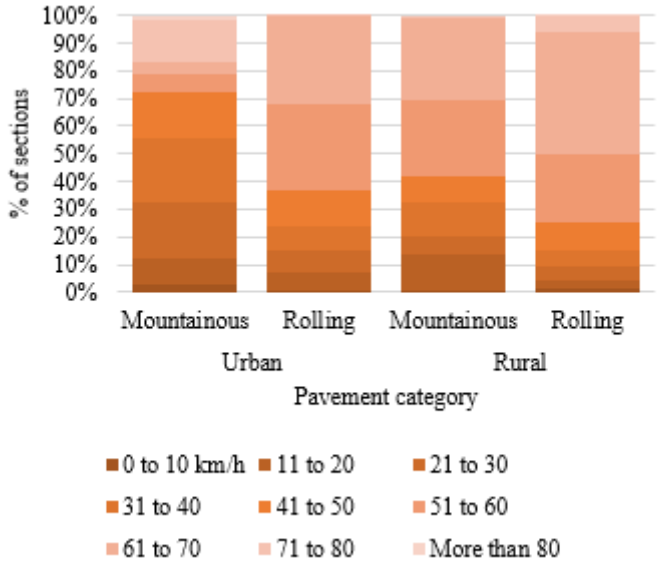

Figure 4.8. Speed achieved on surveyed Ugandan national road sections.

Table 4.4. Average speed (km/h) and set FFS

Development Category	Urban		Rural	
Terrain	Mountainous	Rolling	Mountainous	Rolling
Average speed*	41.68	50.63	47.41	55.54

**Average speed was set as the FFS.*

The parameter $\boldsymbol{\theta}$ and index n were estimated using R programming language as shown in Table 4.5 and Table 4.6. The model calibration results showed that the road condition and volume:capacity ratio were strongly related to the travel time. The condition and volume:capacity ratio parameters had a low standard error, with a significant *t*-value and *p*-value for a 95% confidence interval. This result empirically shows that the road condition and volume:capacity ratio have a significant effect on the travel time. The positive sign for the condition parameter indicates that as the condition worsens, the travel time increases. The same can be inferred for the volume:capacity ratio. Also, the estimated θ_2 value was close to that of the original BPR equation.

The n value was insignificant; hence, it was also fixed to 1. Other nonlinear relationships were tested with y free or fixed to other values but the results were not any better. Figure 4.9 shows the plots of the estimated vs. measured time with points generally falling close to the 45° line. The results for the 2018 data in Table 4.6 showed the best parameter estimate. It should be noted that the inaccuracy in the model is due to noise in the data because the travel time is also affected by other factors such as the road geometry and driver behavior, but not only the road condition and traffic volume as considered in this study.

Table 4.5. Estimated parameter values with *n* free for 2018

R^2	Variable	Parameter	Estimated value	Standard error	*t*-value	Pr (>|t|)	Significance code
0.5778	Condition	θ_1	0.3157	0.04651	6.79	2.91e-08	***
	Volume/ capacity	θ_2	0.4385	0.12576	3.49	0.00116	**
	Power	n	0.5479	0.35498	1.54	0.13024	

*Significance codes: ***: 0, **: 0.001, *: 0.01*

Table 4.6. Estimated parameter values with *n* fixed for 2018

R^2	Variable	Parameter	Estimated value	Standard error	*t*-value	Pr (>|t|)	Significance code
0.5615	Condition	θ_1	0.3331	0.04387	7.59	1.8e-09	***
	Volume/ capacity	θ_2	0.3481	0.09740	3.57	0.00088	***
	Power	n	1				

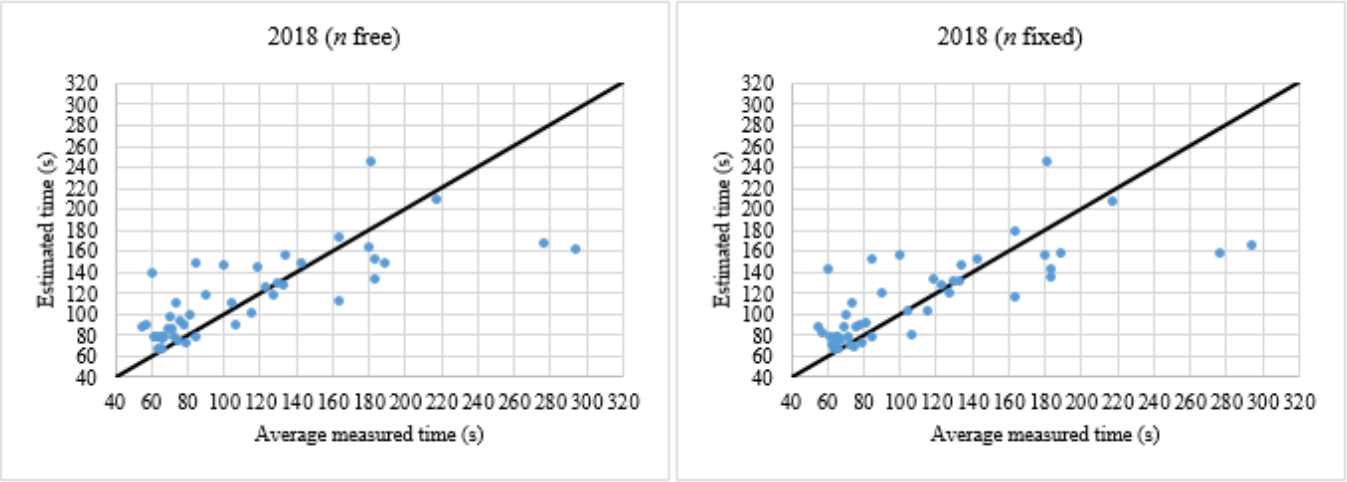

Figure 4.9. Estimated vs. average measured time plots.

From the results in Table 4.6, it can be seen that 1 unit improvement in condition i^{kg} results in a reduction of 0.3331/(1 + 0.3331i^{kg}) in the travel time if v^{kg}/c^{kg} is held constant. This shows that a unit improvement in the condition for roads in fair condition (smaller i^{kg}) has a larger net reduction in the travel time compared to that for roads in a worse condition (larger i^{kg}). Similarly, a unit improvement in v^{kg}/c^{kg} results in a reduction of 0.3481/(1 + 0.3481(v^{kg}/c^{kg})) in the travel time if i^{kg} is held constant.

4.5.4 Pavement Intervention

Pavement management decisions such as improving the condition, increasing the capacity, and no action are considered to be undertaken by the road agency. Action A_i is taken to improve the section condition, action A_c to increase the section capacity, and action A_0 is no action. This attracts an intervention unit cost $C^{kg,A}$ considering a specified intervention $\boldsymbol{A}(A = A_i, A_c, A_0)$ for section area a_{kg} to be improved ($C^{kg,A_0} = 0$). When intervention occurs, the condition and capacity improve based on Equations (4.7) and (4.8) respectively.

$$i^{kg} = \begin{cases} i^{kg} - \nabla & if\ A_i \\ i^{kg} & otherwise \quad A_0 \end{cases} \tag{4.7}$$

$$c^{kg} = \begin{cases} mc^{kg} & if \quad A_c \\ c^{kg} & otherwise \quad A_0 \end{cases} \tag{4.8}$$

where

m is the percentage change in the capacity; and

∇ is the improvement in the condition.

4.5.5 Social Cost

The social cost $\xi(\tau^{kg}, C^{kg,A})$ is presented as a summation of the travel and the intervention cost as shown in Equation (4.9). Intervention costs were considered to be paid for by the society to maintain public road infrastructure; therefore, they are a form of social cost. It was assumed that the intervention is done once a year on a road section and thus the road user travel cost was

computed for 365 days.

$$\xi = \sum_{g=1}^{G} \left\{ \left(365\omega k^g \overline{v^{kg}} * \overline{\tau^{kg,A}}\right) + \sum_{k^g=1}^{k^g} \sum_{A} a_{k^g} C^{k^g,A} \right\} \tag{4.9}$$

where

ω is the monetary value of one unit of travel time;

$\overline{\tau^{kg,A}}$ is the new average travel time on k^gsections in group g after intervention, $\boldsymbol{A}$; and

$\overline{v^{kg}}$ is the average volume on k^gsections in group g.

4.5.6 Objective Function and Solution Algorithm

The objective of the model is to minimize the total social cost ξ ; hence, the objective function can be expressed as shown in Expression (4.10) with feasibility and budget Constraints; (4.11) and (4.12) respectively.

$$\min_{\boldsymbol{A}} \ \xi \tag{4.10}$$

$$Subject\ to$$

$$\boldsymbol{A} \in \boldsymbol{\Gamma} \tag{4.11}$$

$$\sum_{g=1}^{G} \sum_{k^g=1^g}^{k^g} \sum_{A} a_{k^g} C^{k^g,A} \in \Omega \tag{4.12}$$

where

$\boldsymbol{\Gamma}$ is a set of all feasible actions; and

Ω is the budget limit.

The discrete sections for intervention are selected using a greedy algorithm (GA) (Rinnooy Kan et al. 1993). The discrete candidate sections with the largest reduction in social cost $\left(\xi_0 - \xi_A^{k^g}\right)$ are

selected first by the GA until the entire budget is consumed in a typical knapsack procedure. If the reduction in social cost ($\xi_0 - \xi_A^{k^g}$) is the same for several sections, this may result in their clustering in the same position for intervention forming a Pareto frontier. To overcome this challenge, a second decision level based on the priority weight W^{k^g}, prioritizing sections based on traffic volume v^{k^g} and condition i^{k^g}, may be introduced as an application of the AHP. This can be explicitly expressed as follows:

$$\underset{\boldsymbol{A}}{max}\ \left(\xi_0 - \xi_A^{k^{g\prime}}\right) + \delta W^{k^{g\prime}} \qquad A^{k^g} = 0\ for\ \forall\ k^g \neq k^{g'} \tag{4.13}$$

$$W^{k^g} = \frac{v^{k^g}}{v_{max}^{k^g}} \times \frac{i^{k^g}}{i_{max}^{k^g}}$$

$$\delta = \begin{cases} 1 & if\ \ \left(\xi_0 - \xi_A^{k^g}\right)\ is\ the\ same\ for\ sections\ k^g \\ 0 & if\ \ \left(\xi_0 - \xi_A^{k^g}\right)\ is\ different\ for\ sections\ k^g \end{cases}$$

where

ξ_0 is the initial social cost;

$\xi_A^{k^g}$ is the social cost if action A is taken for section $k^{g\prime}$ and nothing is done for other sections k^g;

W^{k^g} is the priority weight;

$v_{max}^{k^g}$ is the maximum v^{k^g} for all sections;

$i_{max}^{k^g}$ is the maximum i^{k^g} for all sections;

δ is a dummy variable to avoid clustering at one intervention position; and

the symbol [′] is used to distinguish $k^{g\prime}$ from other sections k^g.

The solution algorithm is shown in Figure 4.10. The steps of the algorithm are detailed below.

1) Set the safety limit $\underline{i^{k^g}}$.
2) Propose interventions that prioritize safety; hence, sections with $i^{k^g} > \underline{i^{k^g}}$ are repaired first. For sections above the safety limit, the worst sections are prioritized (repaired first).
3) Check that the feasibility constraint has been met for unsafe sections selected for repair.
4) Check that the budget constraint has been satisfied for the repair work for the unsafe

sections.

5) Propose interventions (A_i , A_c) for all remaining sections k^g with $i^{k^g} > i^{k^g*}$ and $v^{k^g}/c^{k^g} > (v^{k^g}/c^{k^g})^*$ and calculate the social cost $\xi_A^{k^g}$ each time for each candidate section and each proposed intervention.
6) Check that the feasibility constraint has been met again for the proposed interventions.
7) Calculate $\xi_A^{k^{g\prime}}$ for each candidate section $k^{g\prime}$ given that $A^{k^g} = 0$ for $\forall k^g \neq k^{g\prime}$.
8) Select the candidate sections for intervention using a GA based on $\underset{\boldsymbol{A}}{max} \left(\xi_0 - \xi_A^{k^{g\prime}}\right) + \delta W^{k^g}$.
9) Calculate ξ cumulatively for the selected sections and the change in cumulative social cost $\Delta\xi(k^g)$ for each candidate section k^g and discard action for candidate sections with an increase in ξ.
10) Check that the budget constraint has been satisfied and cut off actions for candidate sections that are outside the budget limit.
11) Determine the optimum intervention strategy and social cost for each set $\underline{i^{k^g}}$.

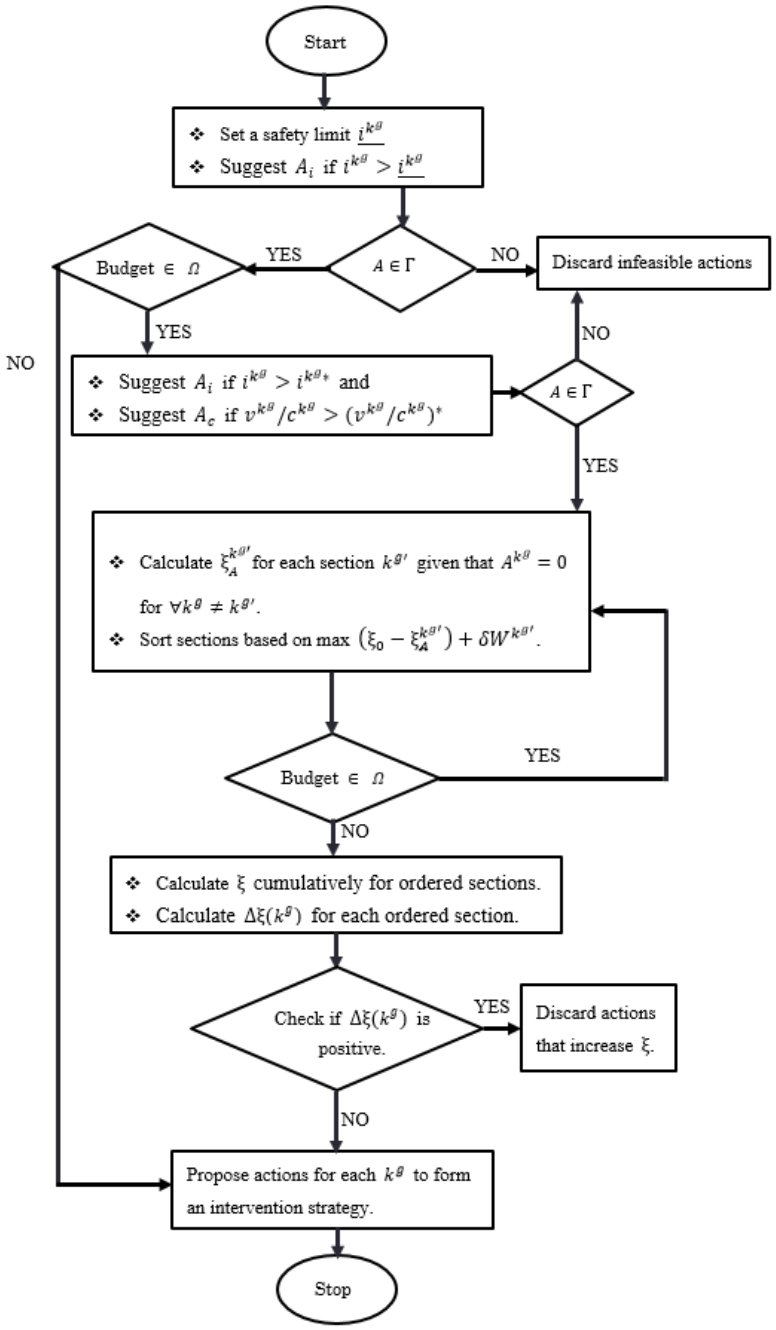

Figure 4.10. Solution algorithm.

4.6 Model Application

4.6.1 Optimum Intervention Strategy for Surveyed Paved Ugandan Roads

This subsection describes the application of the model to determine the optimum intervention strategy for paved Ugandan road sections. Intervention costs were set based on Ugandan road maintenance costs. The data for 2018, with the best estimate of the travel time model, was used in

the determination of the optimum strategy. The cost of the interventions was set according to Table 4.7. No action was taken for sections in good condition with an IRI $\leq$ 4.00 mm/m and uncongested sections with $v^{kg}/c^{kg} < 0.5$. When repair was done, section roughness was assumed to improve by $\nabla = 1\ \mathrm{mm/m}$ roughness. When capacity was increased, section capacity was doubled; i.e., from a two-lane (c^{kg} = 2,200 PCU/h) to a four-lane section (c^{kg} = 4,400 PCU/h). For sections below the safety limit $\underline{i^{kg}}$, the section condition was considered to improve to the best condition (about $2\ \mathrm{mm/m}$ roughness) when it was repaired and the safety improvement cost was set to twice the repair cost. The traffic was assumed to flow for 12 h in a day because night traffic is normally negligible. It was also assumed that technological improvements restricted the repair (overlay cost) at the lower boundary and the capacity improvement cost at 70% of the current cost. The current Ugandan national road maintenance budget is mainly allocated to paved roads because it is still a deficit. The budget was US$138.3 (hereafter $ is used), $145.2, $118.8, and $166.1 million in fiscal year 2013/14, 2014/15, 2015/16, and 2016/17, respectively, for the entire 4,551 km paved network (MoWT 2011–2017). This averaged to about $31,223/km, which was set as the current budget level. For 2,404 km paved roads, the current budget limit was set to $75.06 million.

Table 4.7. Cost of interventions (MoWT 2011–2017, UNRA 2018)

Action	Unit cost*
Repair (A_i)	(280-497.5)
Capacity increase (A_c)	2,360

**Value in 1,000 $/km (in 2017). Range shows the value for low- and high-traffic roads.*

The proposed intervention policies were evaluated within a period of one year; hence, discounting of costs was unnecessary. The monetary value of one unit of travel time in Uganda was estimated based on the transport charges in Uganda and its environs. In 2015, road freight charges from Kampala to Nairobi, a distance of about 688 km, were approximately $500 (0.73 $/km) (NCTTA 2015). Based on the Ugandan freight charges and the average time required to travel one kilometer (76.04 s), the exogenous variable ω was set to 34.56 $/PCU/h. The estimated variable ω excludes other important considerations for unit travel cost such as costs to other road users because of the lack of more accurate travel cost data on Ugandan roads. Also, the results may not change significantly if other unit travel cost values were used. Four safety limits $\underline{i^{kg}}$ were considered to be set by the road agency, as shown in Table 4.8. Two intervention batches were considered. The

first batch involved repairing sections to meet the safety levels and the second batch involved setting interventions that optimized the social cost.

Table 4.8. Social cost per set safety limit for surveyed Ugandan national roads at current budget level

$\underline{\iota^{k^g}}$	ξ ($million)	Reduction in ξ (%)	No. of sections repaired out of 762 candidates			No. of sections with capacity increased out of 815 candidates
			*Batch 1	*Batch 2	Total	
Do nothing	11,562.6899	0.00	0	0	0	0
4	10,975.3483	5.08	134	0	134	0
5	10,975.3483	5.08	134	0	134	0
6	10,843.9522	6.22	103	3	106	10
7	10,749.2520	7.04	48	6	54	28

**Batch 1 contains sections above the safety limit that were repaired and batch 2 contains sections within the safety limit but repaired to optimize the social cost.*

An optimization program, which was developed in Python programming language based on the solution algorithm, produced the optimum results for each set safety limit and at different budget levels. Data preparation was done in Microsoft Excel with each section having free-flow travel time, condition, volume:capacity ratio, traffic volume, and a group label. It was empirically shown that the stricter the safety limit (smaller IRI) for the surveyed paved Ugandan national roads, the higher the social cost (Table 4.8 and Figure 4.11). At stricter safety limits, there was less flexibility in optimizing the social cost as more sections were preselected for repair. The opposite was true for less strict safety limits (higher IRI), in which case more sections were selected for capacity increase by the optimization algorithm. The results showed that at the stricter safety limit of 6 mm/m, more sections (103) were preselected for repair in the first batch with low flexibility for optimization resulting in the higher total social cost (about $10.84 billion) compared to the less strict safety limit of 7 mm/m with a social cost of $10.75 billion and 48 first batch sections.

Also, at the less strict safety limit of 7 mm/m, more sections (28) were selected for capacity increase compared to the 10 sections selected at the stricter 6 mm/m safety level in the second batch. This framework could therefore be useful for road administrators to evaluate the trade-off off between safety and social cost; and between capacity increase and condition improvement for multiple road sections (Figure 4.12).

The largest reduction in social cost (7.04%) at the current budget level for Uganda's case was realized at the safety limit of 7 mm/m road roughness and the second-largest reduction was 6.22% at a 6 mm/m safety limit. Based on the set standards, the road agency may choose the appropriate safety limit but not necessarily the lowest cost option.

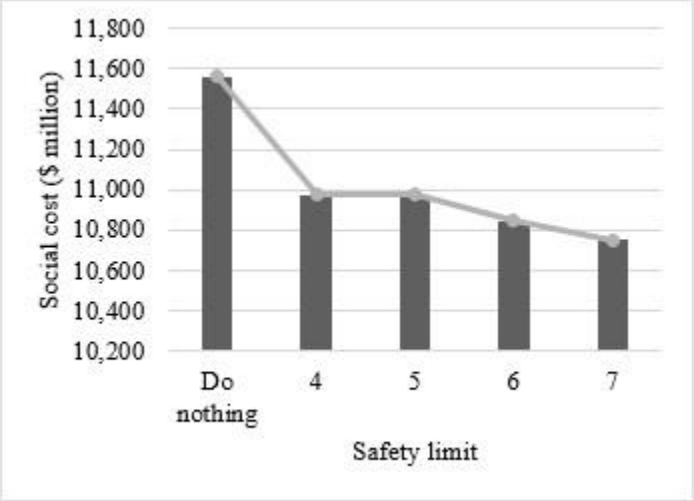

Figure 4.11. Social cost at safety levels at the current budget level.

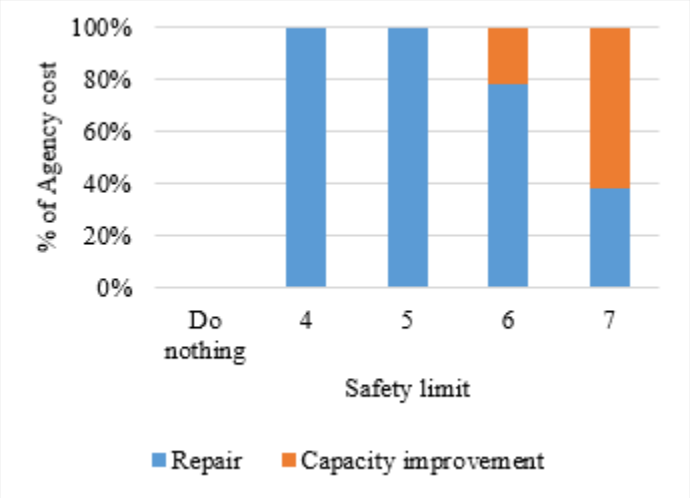

Figure 4.12. Percentage of repair or capacity improvement cost at each safety limit at current budget level.

At a 6 mm/m safety limit, the social cost was reduced by 13.83%, the largest reduction, when the

budget was increased up to about 535%, beyond which the social cost stagnated (Table 4.9 and Figure 4.13). To carry out interventions on all candidate sections in the surveyed paved network (i.e., when a limitless budget was considered), a budget level of $1,588.58 million, a 2,017% increase, was found to be sufficient; however, there was no improvement in the social cost reduction. A similar trend was observed for other safety limits. This suggested that it was counterproductive to increase the road maintenance budget arbitrarily.

Table 4.9. Social cost per set budget level for surveyed Ugandan national roads at $\underline{i^{kg}} = 6$

% increase in Ω	ξ ($million)	Reduction in ξ (%)	No. of sections repaired out of 762 candidates			No. of sections with capacity increased out of 815 candidates
			Batch 1	Batch 2	Total	
Current	10,843.9522	6.22	103	3	106	10
5	10,805.0146	6.55	103	4	106	12
10	10,753.7840	6.70	103	6	109	14
25	10,703.8913	7.43	103	6	109	21
50	10,603.0933	8.30	103	13	116	31
100	10,490.2514	9.27	103	23	126	52
200	10,379.1245	10.24	103	43	146	94
500	9,993.4319	13.57	103	305	408	186
535	9,963.9635	13.83	103	316	419	200
600	9,963.9635	13.83	103	316	419	200
750	9,963.9635	13.83	103	316	419	200

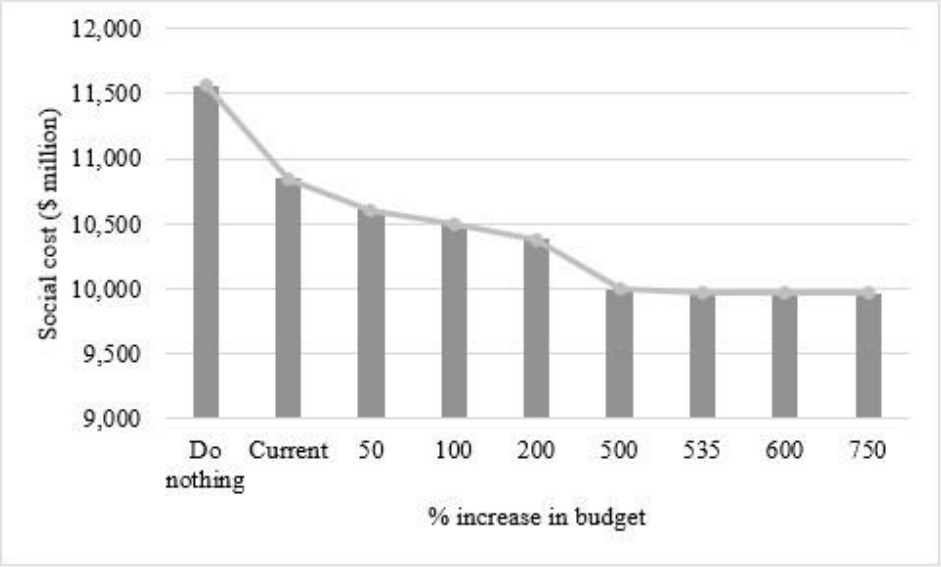

Figure 4.13. Social cost at different budget levels at $\underline{i^{kg}} = 6$.

After the safety limit had been met, the priority order of candidate sections for intervention varied based on interventions that optimized the social cost. The change in order is inferred in Table 4.8 where the number of sections for repair reduced, whereas the number of sections for capacity improvement increased as the safety limit was made less strict.

4.6.2 Discussion of Main Results

The main results in this study include the calibration of the travel time function and the model application to Ugandan road pavements. Based on the Ugandan pavement data, the significant values i^{k^g*} and $(v^{k^g}/c^{k^g})^*$ were fixed at 4.00 mm/m IRI and 0.5, respectively, for the empirical application of the travel time function. Other significant values did not generate better results. Also, model calibration considering individual sections did not generate better results compared to calibration considering groups. The results for the 2018 data shown in Table 4.6 gave the best estimate. The model calibration results showed that the road condition and volume:capacity ratio had a strong relationship with the travel time. The condition and volume:capacity ratio parameters had a low standard error, with a significant *t*-value and *p*-value for a 95% confidence interval. This result empirically shows that the road condition and volume:capacity ratio have a significant effect on the travel time. The positive sign for the condition parameter indicates that as the condition worsens, the travel time increases. The same can be inferred for the volume:capacity ratio. Also, the estimated θ_2 value was close to that of the original BPR equation.

In the model application, when stricter safety limits were set, more sections could be preselected for repair with low flexibility for optimization resulting in a higher total social cost. As the safety limit was made less strict, more sections could be selected for capacity increase due to the increase in the pool of candidate sections for optimization. With a larger pool of sections for optimization, a more optimum intervention strategy and hence lower social cost could be achieved. Therefore, the model can be a useful tool for road managers to evaluate the trade-off between safety and social costs; and between repair and capacity increase for multiple road sections at different safety limits.

At the 6 mm/m safety limit, the largest reduction in the social cost was achieved at a budget increase of about 535%, above which the social cost stagnated for the paved Ugandan roads. Beyond this point, the intervention costs increased yet the travel costs generally remained stagnant;

hence, the algorithm did not select more sections for intervention. This was because carrying out intervention on less congested sections in good condition was counterproductive.

4.7 Conclusion

This study developed a model to aid the decision process on simultaneous pavement interventions (condition improvement and capacity increase) by optimizing the social cost for multiple road sections. A framework to evaluate the trade-off between pavement repair and capacity increase at set safety limits and a model with a modified BPR function that incorporated a condition variable were developed. After calibrating the travel time function, an empirical study was carried out on the surveyed paved Ugandan national road network at different safety limits and budget levels.

The calibration of the travel time function empirically showed a significant relationship between the travel time and condition and volume:capacity ratio for Uganda's case. When applying the model to the surveyed paved Ugandan road network, the use of less strict safety limits resulted in a larger reduction in the social cost because there was more flexibility in the choice of sections for optimum intervention. It was also empirically shown that it was counterproductive to carry out intervention action on less congested sections in good condition, so the budget need not be arbitrarily increased beyond productive limits. By setting different model input values; i.e., cost of capacity increase, repair, and effect of each intervention, safety and budget limit, it is possible to obtain different social costs and order of sections for intervention work with different trade-off levels for various interventions.

This research can be extended by considering multiple assets, e.g., bridges, tunnels and road pavements; tolling, and network equilibrium. This work can also be formulated as a time series problem in which infrastructure life cycle costs can be optimized. When tolling is considered, incentives to change route or stop travel (i.e., free-flow conditions or no charge) may exist; hence, the volume on sections may change from time to time (different equilibrium points).

Bibliography

Adey, B. T., Burkhalter, M., and Martani, C., 2020. Defining road service to facilitate road infrastructure asset management, *Infrastructure Asset Management*, 7(4), 240–255, doi: https://doi.org/10.1680/jinam.18.00045.

Adey, B. T., Lethanh, N., Hartmann, A. and Viti, F., 2014. Evaluation of intervention strategies for a road link in the Netherlands, Built Environment Project and Asset Management, 4(2), 180–198, doi: https://doi.org/10.1108/BEPAM-06-2013-0020.

Adey, B.T. 2019. A road infrastructure asset management process: Gains in efficiency and effectiveness, *Infrastructure Asset Management*, 6(1), 2–14, DOI: 10.1680/jinam.17.00018.

Adey, B.T., Hermann, T., Tsafatinos, K., Luking J., Schindele, N., Hajdin, R. 2012. Methodology and base cost models to determine benefits of road preservation interventions in Switzerland, *Structures and Infrastructure Engineering*, 8(7), 639–654 DOI: 10.1080/15732479.2010.491119.

Bennett, C. R. and Greenwood, I. D., 2002. Modelling road user and environmental effects in HDM-4, *The Highway Development and Management Series Collection*, Vol. 4, 44–81, The World Road Association, Paris, France.

Bird, J. and Venables, A. J., 2020. Land tenure and land-use in a developing city: A quantitative spatial model applied to Kampala, Uganda. *Journal of Urban Economics*, 119, 103268.

BPR (Bureau of Public Roads), 1964. Traffic Assignment Manual, U.S. Department of Commerce, Urban Planning Division, Washington D.C.

Chandra, S., 2004. Effect of Road Roughness on Capacity of Two-Lane Roads, *Journal of Transportation Engineering*, 130 (3), 360–364.

Dabous, S. A., Zeiada, W., Tarek Zayed, T. and Al-Ruzouq, R. 2019. Sustainability-informed multi-criteria decision support framework for ranking and prioritization of pavement sections, *Journal of Cleaner Production*, 244 (2020), 1187552.

FHWA (Federal Highway Administration), 2018. Traffic Data Computation Pocket Guide, No. FHWA-PL-18-027.

FHWA (Federal Highway Administration), USDoT (US Department of Transportation), 2014. Vehicle Classification Manual; FHWA-HRT-13-091.

Iryo, T., Inoue, K., Tohyama, T. and Asakura, Y., 2005. Time dependent correlations between travel time and traffic volume on expressways, *Journal of the Eastern Asia Society for Transportation Studies*, 6, 1557–1569.

Kobayashi, K., Eguchi, M., Oi, A., Aoki, K., Kaito, K., 2013. The optimal implementation policy for inspecting pavement with deterioration uncertainty. *Journal of Japan Society of Civil Engineers*, 1(1), 551–568.

Lethanh, N., Adey, B. T. and Fernando, D. N., 2015. Optimal intervention strategies for multiple objects affected by manifest and latent deterioration processes, *Structure and Infrastructure Engineering*, 11(3), 389–401, DOI: 10.1080/15732479.2014.889178.

Lin, K. and Lin, C., 2011. Applying Utility Theory to Cost Allocation of Pavement Maintenance and Repair, *International Journal of Pavement Research and Technology*, 4 (4), 212–221.

Liu, H. and Wang, D. Z. W., 2016. Modeling and solving discrete network design problem with stochastic user equilibrium, *Journal of Advanced Transportation*, 50 (7), 1295–1313.

Lu, Z., Meng, Q. and Gomes, G., 2016. Estimating link travel time functions for heterogeneous traffic flows on freeways, *Journal of Advanced Transportation*, 50 (8), 1683–1698.

Luis G. W., 2008. Handbook of Transport Modelling, Elsevier: Handbooks in Transport, 1, 203–220.

Madanat, S. and Ben-Akiva, M., 1994. Optimal inspection and repair policies for infrastructure facilities. *Transportation Science*, 28(1), 55–62, doi:10.1287/trsc.28.1.55.

Moazami, D., Muniandy, R., Hamid, H. and Yusoff, Z., 2011. The use of analytical hierarchy process in priority rating of pavement maintenance, *Scientific Research and Essays*, 6 (12), 2447–2456, doi:10.5897/SRE10.764.

MoWT (Ministry of Works and Transport) – Uganda, 2010. *Road Design Manual, Volume 1 Geometric Design Manual, Volume 3: Pavement Design; Part I: Flexible Pavements*. Kampala, Uganda: MoWT.

MoWT (Ministry of Works and Transport) – Uganda, 2011–2017. Annual Sector Performance Reports (ASPR); http://www.works.go.ug/document-category/jtsrw/.

NCTTA (Northern Corridor Transit and Transport Coordination Authority), 2015. Road Freight Charges in Uganda, http://top.ttcanc.org/indicators.

Newbery, D. M., 1988. Road damage externalities and road user charges, *Econometrica*, 56 (2), 295–316.

Newbery, D. M., 1989. Cost Recovery from Optimally Designed Roads, *Economica*, 56 (222), 165–185.

Ravi Sekhar. Ch., Nataraju, J., Velmurugan, S., Pradeep, K. and Sitaramanjaneyulu, K., 2016. Free Flow Speed Analysis of Two Lane Inter Urban Highways, *Transportation Research Procedia*, 17, 664–673.

Richmond, C., Saeed, T. U., Adey, B. T., 2021. Non-parametric infrastructure deterioration curves from differenced condition measurements: method and examples. Preprint @ ETH Zurich, doi: https://doi.org/10.3929/ethz-b-000479524.

Rinnooy Kan, A. H. G., Stougie, L. and Vercellis, C., 1993. A class of generalized greedy algorithms for the multi-knapsack problem, *Discrete Applied Mathematics*, 42, 279–290.

Sinha, K. C., and Labi, S., 2007. Transportation Decision Making: Principles of Project Evaluation and Programming, John Wiley & Sons, Inc., Hoboken, New Jersey.

Small, K. A. and Winston, C., 1988. Optimal highway durability, *The American Economic Review*, 78 (3), 560–569.

Small, K. A. and Yan, J., 2001. The value of "value pricing" of roads: second best pricing and product differentiation, *Journal of Urban Economics*, 49, 310–336.

Small, K. A., Winston, C. and Evans, C. A., 1989. Road Work: A New Highway Pricing and Investment Policy, The Brookings Institution, Washington, D.C.

Smilowitz, K. and Madanat, S., 2000. Optimal inspection and maintenance policies for infrastructure networks, *Computer‐Aided Civil and Infrastructure Engineering*, 15(1), 5–13, doi: https://doi.org/10.1111/0885-9507.00166.

TRB (Transport Research Board), 2000. Highway Capacity Manual. National Research Council, Transportation Research Board, Washington, D.C.

TRB (Transport Research Board), 2010. Highway Capacity Manual. National Research Council, Transportation Research Board, Washington, D.C.

UNRA (Uganda National Roads Authority), 2018. Annual Performance Report, FY2017/18.

UNRA (Uganda National Roads Authority), 2019. Database (Available on request from UNRA).

Verhoef, E. T. and Small, K. A., 2004. Product Differentiation on Roads: Constrained Congestion Pricing with Heterogeneous Users, *Journal of Transport Economics and Policy*, 38 (1), 127–156.

Vlahogianni, E. I., 2007. Some empirical relations between travel speed, traffic volume and traffic composition in urban arterials, *IATSS Research*, 31(1), 110–119.

Volovski, M., Murillo-Hoyos, J., Saeed, T.U. and Labi, S., 2017. Estimation of routine maintenance expenditures for highway pavement segments - accounting for heterogeneity using random-effects models, *Journal of Transportation Engineering Part A: Systems*, 143(5), 04017006.

Wang, T., Harvey, J., Lea, J. and Kim, C., 2014. Impact of Pavement Roughness on Vehicle Free-Flow Speed, *Journal of Transportation Engineering*, 140 (9), 04014039.

Wardrop, J. 1952. Some Theoretical Aspects of Road Traffic Research, *Proceedings of the Institution of Civil Engineers*, Part II 1, 325–362.

Watanatada, T., Dhareshwar, A. M. and Lima, P. R. S. R., 1987. *Vehicle speeds and operating costs: models for road planning and management,* John Hopkins University Press, Baltimore, MD.

Yang, C., Remenyte-Prescott, R. and Andrews, J., 2015. Road maintenance planning using network flow modelling, *IMA Journal of Management Mathematics*, 2017(28), 387–402, doi:10.1093/imaman/dpv031.

Chapter 5

5 Pavement Management Using Deep Learning

"I think A.I. is probably the single biggest item in the near term that's likely to affect humanity." – Elon Musk

5.1 Introduction

This chapter's main theme involves improving civil infrastructure management using advanced computing techniques. Specifically, the chapter looks at image processing techniques and deep learning to support asset management decisions by improving their efficiency, accuracy and cost effectiveness. Pavement management decisions have traditionally been made by engineers (human-based). However, the pavement stock has recently increased in many countries yet management expert numbers are reducing, posing a challenge of how to manage road infrastructure with fewer resources efficiently. Human-based methods are prone to errors that compromise analysis and decisions. More efficient computer-based techniques could offer viable solutions. This research builds a pavement management model with a safety metric output using inputs from image processing. The study explored image processing techniques considering a trade-off between processing cost and output accuracy, with the annotation precision and Intersection over Union (IoU) set objectively. The robustness of the model was tested by comparing its output with the judgement of expert engineers on pavement safety level and its applicability was empirically shown for select roads in Japan.

5.2 Pavement management

Pavement management decisions may be based on the predicted performance of the pavement structure. Infrastructure performance models can be placed into three broad categories; i.e., stochastic (probabilistic), deterministic and computer techniques (Tsuda et al. 2006, Kobayashi et al. 2010, Tabatabaee and Ziyadi 2013, Pérez-Acebo et al. 2019, Obunguta and Matsushima 2020). The Bayesian approach has also been used to improve the prediction of infrastructure performance through updating whenever more data is available (Kobayashi et al. 2012, Tabatabaee and Ziyadi 2013).

Infrastructure asset management is heavily dependent on infrastructure condition which requires significant amounts of data. Stochastic and deterministic techniques may require a minimum of two-point data to predict the performance of infrastructure systems; however, cases of incomplete data including one-point sometimes occur due to a lack of resources such as human and equipment to carry out surveys. Lethanh and Adey (2012) applied the improved stochastic hidden Markov model to model pavement deterioration in case of incomplete monitoring data. Additional data may be generated through multiple imputation (Rubin 1976, 1987) and/or computer techniques could be used to process one-point data and output useful information to support management decisions (Maeda et al. 2018, Zou et al. 2022).

In the past, data had been collected by engineers through periodic inspection which is prone to a number of errors such as miss-reporting, omission and/or wrong data entries especially as the infrastructure stock increases. Human-based detection and measurement of defects is a highly subjective process liable to bias. The use of expensive specialized damage measurement equipment may not be feasible in some settings and may also disrupt normal traffic flow. A shortage of experts has also resulted in less inspection coverage (Maeda et al. 2018). Furthermore, the collected data is normally manually sorted by a data analyst to eliminate unusable data, a process that may introduce additional errors. The poor data problem is further augmented at the data cleaning stage, where a lot of data is eliminated affecting the power of estimates obtained from prediction models; which blurs management decisions (Obunguta and Matsushima 2020). Accurate and effective computer-based infrastructure management using fewer resources (both human and material) could thus be desirable.

Pavement management decisions are made to minimize costs typically Life Cycle Costs (LCC) for a projected period of operation. Kobayashi et al. (2013) developed a pavement management model that optimized inspection and repair for pavements by minimizing LCC. Obunguta and Matsushima (2020) optimized the LCC of a pavement system by considering different management policies; i.e., time-dependent and condition-dependent, and explored the effect of preventive maintenance on LCC. Pavement intervention may also be determined by optimizing road usage and utility (Lin and Lin 2011, Liu and Wang 2016, Mizutani et al. 2020).

5.3 Image processing techniques

5.3.1 Datasets, simple segmentation and deep learning

Recent technological advancements have led to the development of comparatively lower cost but high quality smartphones which has resulted in the production of abundant smartphone road image data. The images may be stored in datasets such as ImageNet (Deng et al. 2009) and PASCAL VOC (Everingham et al. 2015), CamVid (Cambridge University 2021) and Road Damage Dataset – 2020 (RDD-2020) (Arya et al. 2020a).

For infrastructure systems such as road networks, images are normally collected by taking photos through the car windshield using a smartphone mounted on the dashboard (Figure 5.1). Car windshield images are complex because they contain a lot of noise (many objects) and are in perspective view. The images may additionally be affected by weather; e.g., lighting and shadows. Plan view images, taken directly above the road surface; for example, using a drone may be simpler but are legally prohibited in many jurisdictions.

Image processing has been applied to many fields such as forestry to evaluate the impacts of policies addressing deforestation (The Mathworks Inc. 2021), transportation infrastructure for road damage detection (Maeda et al. 2018, Arya et al. 2020a, 2021), and dermatology to determine the severity of skin cancer (Kinyanjui et al. 2019) and skin lesions (Mirikharaji et al. 2021). A study by Zou et al. (2022) applied deep learning using the You Only Look Once v4 (YOLOv4) algorithm to detect defects in structures after an earthquake disaster. Maeda et al. (2018) developed a road damage detection system based on the YOLO algorithm using smartphone images in Japan. Thuyet et al. (2022) developed an autonomous road inspection system using deep learning and data obtained using a Laser Crack Measurement System to detect cracks and patches. Other studies such as Goncalves and Givigi (2016), Hong et al. (2020) have developed methods to detect and measure crack defects in civil infrastructure from simple image data that contains a few objects.

Figure 5.1. Setup of smartphone in car (Arya et al. 2021).

Object recognition systems can be broadly divided into three groups. First, human-based methods, where an inspector observes and measures defects using traditional measurement equipment. Second, microscopic inspection using specialized tools; and third, machine vision, in which defects are identified and quantified automatically by image analysis. Machine vision has proved to be the most efficient and accurate of the three. Within machine vision, Artificial Neural Networks (ANNs) and convolutional neural networks (CNNs); and pattern recognition using colour models have emerged as the most popular (Goncalves and Givigi 2016). Colour models were an advancement of simple threshold segmentation (e.g., Otsu 1979). Other segmentation methods including graph-based segmentation using the lazysnapping technique and region growing from a seed point have been developed (The Mathworks Inc. 2021).

In deep learning, algorithms built using region proposals and CNNs (R-CNN) have achieved higher accuracy. The Mask R-CNN algorithm (He et al. 2018); an advancement of Faster R-CNN (Ren et al. 2015), Fast R-CNN (Girshick 2015) and R-CNN (Girshick et al. 2014), is the current state-of-the art algorithm in the family of object detection and segmentation algorithms using region proposals. Mask R-CNN extended Faster R-CNN by adding a branch for predicting segmentation masks from each Region of Interest (RoI) and also replaced the RoIPool layer with the RoIAlign layer that is quantization-free which solved the misalignment challenge in earlier algorithms (Figure 5.2).

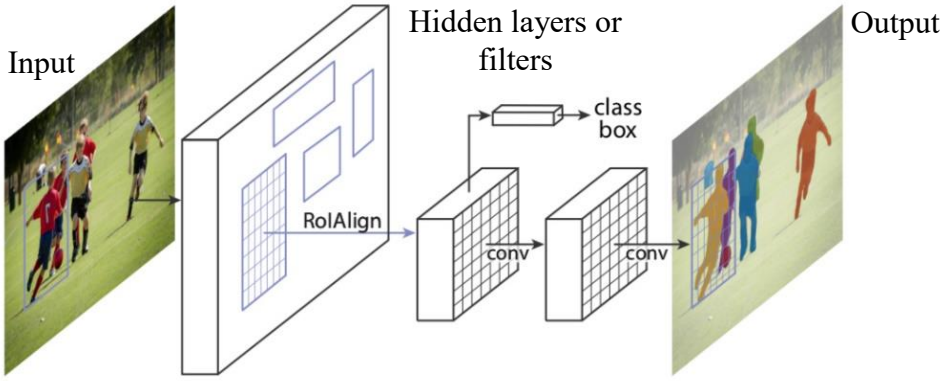

Figure 5.2. Facebook AI Research's Mask R-CNN (He et al. 2018).

Object detection techniques build a bounding box based on the object category as shown in Figure 5.3 and therefore do not provide information about the size and shape of defects. Image detection and segmentation algorithms such as Mask R-CNN provide a pixel-wise mask for an object which gives more details about its shape and size, and may also be more suitable for segmentating complex images containing overlapping objects, different colours, textures, contrasts and light intensities. The severity of defects, obtained through quantification, is important for the asset management decision process especially considering user safety.

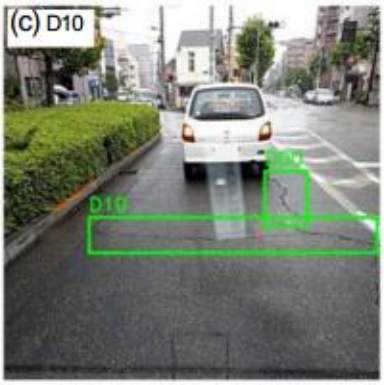

Figure 5.3. Crack detection (Maeda et al. 2018).

5.3.2 Image Annotation

Annotation is a vital preliminary step, despite being labour-intensive, before training a deep learning model and therefore should be done as efficiently and as accurately as possible. For object detection, bounding boxes and object labels are manually added to the images at every instance an object is identified by the annotator. For object segmentation, a pixel-wise mask and object label are manually added to the images at each instance. Higher quality and more precise annotations

may increase accuracy, however, they require a higher time cost to achieve. Past studies including Greenwald et al. (2022) have attempted to optimize the time cost for annotating images by combining expert, crowd and computer input while ensuring required accuracy levels are met. Xu et al. (2021) applied partial annotation to leverage the advantages of using annotated and unannotated regions in the training process for crowd counting tasks. More informative annotations may involve detailed manual boundary drawings for a feature of interest, whereas less informative approximate annotations (e.g., bounding boxes or simplified polygons) may require simpler drawings. Therefore, a trade-off may exist between the quality and time cost of annotating images (Mirikharaji et al. 2021). For infrastructure performance evaluations, the accuracy requirements for measurements may not be as strict compared to fields such as health because classification of the defect level need only fall within a specified range. Practitioners may decide the needed annotation quality for specific purposes more efficiently based on the accuracy-time cost trade-off.

5.4 Problem statement

Road infrastructure asset management is faced with the challenge of an increasing infrastructure stock yet management expert numbers are dwindling that results in low coverage and the neglect of some infrastructure as discussed above which may be unsafe for road users. This challenge is further exacerbated by the inaccuracy of human-based inspection and data preparation which compromises pavement performance results and subsequent management decisions. Road infrastructure asset management may capitalize on the gains in the technological industry that have seen the development of low cost smartphones. Pavement smartphone images from a wider road infrastructure stock may be taken and analysed using more efficient and accurate image processing techniques compared to human-based methods. For image processing, less accurate simple segmentation methods which do not require costly annotations and the more accurate deep learning process that requires the costly annotations exist. A trade-off between accuracy and annotation cost may therefore be evaluated by varying annotation precision requirements from no annotation (for simple segmentation methods), less detailed to more precise annotations (for deep learning). This trade-off may be used to evaluate the most appropriate image processing methods and requirements for pavement defect detection tasks because in pavement asset management very precise defect measurements may be unnecessary since the defects need only fall within a specified

range for appropriate intervention prescription. Also noted in the previous sections is the subjectivity of annotation and deep learning model inputs such as IoU which this research work attempts to set objectively by building a probabilistic pavement asset management model that is validated by expert analysis. The study also shows how the output from deep learning can be applied to pavement asset management to encourage adoption of more efficient technologies in the asset management practice.

5.5 Study objectives

The main objective of this study is to explore the possibility of arriving at sound pavement management decisions with minimal human dependence. Specifically, the objectives are:

1) Carry out an experimental comparison between simple segmentation methods and deep learning.
2) Develop a probabilistic pavement management model based on safety and set annotation precision and Intersection over Union (IoU) objectively.
3) Empirically show the applicability of the model using deep learning output from the processed RDD-2020.

As far as is known, no other study develops a model that sets the IoU and annotation precision objectively including expert validation and empirically shows the applicability of image processing outputs as inputs for asset management decisions. The rest of this chapter is organised as follows. The next section develops the probabilistic asset management model followed by an empirical model application including deep learning on the RDD-2020. Conclusions and suggestions for possible future work are presented at the chapter end.

5.6 Probabilistic Asset Management Model

5.6.1 Model definition and overview

Consider that a road pavement section $k(k = 1,2, \dots, K)$ has defect density d_k^n estimated from processed image data with $n(n = 1,2, \dots, N)$ indicating the class of the defects; e.g., cracks and potholes. From the estimated d_k^n, an input vector $\boldsymbol{d_k} = [d_k^1, \dots, d_k^N]$ can be created that generates an output, the safety metric $S_k = f(\boldsymbol{d_k})$. The safety metric may be the Maintenance Control Index (MCI) that is commonly used in Japan (JARA 2013). Each section k, can thus have an estimated

MCI_k. Based on the severity of MCI_k, road managers may propose the appropriate intervention A on a section with options; do nothing A_0, sealing or patching A_1, overlay A_2, and reconstruction A_3. The estimated defect densities d_k^n may vary based on image processing; i.e., set annotation case i and IoU threshold. The defect densities may also vary due to other factor including image quality such as lighting conditions, e.g., shadows; scale, e.g., perspective view and/or pavement infrastructure properties, e.g., material colors. In this study, processing methods were emphasized and the goodness of fit of annotation case i and IoU in defect detection was validated using the pavement condition estimates by experts $e(e = 1,2, \dots, E)$. The priority for intervention on a section k is determined based on the magnitude of the safety metric on that particular section in comparison with other sections and the intervention is proposed following an intervention matrix. This is illustrated in Figure 5.4 with $MCI_{k=1} < MCI_{k=2}$, which implies that worse section $k = 1$ should receive priority for intervention. The defect densities used to estimate MCI_k are obtained probabilistically by maximizing the probability of detection of defects considering different annotation cases i and IoU threshold against the expert benchmark. The annotation cases are of number n_i and MCI_k^* is the MCI determined after optimizing i and IoU.

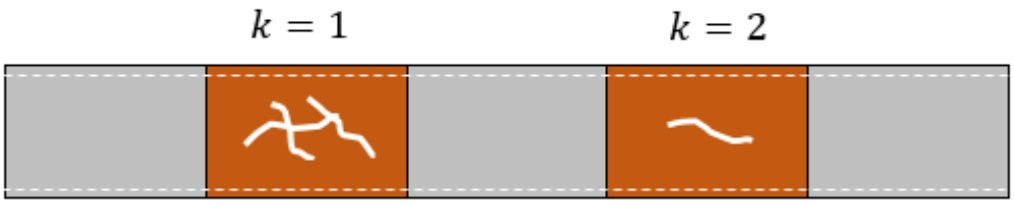

Figure 5.4. Illustration of two pavement sections.

The MCI_k is defined as (Minami and Suzuki 2008, Miyamoto and Yoshitake 2009, JARA 2013, Yoshida 2016, Kubo 2017);

$$MCI_{k,0} = 10 - 1.48{C_k}^{0.3} - 0.29{D_k}^{0.7} - 0.47{\sigma_k}^{0.2} \quad (5.1)$$

$$MCI_{k,1} = 10 - 1.51{C_k}^{0.3} - 0.30{D_k}^{0.7}$$

$$MCI_{k,2} = 10 - 2.23{C_k}^{0.3}$$

$$MCI_{k,3} = 10 - 0.54{D_k}^{0.7}$$

$$MCI_k = min(MCI_{k,j}) \quad j(j = 0, \dots, 3)$$

where C_k is the cracking ratio in %, D_k is the rutting depth in mm and σ_k is the roughness in mm.

5.6.2 Probabilistic annotation and IoU setting

Consider that the quality of annotations for images and set IoU applied in deep learning can be varied. Assume that the defect densities $\boldsymbol{d_k}$ for a given annotation case i and IoU can be estimated using a computer and give an output MCI_k. Consider that experts $e(e = 1,2, \dots, E)$ analyse the same *K* images and grade them using a similar point scale used for computer analysis. Considering the expert analysis as the benchmark, a successful computer match is established if MCI_k falls within $[MCI_{min}^k, MCI_{max}^k]$ from the expert analysis, otherwise it is considered a failure (no match). Using multiple logistic regression, the probability $\in [0,1]$ of predicting a binary outcome (match = 1, or no match = 0) can be estimated given annotation case i and IoU. The explanatory variable *i* may be considered as categorical and the IoU as continuous within the limits [0,1].

$$\Pr\{MCI_{min}^k \leq MCI_k < MCI_{max}^k | i, IoU\} = p(i, IoU) \tag{5.2}$$

$$p(i, IoU) = \frac{exp(\beta_0 + \beta_1\delta_1 + \cdots + \beta_{n_i-1}\delta_{n_i-1} + \beta_Q IoU)}{1 + exp(\beta_0 + \beta_1\delta_1 + \cdots + \beta_{n_i-1}\delta_{n_i-1} + \beta_Q IoU)} \tag{5.3}$$

where $\boldsymbol{\beta}$ $(\beta_0, \beta_1, \dots, \beta_Q)$ is a vector of unknown parameters to be estimated with $q(q = 0, 1, \dots, Q)$ denoting number of explanatory variables; and δ_i $(i = 1, \dots, n_i - 1)$ are dummy variables for annotation case. The base annotation case I has all the dummies equal to zero. For three annotation cases, $\delta_1 = \delta_2 = 0$ for the base case I; $\delta_1 = 1$ and $\delta_2 = 0$ for case II; and $\delta_1 = 0$ and $\delta_2 = 1$ for case III. The dummies δ_1 and δ_2 are comparative between cases II and III with the base case, respectively. This definition of dummies is important to avoid indeterminate model coefficients that may occur due to singularities as a result of the violation of the perfect collinearity property.

Assuming that the probabilities of detection are mutually independent then the log-likelihood expressing the joint probability density of successful defect detection considering all experts and sections is;

$$ln[\boldsymbol{L}(\boldsymbol{\beta})] = ln\left[\prod_{e=1}^{E}\prod_{k=1}^{K}\{p(i,IoU)\}^{\delta_{k,e}}\{1-p(i,IoU)\}^{(1-\delta_{k,e})}\right] \tag{5.4}$$

$$= \sum_{e=1}^{E}\sum_{k=1}^{K}\{\delta_{k,e} ln[p(i,IoU)] + (1-\delta_{k,e}) ln[1-p(i,IoU)]\}$$

$$\delta_{k,e} = \begin{cases} 1 & if\ \ match \\ 0 & if\ no\ match \end{cases}$$

where $\delta_{k,e}$ is a dummy variable for match or no match.

The unknown parameters can be obtained by maximizing the log-likelihood function;

$$\frac{\partial\, ln[\boldsymbol{L}(\boldsymbol{\beta})]}{\partial \beta_q} = 0 \tag{5.5}$$

$$(q = 0, 1, \dots, Q)$$

An iterative method for example the Newton Raphson method could be used to iteratively estimate $\boldsymbol{\beta}$ within a given tolerance level.

For a given annotation case i and IoU to be acceptable to effectively detect and quantify defects, the probability $p(i, IoU)$ should not be less than a set limit p_0 .

$$p(i, IoU)) \geq p_0 \tag{5.6}$$

The annotation case i^* and IoU^* that optimizes the probability of detection of defects is obtained as;

$$\underset{i,IoU}{argmax}\ p(i, IoU) \tag{5.7}$$

The defect densities d_k^{n*} obtained for i^* and IoU^* are used in the calculation of MCI_k^*.

5.6.3 Intervention planning

The choice of intervention A on a section is determined by maximizing the MCI for the entire pavement stock (Obunguta et al. 2022). When action is carried out, it is assumed that the defect density improves and $d_k^{n*} = 0$. The intervention on a given section is determined based on the

MCI following an intervention matrix shown in Table 5.1. This type of intervention decision is used by a number of agencies including the Ministry of Land, Infrastructure, Transport and Tourism of Japan (Miyamoto and Yoshitake 2009, Kubo 2017). The cut off level for each defect class intervention can be varied by a road agency based on their standards.

A Pareto frontier may occur where for two or more elements, the MCI_k value is the same. In this case, other factors may be considered such as the importance factor of a pavement section relative to others. If other factors are insignificant, then the prioritization of intervention for the sections at the Pareto frontier may be done randomly.

Table 5.1 Intervention matrix (Miyamoto and Yoshitake 2009, Kubo 2017).

MCI_k	Intervention			
	A_0	A_1	A_2	A_3
$MCI_k = 10$	o	x	x	x
$4.5 \leq MCI_k < 10$	x	o	x	x
$2.5 \leq MCI_k < 4.5$	x	x	o	x
$MCI_k < 2.5$	x	x	x	o

Note: o means intervention and x means no intervention.

5.7 Empirical application

5.7.1 Outline of application

In the empirical application, simple object segmentation methods that don't require costly annotation were explored, and a deep learning model was trained using the Mask R-CNN algorithm in Python 3.9.1 to detect and quantify defects and road features (RoIs) in the RDD-2020 so as to estimate the defect densities applied in the probabilistic asset management model. To show the practicality of the model, an empirical application was carried out for select roads in Japan. The empirical application was done for Japanese roads due to the unavailability of reliable road image data in Uganda.

5.7.2 Road image dataset

The RDD-2020 contains images of 600 × 600 pixels for road surfaces approximately 10 m ahead taken using a camera mounted on a vehicle traveling at an average speed of about 40 km/h (about 10 m/s) capturing an image every second. The dataset is heterogeneous with more objects and includes images from India, Japan, and the Czech Republic (Figure 5.5).


a)

b)

c)

Figure 5.5. Road images from Japan (a), India (b) and Czech (c).

5.7.3 Simple segmentation methods

5.7.3.1 Overview of methods

There are several segmentation techniques that can be applied to extract features of interest from images. For many images, segmentation needs to be done programmatically as opposed to manually because of computational reasons. This study explored graph-based segmentation using the lazysnapping technique and region growing from a seed point. The segmentation algorithms can be developed in MATLAB and looped through images stored in a specified file directory.

For the lazysnapping technique, the initial background and foreground RoIs are user-dependent. After the RoIs are set, the algorithm programmatically classifies other unallocated image pixels as either background or foreground based on a similarity metric. In Figure 5.6, consider a 5x5 pixel image with a low pixel (dark) foreground and a high pixel (light) background. The foreground (object) region can be segmented out by specifying the RoI with dimensions [xmin,ymin,width,height] and a background RoI with its own dimensions. The RoIs for each group (fore or background) can be as many as necessary. The lazysnapping formular can then be used to group pixels based on similarity.

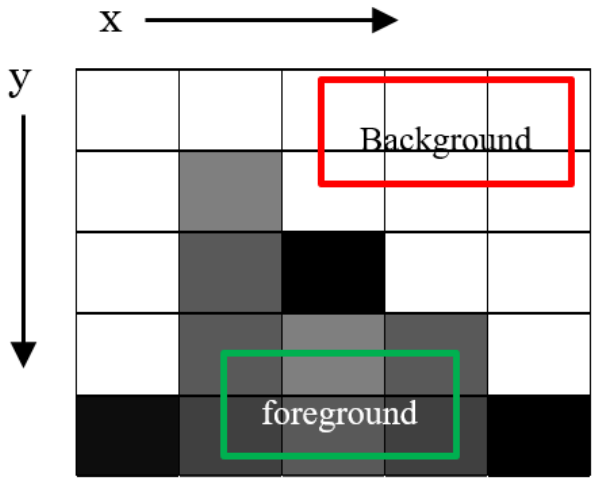

Figure 5.6. Graph-based segmentation by lazysnapping with a foreground and background RoI.

For region growing from seed point(s), the RoI is iteratively grown by comparing all unallocated neighbouring pixels to the RoI based on a similarity measure as illustrated in Figure 5.7 where the initial user-dependent seed point Sp with coordinates [x,y] is grown to cover the low pixel object region (Kroon, 2021).

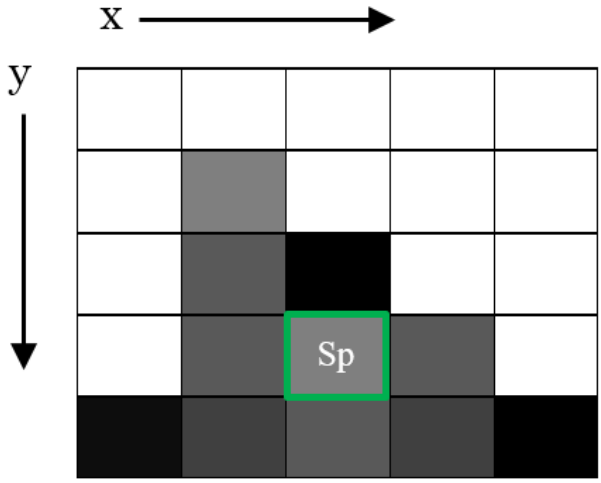

Figure 5.7. Region growing from a seed point (Sp).

To run either algorithms programmatically, the RoIs or the Sp need to be pre-set by the user for the entire dataset. When performed programmatically, the algorithms may generate inaccurate results incase the initial RoIs and Sps do not fall in the pixel area of the feature of interest for all images.

5.7.3.2 Simple segmentation experiments

The segmentation experiments shown in Figure 5.8 and Figure 5.9 highlighted that both lazysnapping and region growing from a seed point were challenged by;

1) Region continuity breakage due to lighting conditions; i.e., dark shadows (Figure 5.9 a), bright shiny surfaces and bright reflections (Figure 5.8 c and Figure 5.9 c) probably from the windscreen due to the camera flash.
2) Breakage in segmentation regions due to the colour difference between the road markings such as zebra crossings and lane separations; and the pavement surface (Figure 5.8 b and Figure 5.9 b).
3) Unwanted regions were segmented (Figure 5.8 d).

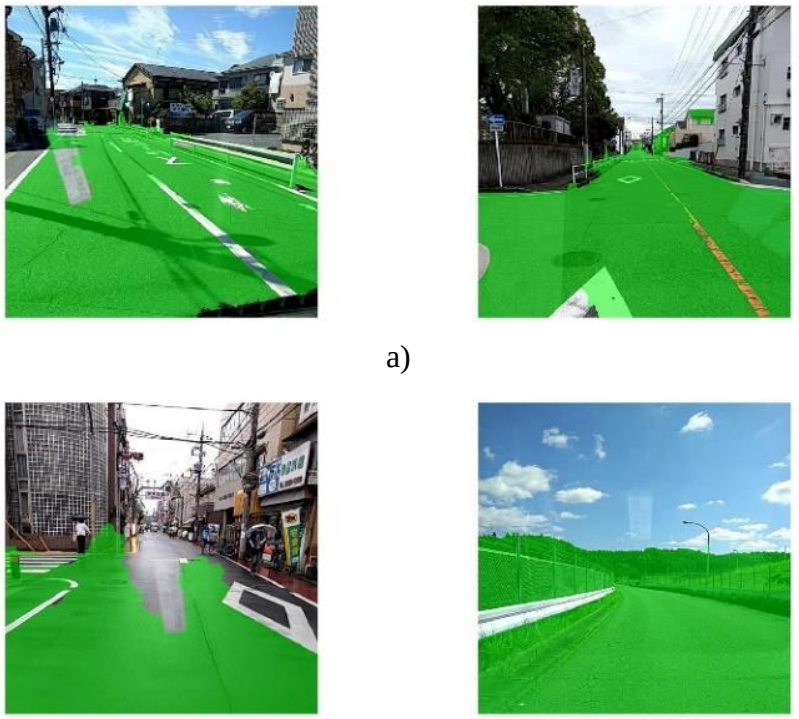

a) b)

c) d)

Figure 5.8. Segmentation trials using the lazy snapping technique on RDD-2020.

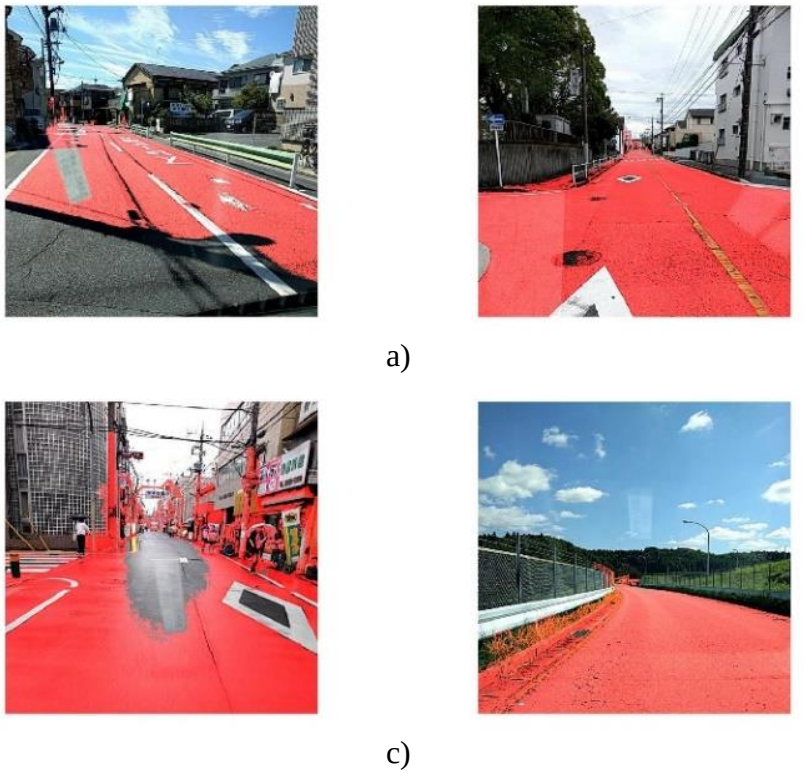

a) b)

c) d)

Figure 5.9. Segmentation trials using region growing from a seed point on RDD-2020.

The simple segmentation experiments showed that both techniques were challenged by the complexities of segmenting features as a result of lighting and colour changes, and unwanted objects were segmented in several cases because segmentation of complex images was challenged by inaccurate initial RoI specification if done programmatically. On the other hand, manual segmentation may be cumbersome, hence, deep learning may offer more accurate segmentation results despite having a higher computational cost (annotation and training) compared to simple segmentation methods.

5.7.4 Deep learning

5.7.4.1 Algorithm

Deep learning involves annotating images then training a model to detect the annotated RoIs. In this study, the deep learning model was trained using the Mask R-CNN algorithm to detect and build a pixel-wise mask on road features and defects. The main steps of the algorithm are detailed in Table 5.2 below.

Table 5.2 Deep learning algorithm.

Algorithm: Deep learning and defect quantification
Start
Step 1: Obtain road pavement images
Step 2: Sort images
Step 3: Annotate images in the training and validation set
Step 4: Input annotated images then train and test the deep learning model
Step 5: Defect quantification
Step 6: Output quantified defects; i.e., defect densities
End

5.7.4.2 Deep learning accuracy

The Mean Average Precision (mAP) is a popular metric in computer vision for evaluating the accuracy of object detectors (Padilla et al., 2020). The measures, precision and recall, are required in the estimation of mAP. Precision is the ratio of true positives to all predicted positives, whereas recall is the ratio of true positives to all actual positives. To explicitly express precision and recall, the following parameters are defined as;

- True Positive (TP): If an object or defect instance is present in the ground truth, and the label and the bounding box of the instance are correctly predicted with Intersection over Union (IoU) ≥ threshold.
- False Positive (FP): If the model predicts an object or defect instance at a particular location in the image, but the instance is not present in the ground truth for that particular image. This also applies to the case when the predicted label doesn't match with the actual label.
- False Negative (FN): If an object or defect instance is present in the ground truth, but the model fails to predict either the correct label or the bounding box of the instance.

The precision and recall are then defined mathematically as;

$$Precision = \frac{TP}{TP + FP} \tag{5.8}$$

$$Recall = \frac{TP}{TP + FN} \tag{5.9}$$

The average precision (AP) is obtained as the average of precision values obtained from the precision-recall (PR) curve for a select set of recall values. The mAP score is the mean of APs over all the object classes, *N*.

$$mAP = \frac{1}{N}\sum_{n=1}^{N} AP_n \tag{5.10}$$

5.7.4.3 Image annotation

This study explored three annotation cases (Figure 5.10) with decreasing labour requirements and precision, and compares their accuracy in determining the right defect classifications and quantifications against expert judgements. The study employed the Visual Geometry Group (VGG) Image Annotator (VIA) software to annotate the RDD-2020 images and the annotations were exported in the JSON format. The annotation of the objects of interest was done following Table 5.3. The road feature was added to the defect classes defined by Arya et al. (2020a) with D00, D10 and D20 defining cracks and D40 mainly potholes based on the Japan Road Maintenance and Repair Guidebook 2013 (JARA 2013). Figure 5.11 shows a select road damage image before and after annotation. It took about 2 to 4 minutes for case I, 1 to 2 minutes for Case II and less than 1 minute for Case III; to annotate a single image using human labour depending on the amount of defects observed in the image by the annotator. The Figure 5.12 and Figure 5.13 show the training and validation data statistics, respectively, with a total of 1,165 annotated objects. The low occurrence of D40 defects in Japan compared to the other countries is probably due to better and more regular maintenance.

Figure 5.10. Different annotation cases in red, green and blue.

Table 5.3 Objects of interest (Arya et al. 2020a).

Object ID	Description	Defects Group
Road	Road surface	
D00	Linear crack, longitudinal	C_k
D10	Linear crack, lateral	
D20	Alligator crack	
D40	Pothole, rutting, bump, separation	D_k


a)

b)

Figure 5.11. Road damage image before (a) and after (b) annotation.

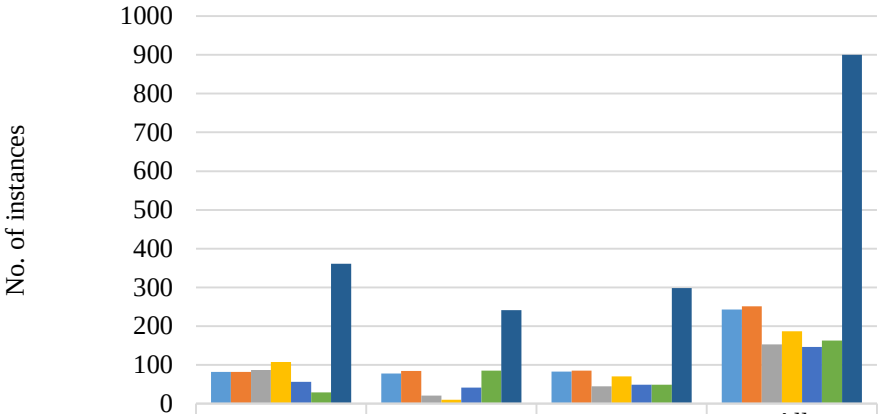

	Japan	India	Czech	All countries
No. of images	82	78	83	243
Road	82	84	85	251
D00	87	21	45	153
D10	107	10	70	187
D20	56	41	49	146
D40	29	85	49	163
Total objects	361	241	298	900

Figure 5.12. Training data statistics.

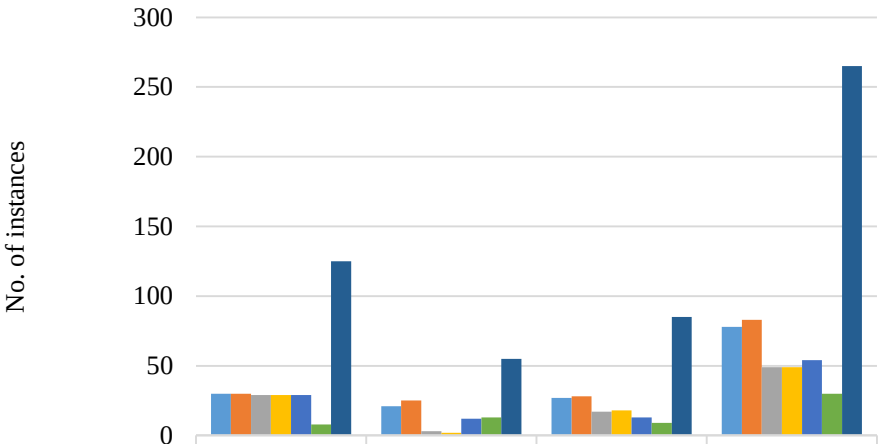

	Japan	India	Czech	All countries
No. of images	30	21	27	78
Road	30	25	28	83
D00	29	3	17	49
D10	29	2	18	49
D20	29	12	13	54
D40	8	13	9	30
Total objects	125	55	85	265

Figure 5.13. Validation data statistics.

5.7.4.4 Deep learning experiments

The model was trained for 50 epochs at a learning rate of 0.001 in Python 3.9.1 using an Intel(R) Core(TM) i5-5200U CPU @ 2.20GHz with 4.00GB RAM and 500GB HDD computer. Model accuracy was tested at different IoU thresholds across different object classes considering varied annotation precision. The model training took about 33 hours. The Table 5.4 shows mAP values per defect class at different IoU thresholds and annotation cases. The Figure 5.14 shows the improved results of the road feature extraction and the defect identification done in parallel without image lighting and colour change inhibitions (Comparing Figure 5.14 a with Figure 5.8 a; and Figure 5.14 c with Figure 5.8 c and Figure 5.9 c) and unwanted segmentation (Figure 5.14 d and Figure 5.8 d). The model showed high confidence values of up to 0.99 for prominent road features.

Comparing across the different annotation cases, the mAP increased by an average of 8.3% from Case I to II and by an average of 5.8% from Case II to III considering all IoU thresholds. This mAP increase was probably because of the increase in the RoI size which resulted in more overlap between the ground truth and prediction, hence more detection. However, the difference in detection accuracy was less than 10% which may arguably be insignificant. Particularly, Case III and II may be competitive because relatively similar mAP levels were achieved at a lower

annotation cost compared to Case I. This result may show the insignificance of annotation precision in generating acceptable defect density estimates for pavement management purposes. It is also important to note that for a given annotation case and IoU, specific defects may be detected better, for instance, the smaller size D00 defect was detected at the highest AP considering annotation case II, which is more precise compared to III, for all IoU thresholds.

The Road object class had the highest AP values because the road feature was very prominent in all the images which made it easy for the algorithm to learn, detect and segment. On the other hand, the linear cracks consisting of lateral and longitudinal cracks had comparatively lower APs because they were generally of much smaller size compared to other objects; hence, their detection and segmentation was poorer. As the IoU was decreased, the APs increased across all object classes except for the Road class because the less strict IoU requirement resulted in more object detection as the ground truth and prediction needed not overlap much. The high AP value for the Road class was stagnant because that was the maximum achievable value.

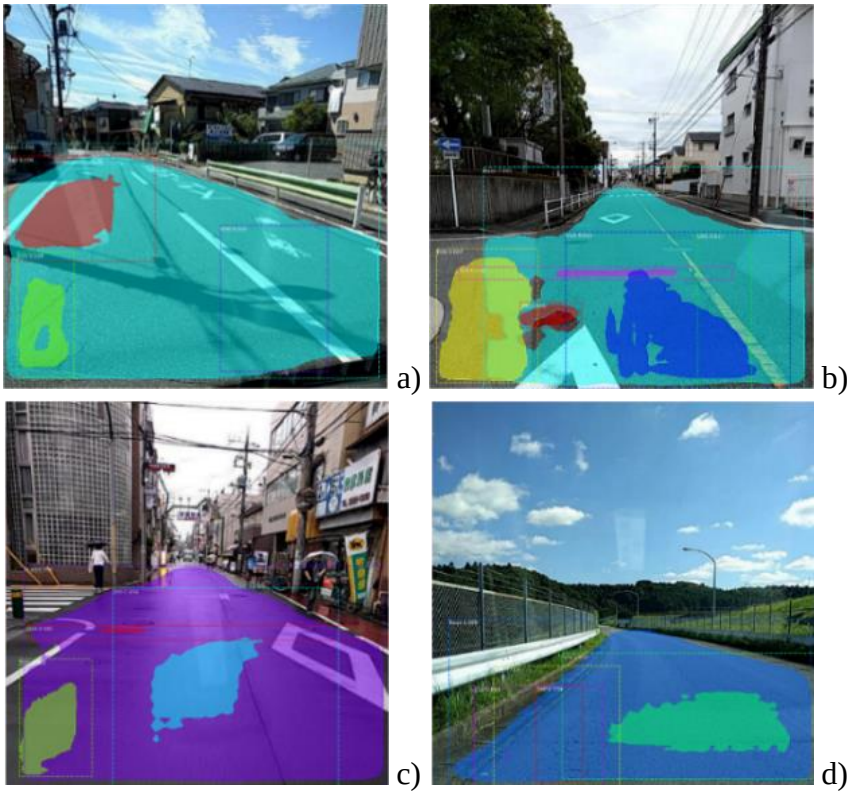

Figure 5.14. Detection and segmentation of road features and defects on RDD-2020 for case I, IoU 0.5.

Table 5.4 AP per object class at different IoU thresholds.

IoU	Object ID	Case I		Case II		Case III	
		AP	mAP	AP	mAP	AP	mAP
0.7	Road	0.9794	0.3436	1.0	0.3963	1.0	0.4097
	D00	0.0833		0.3280		0.1517	
	D10	0.3556		0.0407		0.4520	
	D20	0.1011		0.2045		0.0824	
	D40	0.1985		0.4081		0.3624	
0.5	Road	0.9794	0.5738	1.0	0.6328	1.0	0.6979
	D00	0.3444		0.6472		0.5992	
	D10	0.5799		0.1512		0.7674	
	D20	0.5337		0.5704		0.4843	
	D40	0.4318		0.7951		0.6386	
0.3	Road	0.9794	0.7020	1.0	0.7284	1.0	0.7645
	D00	0.6083		0.7358		0.7258	
	D10	0.5950		0.2523		0.7681	
	D20	0.7291		0.7893		0.6039	
	D40	0.5984		0.8644		0.7245	
0.1	Road	0.9794	0.7046	1.0	0.7309	1.0	0.7645
	D00	0.6083		0.7358		0.7258	
	D10	0.5950		0.2523		0.7681	
	D20	0.7397		0.8019		0.6039	
	D40	0.6005		0.8644		0.7245	

5.7.4.5 Defects density

The extent of defects could be estimated from the segmented images by calculating the ratio of the size of defect pixels to the size of pavement pixels. A ratio was considered because the images may be taken at different perspectives and using different smartphones and hence may have different relative sizes. This estimation of the defect densities d_k^n in an image taken at a specific location was done so as to facilitate comparisons between different road sections. The defect density is also similar to the cracking ratio defined by the Japan Road Association (JARA 2013, Kubo 2017).

$$d_k^n = \frac{No.of\ defect\ pixels}{No.of\ total\ pavement\ pixels} \tag{5.11}$$

The defect densities were estimated for 1,660 select sections in Adachi City, Japan (Figure 5.15). For some sections, the aggregate defect densities were greater than expected probably due to the detection and segmentation of multiple objects at different instances, overlap and partial detection

of road features in the images. From Figure 5.15, more defects were detected when the IoU was reduced because of a less strict IoU that enabled more detection. Also, more severe defects could be detected from annotation case I to II to III, attributable to the increase in RoI size as annotation is made less precise. The variation such as reduction in defect detection for case III could be attributed to annotation subjectivity.

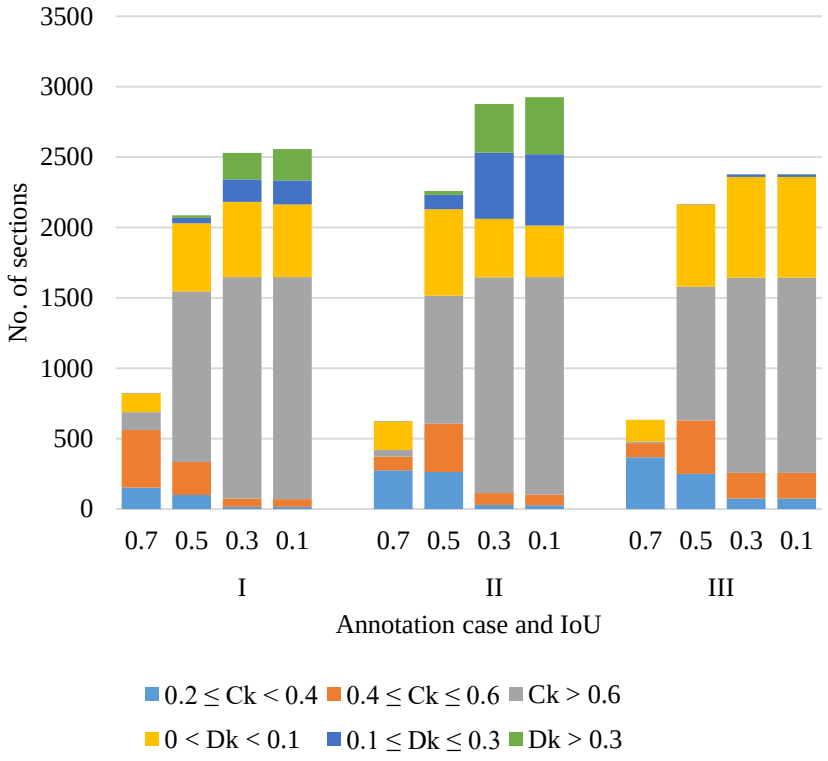

Figure 5.15. Section defect densities.

5.7.5 Estimation of the safety metric

The data preparation stage before application of the probabilistic model generated 12,000 data points for 100 select sections from Adachi City considering 12 possible combinations of annotation case *i* and IoU compared against the judgement of ten expert engineers. The experts classified the pavement images visually based on a three-point scale in Table 5.5 and their experience. To eliminate bias, the experts were presented with the images labeled from 1 to 100 (blind judgement). A comparison was made between the expert image classification and the image analysis results. In the estimation of MCI, instead of the rutting/ pothole depth, the density value was used. The estimated MCI values were compared with the expert analysis to determine a match or no match.

Table 5.5 Evaluation of pavement soundness (Kubo 2017).

	Type	Condition (Deterioration level)	Approximate MCI_k
1	Good	Low and the pavement surface is in a good condition	$4.5 \leq MCI_k \leq 10$
2	Phase to keep surface function	Medium deterioration level	$2.5 \leq MCI_k < 4.5$
3	Repair phase	High and expected to be beyond the permissible level soon	$MCI_k < 2.5$

The Table 5.6 shows a summary of the expert classification aggregated into the worst, best and mode (majority) result from the ten experts for each of the 100 sections. About 71% of the sections were classified as good by majority experts.

Table 5.6 Aggregate expert classification for the selected sections.

Condition state	Number of sections		
	Worst	Best	Mode
1	28	86	71
2	51	13	28
3	21	1	1

The Figure 5.16 shows a comparison of image processing output and expert classification with the highest matching rate of 65.5% achieved for both annotation case II and III at 0.7 IoU considering all experts.

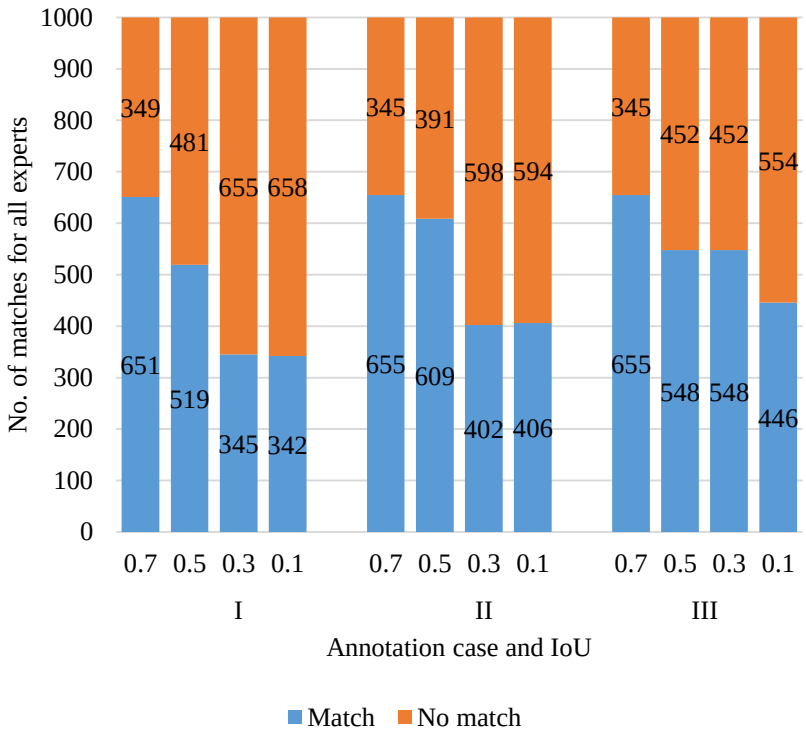

Figure 5.16. Image processing vs expert classification.

The unknown parameters were estimated by maximizing the log-likelihood function using Newton's method as shown in Table 5.7. All the estimated parameters had significant *p*-values (< 0.05) and all had low standard errors. The significant *p*-values mean that *i* and IoU influence the accurate detection of defects. As the annotation case was made less strict; i.e., from I to II to III, the estimated parameters increased which showed that the odds of obtaining a right detection increased by 25.2% from I to II, 28.3% from I to III, and 3.1% from II to III; if other variables were fixed. The increase in odds as annotation was made less strict could be attributed to the increase in the RoI area which increased the probability of detection. There were 574% more odds of right detection if the IoU was increased if annotation precision was fixed. This increase in odds was because increased IoU resulted in less defect detection which generated results that showed road pavements in good condition and matching with the expert judgement. This result showed the need to limit the IoU within given thresholds to avoid erroneous and meaningless detections as IoU approximates the limits of 0 and 1.

Table 5.7 Estimation of unknown parameters.

Parameter	Estimate	Standard error	*exp(β)*	Increase in odds	*p*-value
β_0	-0.9127	0.04734	0.4014	-0.5986	2×10^{-16}
β_1	0.2250	0.04580	1.2523	0.2523	8.98×10^{-7}
β_2	0.2491	0.04581	1.2829	0.2829	5.42×10^{-8}
β_3	1.9074	0.08483	6.7356	5.7356	2×10^{-16}

To evaluate the success rate of the model in making correct predictions, a confusion matrix and hitting rate accuracy were generated. The confusion matrix showing the accuracy rate of the calibrated model in predicting an observed match or no match at a 0.5 cut off is shown in Table 5.8. The model rightly predicted the observations at a 60.42% accuracy rate, showing high goodness of fit of the calibrated model. The model may not need to be an exact match since the expert classification was not based on only observed defects. The expert classification was also based on experience and other defect characteristics including crack patterns and defect colors not considered in the deep learning. For example, diagonal cracks are indicative of shear failure in reinforced concrete structures and reflection linear cracks may show the degeneration of the pavement sub layers; and black colour may be due to bleeding defects where asphalt binder is forced to the pavement surface.

Table 5.8 Confusion matrix.

		Observed		
		Match	No match	Total
Predicted	Match	3637	2363	6000
	No match	2387	3613	6000
	Total	6024	5976	12000
	Accuracy	0.6038	0.6046	0.6042

The Figure 5.17 shows a match in classification between the image processing and majority experts with Figure 5.17 a) and b) classified as 1 and 2, respectively. The Figure 5.18 shows a mismatch in classification between the majority experts (classified as 3) and the image processing (classified as 2) probably attributable to the variation in grouping of the condition states and other factors such as crack pattern not considered in the image processing.

 a)  b)

Figure 5.17. Image processing and expert classification match.

Figure 5.18. Image processing and expert classification no match.

The Table 5.9 shows probabilities of obtaining a match or right detection for each i and IoU combination. The highest probability of 0.66 was achieved if IoU was set to 0.7 and the least precise annotation case III was applied. As noted, the high probabilities for 0.7 IoU were also influenced by no defect detection which led to high MCI values that matched expert results. If p_0 is set to 0.5, then IoUs of 0.3 and below may be inappropriate for pavement defect detection tasks; and high IoUs above 0.7 need to be selected taking into consideration the inability to detect defects at such strict thresholds. This result showed the insignificance of highly precise annotations (case I), and that very low or very high IoUs may be undesirable for road defect detection tasks. From the optimization process, defect densities can be obtained and proposed section intervention can be determined following an intervention matrix after prioritization.

Table 5.9 Probabilities of detecting a match.

Annotation case *i*	IoU	Pr(*i*, IoU)
I	0.7	0.6041
	0.5	0.5102
	0.3	0.4157
	0.1	0.3270
II	0.7	0.6564
	0.5	0.5661
	0.3	0.4712
	0.1	0.3783
III	0.7	0.6619
	0.5	0.5720
	0.3	0.4772
	0.1	0.3839

5.8 Discussion

5.8.1 Annotation precision and cost trade-off

This study evaluated the trade-off between image processing inputs including annotation precision and cost. First, the research experimentation explored using simple segmentation methods that do not require costly annotation on the publicly available RDD-2020. For efficiency reasons, simple segmentation should be done programmatically as opposed to manually as the latter is cumbersome for a large image dataset. Whereas simple segmentation methods incur no annotation cost, they were challenged by region breakage due to poor lighting conditions and colour changes, and unwanted objects were segmented in several cases. These challenges of simple segmentation methods could have potentially resulted in accurate estimation of defect densities.

The shortcomings of simple segmentation methods led to the experimentation on deep learning methods. A deep learning model was trained using the Mask R-CNN algorithm utilizing the RDD-2020. For deep learning, the road images were annotated by varying the degree of precision. Less informative annotations required less annotation time, whereas more informative annotations consumed more time. As annotation precision was reduced, the odds of obtaining a correct match increased from annotation case I, II to III as a result of the increase in the RoI area which increased the probability of detection. These results showed the insignificance of very precise and costly

annotations for pavement defect detection tasks. However, the annotations should be tight enough to avoid erroneous allocation of non object regions as RoIs before model training as this may generate inaccuracies.

5.8.2 Deep learning, objective annotation and IoU

As discussed in the previous subsection, deep learning overcame the challenges faced by simple segmentation methods. Additionally, deep learning in which all objects of interest (road features and defects) were identified and segmented in parallel made it convenient to estimate the defect densities. The deep learning results were also more promising with objects detected and segmented with high AP values. Road features were detected and segmented with the highest AP values because they were very prominent in the images. As IoU was decreased, more defects were detected because a less strict IoU enabled more detection since the ground truth and prediction needed not overlap much. Also, more severe defects were detected from annotation case I to II to III because of the increase in the RoI size that allowed more overlap between the ground truth and prediction.

A probabilistic pavement management model that included setting IoU and annotation precision objectively with validation from experts was developed in this study to facilitate the standardisation of setting model inputs so as to have more uniform outputs that would minimise the variability of infrastructure intervention decisions. The validation of the model by a group of experts ensured that the model could be applied even in areas where expert engineers were very few or absent to hopefully reduce the proportion of infrastructure neglected as a result of personnel shortages. In the empirical application of the model, the estimated parameters were significant which showed that IoU and annotation precision influenced accurate defect detection. The calibrated model also had a high success hitting rate of more than 60%. It was shown that low IoU resulted in more defect detection, whereas the annotation precision was insignificant. As annotations were made less precise, the RoI size increased which resulted in more overlap between the ground truth and the prediction hence more defect detection. As the IoU was reduced, the requirement for area of overlap was made less strict which meant that the ground truth and prediction needed not overlap much increasing detection. However, the IoU needs to be restricted to avoid meaningless and erroneous detections if IoU approximates the limits of 0 and 1. Despite being insignificant, the object annotations need to be as tight as possible to avoid labeling non

object regions as objects and the annotations shouldn't be cumbersome so as to lower the processing cost. The developed model maximized the probability of right defect detection because more detection may encourage proactive intervention and further investigation for the candidate sections which could improve road user safety.

5.8.3 Road asset management application

The optimum model inputs, annotation precision and IoU, could be used to generate the section defects and safety level, MCI in this paper. The obtained MCI that may closely match with the expert classification can then be used to prescribe the appropriate interventions for a road pavement group using an intervention matrix as shown earlier in the article. The intervention on a section can be based on the severity of the defects on a given section in comparison to other sections in the infrastructure group. It may be noted that the intervention in this case could be based on one point image data collected at one time point, however, the appropriateness of intervention decisions could be improved by incorporating future performance prediction models such as the stochastic Markov hazard model since image data is expected to be more available in future. The required performance model could inform the image data collection process so as to generate more consistent and usable data.

5.9 Conclusions

This research proposed a framework to feasibly apply deep learning model results to pavement asset management. The study used the publicly available smartphone road image data from Japan, India and the Czech republic to train and validate a deep learning model built on the Mask R-CNN algorithm. The experiments showed that with fewer resources for management amidst an increasing infrastructure stock, computer vision promises safer and more efficient asset management and planning compared to the current human dependent practice. The research work empirically showed the following:

1) Experimental comparison showed the merits of deep learning compared to simple segmentation in overcoming poor lighting conditions and colour changes to correctly segment objects in images.
2) Choice of the IoU threshold and annotation precision are important for object detection tasks and should be optimally determined. The IoU significantly affected defect detection

and hence should be carefully selected to avoid meaningless and erroneous detections. The annotation precision was insignificant in defect detection and so less costly simplified polygons may suffice.

3) Tests showed that one-point data obtained from a single image dataset can be efficiently used to support intervention choices on infrastructure with less human dependence.

In future, better stochastic asset management models could be developed using consistently obtained data because current state-of-the-art asset management models require at least two-point condition data to model deterioration processes and perform LCC analysis. Building and improving algorithms that detect patterns of defects and their colors is a possible area for future research because defect patterns and colours could indicate the failure type. The efficiency of detection and segmentation algorithms also needs to be generally improved. A positive feedback loop can also be created between data collection and future asset management needs. To make the data more usable for planning the Global Positioning System (GPS) coordinates of the photos could be included in the database so that the road sections can be better identified and linked to road network maps. It is recommended that further studies and methodologies be developed to make annotation more objective than subjective to minimize the variability due to different annotators.

Bibliography

Arya, D., Maeda, H., Ghosh, S. K., Toshniwal, D., Mraz, A., Kashiyama, T. and Sekimoto, Y., 2020a. Transfer Learning-based Road Damage Detection for Multiple Countries, arXiv preprint arXiv:2008.13101.

Arya, D., Maeda, H., Ghosh, S. K., Toshniwal, D., Mraz, A., Kashiyama, T. and Sekimoto, Y., 2020b. Global Road Damage Detection: State-of-the-art Solutions, arXiv preprint arXiv:2011.08740.

Arya, D., Maeda, H., Ghosh, S. K., Toshniwal, D., Mraz, A., Kashiyama, T. and Sekimoto, Y., 2021. Deep learning-based road damage detection and classification for multiple countries, *Automation in Construction*, Vol.132, 103935.

Cambridge University, 2021. CamVid dataset. http://mi.eng.cam.ac.uk/research/projects/VideoRec/CamVid/. Accessed on December 13.

Deng, J., Dong, W., Socher, R., Li, L. -J., Li, K. and Fei-Fei, L., 2009. ImageNet: A large-scale hierarchical image database, *IEEE Conference on Computer Vision and Pattern Recognition*, Florida, doi: 10.1109/CVPR.2009.5206848, pp. 248-255.

Everingham, M., Eslami, S. A., Van Gool, L., Williams, C. K., Winn, J. and Zisserman, A., 2015. The Pascal visual object classes challenge: a retrospective, *International Journal of Computer Vision*, Vol.111, No.1, pp. 98–136.

Girshick, R., 2015. Fast R-CNN, *IEEE International Conference on Computer Vision*, Boston, MA, pp. 1440–1448.

Girshick, R., Donahue, J., Darrell, T. and Malik, J., 2014. Rich feature hierarchies for accurate object detection and semantic segmentation, *IEEE Conference on Computer Vision and Pattern Recognition*, Ohio, pp. 580–587.

Goncalves, L. R. and Givigi, S. N., 2016. Automatic Crack Detection and Measurement Based on Image Analysis*, IEEE Transactions on Instrumentation and Measurement*, Vol.65, No.3, pp. 583–590.

Greenwald, N.F., Miller, G., Moen, E. et al., 2022. Whole-cell segmentation of tissue images with human-level performance using large-scale data annotation and deep learning, *Nature Biotechnology*, 40, https://doi.org/10.1038/s41587-021-01094-0, pp.555–565.

He, K., Gkioxari, G., Dollar, P. and Girshick, R., 2018. Mask R-CNN, Facebook AI Research (FAIR), arXiv:1703.06870v3.

Hong, J.W., Jin, S. and Lee, S.E., 2020. A vision-based approach for autonomous crack width measurement with flexible kernel, *Automation in Construction*, Vol.110, 103019.

JARA, 2012. *Maintenance and Repair Guide Book of the Pavement 2013*, 1st edn., Japan Road Association, Tokyo, Japan.

Kinyanjui, N.M., Odonga, T., Cintas, C., Codella, N.C.F., Panda, R., Sattigeri, P. and Varshney, K.R., 2019. Estimating Skin Tone and Effects on Classification Performance in Dermatology Datasets, *NeurIPS Workshop on Fair ML for Health*, Vancouver, Canada.

Kobayashi, K., Do, M. and Han, D., 2010. Estimation of Markovian transition probabilities for pavement deterioration forecasting, *KSCE Journal of Civil Engineering*, Vol.14, No.3, pp. 343–351.

Kobayashi, K., Eguchi, M., Oi, A., Aoki, K., Kaito, K., 2013. The optimal implementation policy for inspecting pavement with deterioration uncertainty. *Journal of Japan Society of Civil Engineers*, 1(1), 551–568.

Kobayashi, K., Kaito, K. and Lethanh, N., 2012. A Bayesian estimation method to improve deterioration prediction for infrastructure system with Markov chain model, *International Journal of Architecture, Engineering and Construction*, Vol.1, No.1, doi:10.7492/IJAEC.2012.001, pp. 1–13.

Kroon, D., 2021. Region Growing (https://www.mathworks.com/matlabcentral/fileexchange/19084-region-growing), MATLAB Central File Exchange. Retrieved December 13.

Kubo, K., 2017. Pavement Maintenance in Japan, *Road Conference International Symposium*.

Lethanh, N., Adey, B.T., 2012. A hidden Markov model for modeling pavement deterioration under incomplete monitoring data. *International Journal of Civil and Environmental Engineering*, 6(1), 7–14.

Lin, K. and Lin, C., 2011. Applying Utility Theory to Cost Allocation of Pavement Maintenance and Repair, *International Journal of Pavement Research and Technology,* 4 (4), 212–221.

Liu, H. and Wang, D. Z. W., 2016. Modeling and solving discrete network design problem with stochastic user equilibrium, *Journal of Advanced Transportation,* 50 (7), 1295–1313.

Maeda, H., Sekimoto, Y., Seto, T., Kashiyama, T. and Omata, H., 2018. Road damage detection and classification using deep neural networks with smartphone images, *Journal of Computer-Aided Civil and Infrastructure Engineering*, Vol.33, pp. 1127–1141.

Minami, M., and Suzuki, T., 2008. Pavement Maintenance Level and Annual Budget over the Regional Road Network, *Journal of Construction Management, JSCE*, 15, 71-79.

Mirikharaji, Z., Abhishek, K., Izadi, S. and Hamarneh, G., 2021. D-LEMA: Deep Learning Ensembles from Multiple Annotations Application to Skin Lesion Segmentation, *Proceedings of the IEEE/CVF Conference on Computer Vision and Pattern Recognition (CVPR) Workshops*, pp. 1837-1846, Held virtually.

Miyamoto, A., and T. Yoshitake., 2009. Development of a remote condition assessment system for road infrastructure, *International ECCE Conference, EUROINFRA 2009, Current State and Challenges for Sustainable Development of Infrastructure.*

Mizutani, D., Nakazato, Y., and Lee, J., 2020. Network-level synchronized pavement repair and work zone policies: Optimal solution and rule-based approximation, Transportation Research Part C: Emerging Technologies, Vol. 120, https://doi.org/10.1016/j.trc.2020.102797, 102797.

Obunguta, F. and Matsushima, K., 2020. Optimal pavement management strategy development with a stochastic model and its practical application to Ugandan national roads, *International Journal of Pavement Engineering*, Vol.23, No.7, DOI: 10.1080/10298436.2020.1857759, pp. 2405–2419.

Obunguta, F., Matsushima, K. and Bakamwesiga, H., 2022. Social Cost Optimization Model and Empirical Evaluation of Intervention Effects on Ugandan Road Pavements, *Journal of Infrastructure Systems*, Vol.28, No.4, DOI: 10.1061/(ASCE)IS.1943-555X.0000707, 05022005.

Otsu, N., 1979. A Threshold Selection Method from Gray-Level Histograms, *IEEE transactions on systems, man, and cybernetics*, Vol.9, No.1, pp. 62–66.

Padilla, R., Netto, S. L. and da Silva, E. A. B., 2020. A Survey on Performance Metrics for Object-Detection Algorithms, *Proceedings of the International Conference on Systems, Signals and Image Processing (IWSSIP)*, pp. 237–242.

Pérez-Acebo, H., Mindrab, N., Railean, A. and Rojí, E., 2019. Rigid pavement performance models by means of Markov Chains with half-year step time*, International Journal of Pavement Engineering,* Vol.20, pp. 830–843. doi:10.1080/10298436. 2017.1353390.

Ren, S., He, K., Girshick, R. and Sun, J., 2015. Faster R-CNN: Towards real-time object detection with region proposal networks, *NIPS.*

Rubin D.B., 1976. Inference and missing data. *Biometrika*, Vol.63, pp. 581–592.

Rubin D.B., 1987. Multiple imputation for non-response in surveys. New York: John Wiley.

Tabatabaee, N. and Ziyadi, M., 2013. Bayesian approach to updating Markov-based models for predicting pavement performance, *Transportation Research Record: Journal of the Transportation Research Board*, Vol.2366, No.1, doi:10.3141/2366-04, pp. 34–42.

The MathWorks Inc., 2021. (https://uk.mathworks.com/help/images/ref/lazysnapping.html).

Thuyet, D. Q., Jomoto, M., Hirakawa, K., Lei Swe, Y. L., 2022. Development of an Autonomous Road Surface Damage Inspection Program Using Deep Convolutional Neural Network, *Journal of JSCE*, Vol. 10, Issue 1, pp. 235–246, https://doi.org/10.2208/journalofjsce.10.1_235.

Tsuda, T., Kaito, K., Aoki, K. and Kobayashi, K., 2006. Estimating Markovian Transition Probabilities for Bridge Deterioration Forecasting, *Structural Engineering/Earthquake Engineering*, Vol.23, No.2, pp. 241s–256s.

Xu, Y., Zhong, Z., Lian, D., Li, J., Li, Z., Xu, X., and Gao, S., 2021. Crowd Counting with Partial Annotations in an Image, *Proceedings of the IEEE/CVF International Conference on Computer Vision (ICCV)*, pp. 15570-15579, Held virtually.

Yoshida, T., 2016. Composite indicators for assessing maintenance needs for road pavements from the view point of road functions, *Journal of Japan Society of Civil Engineers, Ser. E1 (Pavement Engineering)*, 72(1).

Zou, D., Zhang, M., Bai, Z., Liu, T., Zhou, A., Wang, X., Cui, W., and Zhang, S., 2022. Multi-category damage detection and safety assessment of post-earthquake reinforced concrete structures using deep learning, *Journal of Computer-Aided Civil and Infrastructure Engineering*, https://doi.org/10.1111/mice.12815, pp. 1–17.

Chapter 6

6 Conclusions

6.1 Summary of Presented Research

This thesis has detailed Infrastructure asset management showing the traditional and currently applied methods and has looked at the future directions in this field with a focus on encouraging its full appreciation in developing countries. The dissertation described traditional methods including the subjective human based and reactive management methods that have been in operation for a significant time mainly because of the low infrastructure stock in developing countries that are still in the infrastructure development stage and are transitioning into the maintenance phase. With current increases in the stock due to improved access to finance, the developing world will definitely face similar challenges including aging infrastructure that the developed world is currently facing after the rapid economic growth period in the 20th century. The first sections of the dissertation looked at deterioration forecasting, important for proactive planning using stochastic Markov models. Then the challenge of intervention decision making for multiple sections in an infrastructure group was looked at. The thesis then explored the applications of computing specifically deep learning to infrastructure asset management. Below are the specific research directions taken in this dissertation.

Firstly, the studies undertaken in this dissertation encouraged the adoption of proactive infrastructure management; i.e., the condition-dependent policy and preventive maintenance, that utilizes objective and mathematical methods to estimate the deterioration trends of public infrastructure such as roads, bridges, tunnels and pipelines to delay their total dilapidation and avoid disastrous failures and disruptions. The study detailed the stochastic Markov hazard model to estimate deterioration trends and included an empirical application using real world data.

Secondly, the challenge of intervention planning for multiple sections and the effect of road intervention on travel time was looked at as this is an emerging planning problem for infrastructure managers in both developing and developed countries. Decisions on new developments and repair of existing infrastructure have traditionally been made subjectively but this dissertation proposed a more objective way to make these decisions optimally while ensuring that the society that uses this public infrastructure benefits maximally.

Finally, this dissertation looked at the application of new computing technologies to manage infrastructure given the challenges of reduced management personnel and increasingly dangerous conditions for inspectors to access damaged infrastructure for instance after a disaster, and the need for more accurate data for planning. This section of the thesis looked at artificial intelligence specifically computer vision to improve the accuracy of quantification of infrastructure defects and efficiently plan for appropriate intervention. This section suggested a probabilistic method of setting the annotation quality and Intersection over Union objectively rather than subjectively in an attempt to standardize these important pre-steps to deep learning.

The thesis included empirical application cases using data mainly obtained from Uganda and Japan to empirically show the applicability of the proposed models.

6.2 Conclusions and Recommendations

The main takeaways from this dissertation include the following;

- A shift from the time-dependent to the condition-dependent management policy that incorporates infrastructure deterioration rates in planning may improve infrastructure planning and lower the LCCs. Additionally, the gains from this proactive policy can be further realized if preventive maintenance is adopted by the management agency (Chapter 3). This kind of policy shift mainly in developing countries may play a role in improving the quality of transportation infrastructure mainly road pavements.
- With proper intervention planning that balances the kind of actions performed on elements of an infrastructure group, it may be unnecessary to arbitrarily increase intervention budgets. This thesis showed the possibility of optimizing interventions by lowering social costs if key bottlenecks in the road infrastructure system including poor pavement

condition and inadequate capacity were optimally cleared to facilitate traffic flow and hence shorten travel times (Chapter 4).

- Infrastructure asset management should capitalize on the advances in computing to handle the challenges currently faced including shortage of experts and poor access in areas affected by disasters. It was shown that road pavement smartphone image processing may offer viable solutions in the detection and quantification of road infrastructure defects using cheaper methods for data collection (only a smartphone) and analysis. This could improve infrastructure management efficiency, inspection coverage, measurement accuracy and facilitate access to dangerous sites e.g. after a disaster (Chapter 5). This chapter also showed that the setting of annotation precision and Intersection over Union setting could be standardized so as to reduce the variability of object (defect) detection.

To conclude, the following recommendations are made to improve asset management especially in developing countries;

- It is recommended to improve data collection by sectioning roads at about 100 m per section due to the variability of pavement condition as length increases. Data collection should also be more specific and based on how critical sections are, for example bridge and intersection approach sections, for better management. A positive feedback loop can also be created between data collection and future asset management needs. For instance, to make the data more usable for planning the GPS coordinates of the photos could be included in the database so that the road sections can be better identified and linked to road network maps.
- As infrastructure monitoring data changes from written or typed data to image mainly photogrammetric data, the analysis methods need to be improved and simplified to enable larger coverage, and more efficient and effective decision making. Also, algorithms could be developed and improved to handle various situations such as incomplete data and detailed image features including defect colours and patterns.